

Esm1 modulates spinal cord vascularization in Vegfaa gain-of-function zebrafish models

Zur Erlangung des akademischen Grades einer

DOKTORIN DER NATURWISSENSCHAFTEN

(Dr. rer. nat.)

von der KIT-Fakultät für Chemie und Biowissenschaften

des Karlsruher Instituts für Technologie (KIT)

genehmigte

DISSERTATION

von

M.Sc. Silvana Maria Knapp

1. Referent/in: Prof. Dr. Ferdinand le Noble

2. Referent/in: Prof. Dr. Martin Bastmeyer

Tag der mündlichen Prüfung: 6. Februar 2020

Acknowledgements

I thank Ferdinand le Noble for great support during the last years. I could freely pursue my own ideas and could independently work on interesting projects. Your dedication to science and constant enthusiasm is impressive and exemplary.

Special thanks go my academic colleagues, especially to Dietmar Gradl, Laëtitia Préau, Anne Ramms and Andria Michael, who accompanied me most of my time as a PhD student. You were always motivating, supportive and helpful.

I am grateful for all the help I got from every single member of the lab. Special thanks go to Esther Fuchs, Karolin Rahm and Stefanie Kalb. I really valued your great assistance in all matters concerning experiments.

The entire time of my PhD, my family and my partner were always encouraging me. You were cheering me up during difficult times, kept me sane and showed me what really matters in life.

Table of Contents

1	Summary	6
2	Zusammenfassung	7
3	Introduction	9
3.1	<i>The vascular system</i>	9
3.1.1	The development of vascular network.....	9
3.1.2	Architecture of blood vessels	10
3.1.3	From endothelial precursors to tubular structures: vasculogenesis	11
3.1.4	Expanding the vessel network: angiogenesis.....	12
3.1.5	Arteries and veins: differences between the tubular systems.....	13
3.1.6	The vascular system makes difference between health and disease	14
3.2	<i>The zebrafish vascular system</i>	15
3.2.1	The zebrafish is a great model organism	15
3.2.2	Development of the zebrafish trunk vasculature	16
3.2.3	Development and function of the zebrafish spinal cord	21
3.2.4	Friendship between nerves and blood vessels.....	21
3.3	<i>The VEGF family – main effectors of vascular guidance</i>	22
3.3.1	The VEGF ligands	23
3.3.2	The VEGF receptors.....	24
3.3.3	Clinical suitability of VEGFR-2, VEGFR-1 and VEGF-A.....	27
3.4	<i>Endothelial cell-specific molecule 1</i>	28
3.4.1	Proteoglycans are important modulators of cellular responses	28
3.4.2	Endocan – a distinctive proteoglycan.....	29
3.4.3	Endocan and its role in pathological conditions.....	30
3.4.4	VEGF-A signaling and ESM1 expression are linked to each other	31
3.5	<i>Aim of the work</i>	31
4	Results	33
4.1	<i>Esm1 is expressed during early zebrafish development and levels are increased upon loss of flt1</i>	33
4.2	<i>Esm1 mRNA is expressed in developing and developed ISVs</i>	34
4.3	<i>Esm1 promoter activity in the vasculature and cells of the spinal cord</i>	37
4.3.1	The <i>esm1</i> promoter is active in the endothelium of various regions	37

4.3.2	Active <i>esm1</i> promoter in developing and developed trunk vasculature	38
4.3.3	<i>Esm1</i> promoter activity in <i>flt1</i> mutants is comparable to that in the wildtype and is present in the spinal cord vasculature	39
4.3.4	The <i>esm1</i> promoter is preferentially active in arterial endothelial cells	41
4.3.5	Neurons of the spinal cord show <i>esm1</i> promoter activity	43
4.4	<i>Altered esm1 levels influence degree of ectopic sprouting at the neuro-vascular interface in the zebrafish trunk</i>	43
4.4.1	Loss of <i>esm1</i> rescues hypersprouting in <i>flt1</i> mutants.....	44
4.4.2	Number of tertiary sprouts is decreased in <i>esm1</i> mutants upon <i>flt1</i> knock down	49
4.4.3	<i>Esm1</i> gain-of-function promotes vascular sprouting.....	50
4.5	<i>The effects of esm1 on tertiary sprouting was recapitulated in another Vegfaa GOF model, the vhl mutant</i>	53
4.6	<i>The development of the trunk vasculature is not distinctively altered upon loss of esm1</i>	56
5	Discussion	59
5.1	<i>Gene expression pattern of esm1</i>	59
5.1.1	<i>Esm1</i> gene expression is enhanced in Vegfaa GOF models	60
5.1.2	<i>Esm1</i> is expressed in the vasculature of zebrafish embryos	60
5.1.3	<i>Esm1</i> is active preferentially in arterial endothelial cells and subset of neurons.....	62
5.1.4	BAC transgenesis as an alternative tool to study gene expression	62
5.2	<i>Esm1 alone does not influence the vascular architecture in the trunk</i>	63
5.3	<i>Esm1 has minor effect on ISV morphology and endothelial cell proliferation</i>	63
5.4	<i>Spinal cord vascularization is modulated by Esm1 when Vegfaa/Kdrl signaling is highly active</i>	64
5.5	<i>Esm1 affects binding efficiency of Vegfaa to Kdrl</i>	66
5.6	<i>Using Esm1 for treating vascular conditions in medicine</i>	67
6	Material and Methods	69
6.1	<i>Material</i>	69
6.1.1	Transgenic and mutant zebrafish lines used	69
6.1.2	Solutions and buffer	70
6.1.3	Enzymes, chemicals and kits	71
6.1.4	Oligonucleotides	72
6.1.5	Tools for mutant generation	74
6.1.6	Plasmids	74
6.1.7	Online tools and softwares.....	75

6.2	<i>Methods</i>	76
6.2.1	Ethics statement	76
6.2.2	Zebrafish methods	76
6.2.3	Molecular biological methods.....	77
6.2.4	Staining methods.....	80
6.2.5	BAC Recombineering	81
6.2.6	Cloning of pGEMT_ <i>esm1</i> cds	82
6.2.7	Cloning of pCS2+_ <i>esm1</i> cds	82
6.2.8	Cloning of pME_eGFP-p2a- <i>esm1</i> cds.....	84
6.2.9	Generation and verification of <i>esm1</i> and <i>esm1;flt1</i> mutants.....	85
6.2.10	Genotyping	86
6.2.11	Microscopy	87
6.2.12	Computational methods	87
7	Bibliography	91
8	List of figures	122
9	List of tables	123
10	Abbreviations	124
11	Publications	126

1 Summary

The vascular and neuronal network are closely associated throughout embryonic development, in adulthood and during tissue regeneration. Both tissue meshes interact through reciprocal cross-talk involving diffusible molecules, thus being important for physiological functions in both domains.

Ectopic blood vessels are prematurely formed at the level of the spinal cord under certain conditions during early zebrafish development, thus demonstrating molecular cross-talk between the developing peripheral nervous system and the surrounding vascular network. This hyperbranching phenotype revealed a type of angiogenic sprouting form termed “tertiary sprouting” and is regulated by Vascular Endothelial Growth Factor (Vegf) aa/Kdr1 signaling. The onset and extent of spinal cord vascularization is controlled *via* bimodal adjustment of Vegfaa and the soluble form of its decoy receptor Flt1 in the neuronal tissue. The endothelial cell-specific molecule 1 (*esm1*), among others, was significantly deregulated during this process in *flt1* zebrafish mutants. ESM1 is a structurally distinctive secreted proteoglycan upregulated during various pathological conditions of the vascular system and is implied a role in angiogenic processes. However, its function during vascular remodeling remains elusive.

This project has the objective to get insight into the role of Esm1 in remodeling of the vascular architecture of the zebrafish trunk. First, *esm1* gene expression was quantitatively analyzed in models with increased Vegfaa bioavailability during stages of hypersprouting. Its spatial expression pattern was investigated using a BAC promoter-reporter construct and whole mount *in situ* hybridization during early zebrafish development. In addition, alterations in the trunk vascular pattern were analyzed when *esm1* levels were varied in the wildtype and Vegfaa gain-of-function models.

Esm1 was active in developing blood vessels during formation of the trunk vasculature in zebrafish embryos and may be specifically expressed in arterial endothelial cells and in a subset of neurons in the spinal cord. In the wildtype, changes in *esm1* levels did not affect the vascular architecture. However, in Vegfaa-gain-of-function scenarios, spinal cord vascularization is altered concurrent to Esm1 abundance. Accordingly, Esm1 is a modulator of the Vegfaa/Kdr1 signaling cascade by regulating the levels and gradient of Vegfaa in the extracellular matrix in the zebrafish. Moreover, *esm1* seems to have an anti-proliferative effect on endothelial cells attributed to its function as a proteoglycan.

2 Zusammenfassung

Die Netzwerke aus Gefäßen und Nerven sind in der Entwicklung vom Embryo zum ausgewachsenen Organismus sowie in der Regeneration nah miteinander verbunden. Beide Geflechte interagieren durch wechselseitige Kommunikation mit diffusionsfähigen Molekülen, welche für physiologische Funktionen wichtig sind.

Während der frühen Zebrafiscentwicklung können sich unter bestimmten Bedingungen frühzeitig ektopische Blutgefäße auf Höhe des Rückenmarks bilden, was molekulare Wechselwirkungen zwischen dem sich entwickelnden peripheren Nervensystem und dem umgebendem vaskulären Netzwerk demonstriert. Der Phänotyp der übermäßigen Blutgefäßbildung offenbart eine Art von angiogener Sprossung, auch „tertiäre Sprossung“ genannt, welche durch den vaskulären endothelialen Wachstumsfaktor (Vegf) aa/Kdr1 Signalweg reguliert wird. Der Beginn und Ausmaß der Rückenmarksneugefäßbildung wird durch eine bimodale Anpassung von Vegfaa und der löslichen Form seines Lockrezeptors Flt1 im neuralen Gewebe kontrolliert. In *flt1* Zebrafischmutanten ist unter anderem das Endothelzell-spezifische Molekül 1 (*esm1*) während dieses Prozesses signifikant dereguliert. ESM1 ist ein Proteoglykan, welches in seiner Struktur besonders ist. Es ist in verschiedenen pathologischen Konditionen des vaskulären Systems hochreguliert und spielt eine Rolle in angiogenen Prozessen. Seine Funktion mit Bezug auf vaskuläre Umformung ist allerdings immer noch schwer definierbar.

Das Ziel dieser Untersuchungen ist Einsicht in die Rolle von Esm1 bei der Umgestaltung der vaskulären Architektur des Zebrafischrumpfes zu bekommen. Zunächst wurde die Genexpression von *esm1* quantitativ in Modellen mit erhöhter Vegfaa Bioverfügbarkeit in Stadien der übermäßigen Sprossung analysiert. Das räumliche Expressionsmuster wurde mittels BAC Reporterkonstrukten und *in situ* Hybridisierungen während der frühen Zebrafiscentwicklung untersucht. Des Weiteren wurden die Auswirkungen von verschiedenen Expressionsniveaus von *esm1* auf das vaskuläre Muster im Wildtyp und in Vegfaa Überexpressionsmodellen ermittelt.

Esm1 war in sich entwickelnden Blutgefäßen während der Bildung des Zebrafischrumpfes aktiv und scheint gezielt in arteriellen Endothelzellen und in einer Untergruppe von Neuronen im Rückenmark exprimiert zu sein. Im Wildtyp hatten Veränderungen von *esm1* keinen Einfluss auf das Gefäßmuster, während sich in Modellen mit Vegfaa Überexpression die Rückenmarksgefäßneubildung jedoch übereinstimmend mit der Esm1 Verfügbarkeit verändert. Demnach ist Esm1 ein Modulator des Vegfaa/Kdr1 Signalweges, in dem es das Niveau und den Gradienten von Vegfaa in der extrazellulären

Matrix im Zebrafisch reguliert. Des Weiteren scheint *esm1* Zellproliferation entgegenzuwirken, was seiner Funktion als Proteoglykan zugeschrieben werden kann.

3 Introduction

3.1 The vascular system

Every organ of the body is connected to the vascular system. The highly branched vessel network traverses the entire organism (Herbert and Stainier, 2011). The vasculature does not only supply the organisms with nutrients and oxygen, but it transports hormones and waste products through the vertebrate body and enables immune surveillance (Adams and Eichmann, 2010).

The blood vessel system is one of the first functional organs to be formed in the early development of a vertebrate and is crucially involved in organogenesis (Risau, 1995, 2008). Developing and developed organs rely on access to the vessels. Vascular malformations belong to the most common causes for embryonic lethality, which emphasizes the significance of this network during early developmental stages in mice and zebrafish (Feucht, Christ and Wilting, 1997; Krebs *et al.*, 2004).

3.1.1 The development of vascular network

In the first stages of embryonic development nutrients and oxygen are provided by diffusion. With ongoing growth of the organism, a complex system has to evolve to meet the physiological requirements to maintain a healthy organism: the cardiovascular network. This ends up in hierarchically arranged tube-like structures forming the blood vessel system of adult vertebrates. Blood rich in oxygen is transported from the heart towards the tissue *via* arteries, smaller arterioles and capillaries. The capillary network ensures optimal supply of the surrounding tissue with nutrients and oxygen. The blood is returned back to the heart through small venules and veins (Adams and Eichmann, 2010; Herbert and Stainier, 2011).

The vasculature develops in three temporarily distinguishable processes. First, a primitive vascular network is formed *de novo* during vasculogenesis (Flamme and Risau, 1992; Flamme, Frölich and Risau, 1997). Next, this vascular labyrinth is remodeled into a tubular system in the process of angiogenesis (Risau, 1997; Carmeliet, 2003). Last, the vessel identity is determined by arterial-venous differentiation (Wang, Chen and Anderson, 1998; Shin *et al.*, 2001; Eichmann *et al.*, 2005; Herzog, Guttmann-Raviv and Neufeld, 2005; Jones, 2011; Niklason and Dai, 2018)

3.1.2 Architecture of blood vessels

Two circulatory systems exist in higher vertebrates: blood vessel and lymphatic network. The first is a closed tubular framework, whereas the latter consists of a blind-ended tubular network transporting lymph, fluid rich in protein, from tissues towards the veins. In both tubular networks the lumen is lined by endothelium. Endothelial cells (ECs) form a highly heterogeneous cell population with distinct functions and gene expression patterns. Mural cells, smooth muscle cells and pericytes attached to the abluminal surface of certain vessels assist in vessel stability and blood pressure regulation (Annika, Alexandra and Christer, 2005; Adams and Alitalo, 2007; Eilken and Adams, 2010).

The vasculature consists of arterial and venous blood vessels and capillaries. Arteries and veins are made up of three different layers: the tunica intima facing the vessel lumen, the tunica externa the outermost abluminal layer and tunica media sandwiched in between. These layers harbor different cell types: ECs in the tunica intima, smooth muscle cells in the tunica media and fibroblasts in the tunica adventitia (Zhao, Vanhoutte and Leung, 2015). The architecture differs between veins and arteries, reflecting their respective function. In general, veins can be physiologically and histologically distinguished from arteries due to the lower blood pressure, thinner vessel wall and the presence of valves (Kume, 2010; Herbert and Stainier, 2011).

The blood is pumped from the heart into the aorta and distributed through the entire organism through large arteries. Subsequently, the blood reaches the various organs through small arteries and arterioles. Next, the blood passes capillaries where nutrients, oxygen and carbon dioxide are exchanged. The blood returns to the heart through venules, small and large veins. The architecture of blood vessels and the make-up of the vascular network are shown in figure 3-1.

With various substances, such as nitric oxide and angiotensin II, the vascular tone is fine-tuned (Pollman *et al.*, 1996). Furthermore, organ perfusion can be regulated also through sympathetic nerves innervating the arteries (Charkoudian and Rabbitts, 2009).

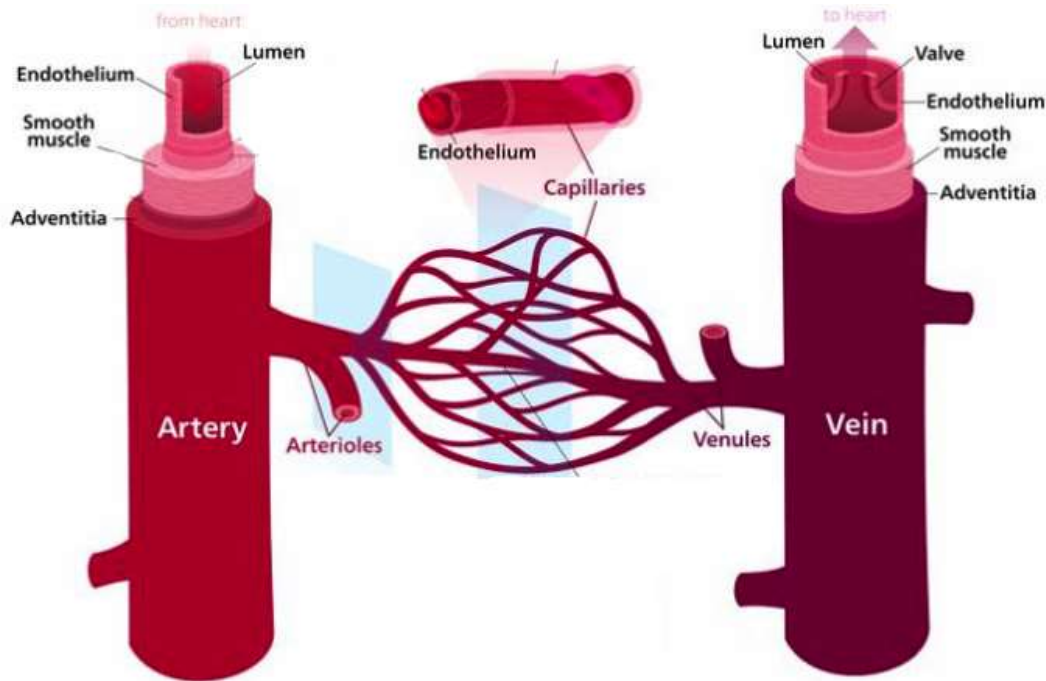


Figure 3-1. The architecture of blood vessels. Arteries, veins and capillaries form the vascular network. Arteries and vein are distinct in their make-up which corresponds to their respective function. The main layers of arteries and veins are the tunica intima, tunica media and tunica externa (from lumen side to the outermost layer). The heart pumps the blood *via* arteries and smaller arterioles towards capillaries, where it flows into the venous circulation and is transported through smaller venules and veins back towards the heart. Endothelial cells line the lumen, smooth muscle cells inhabit the tunica media. The basic structure of arteries and veins is comparable, but valves are specific for veins. Modified from: <https://www.bioexplorer.net/differences-between-arteries-and-veins.html/>

3.1.3 From endothelial precursors to tubular structures: vasculogenesis

The development of the cardiovascular system is initiated by vasculogenesis, a highly regulated process during which a primitive vascular network is formed *de novo* (Fig. 3-2; Adams and Alitalo, 2007).

First, mesodermal precursors, so called hemangioblasts, assemble and aggregate, thereby forming blood islands along the body axis in the extra embryonic tissue. The cells in the center of the blood islands differentiate towards the hematopoietic lineage, whereas the outer progenitors are committed to become angioblasts (Flamme, Frölich and Risau, 1997). These angioblasts are already specified to become arterial or venous ECs and eventually gives rise to primitive tubular structures, the dorsal aorta (DA) and the cardinal vein, at or near the site from which they originate (Risau and Flamme, 1995; Zhong *et al.*, 2001; Coultas, Chawengsaksophak and Rossant, 2005; Roca and Adams, 2007). Consequently, the primitive vascular plexus develops without the need of a pre-existing

structure. Next, the vascular structure grows and is remodeled in a process called angiogenesis (Flamme, Frölich and Risau, 1997).

3.1.4 Expanding the vessel network: angiogenesis

After vasculogenesis, a highly orchestrated vascular network is established by expansion and remodeling of the tubular system. Angiogenesis allows tissue devoid of blood vessels to get access to the vascular system (Patan *et al.*, 2001).

Angiogenic processes occur during the entire life of an organism. Excessively prevalent during the early development of an organism, it proceeds in several physiological (e.g. tissue repair and female reproduction cycle) and pathological (e.g. tumor growth) conditions in adulthood (Folkman, 1995; Meduri, Bausero and Perrot-Applanat, 2000; Carmeliet, 2003; Wang and Olson, 2009).

The formation of vascular segments in the embryo and in the adult organism occurs in a similar manner. Therefore, increased knowledge about blood vessel growth during embryogenesis might aid in understanding pathological conditions in the adult. Research in animal models, such as chicken embryos, zebrafish embryos, fetal/neonatal mice, revealed new insights into angiogenic processes (Pudliszewski and Pardanaud, 2005; Deryugina and Quigley, 2008; Chávez *et al.*, 2016).

New vessels are formed from pre-existing ones *via* different mechanisms: sprouting and splitting angiogenesis (intussusception) (Fig. 3-2). The former is characterized through outgrowth of ECs (Risau and Flamme, 1995; Flamme, Frölich and Risau, 1997), while the latter describes the separation of a tubular structure through insertion of translumen pillars (Burri, Hlushchuk and Djonov, 2004).

Sprouting of a new vessel is induced under hypoxic conditions, which subsequently upregulates angiogenic genes, such as the vascular endothelial growth factor (VEGF). Due to intensified levels of VEGF, ECs loosen intercellular junctional contacts and gain motility. Ultimately, permeability of the endothelium is improved and vessel sprouting can be initiated (Moses, 1997; Mehta and Malik, 2006). The so-called tip cell guides the emerging sprout, which is then lengthened through proliferation of adjacent stalk cells. Subsequently, a lumen is formed (Gerhardt *et al.*, 2003). The sprouting process is finished when the tip cell fuses and anastomoses with the target vessel. Eventually, a functional vascular labyrinth is established (Carmeliet, 2003; Burri, Hlushchuk and Djonov, 2004).

Splitting angiogenesis is the preferred mechanism in small vessels and capillaries. If redundant or inefficient vascular segments are pruned, the angle of bifurcating vessels

needs to be modified or existing vessels need to be duplicated (Mentzer and Konerding 2014). An interstitial tissue column spanning the vessel lumen, the intussusceptive pillar, characterizes this type of angiogenesis (Burri, Hlushchuk and Djonov, 2004; Djonov and Makanya, 2005; Mentzer and Konerding, 2014).

3.1.5 Arteries and veins: differences between the tubular systems

Genetics and hemodynamics determine if vessels acquire either arterial or venous identity during development (le Noble *et al.*, 2004; Jones, le Noble and Eichmann, 2006).

Remodeling of the blood vessel network and establishment of the ultimate vascular architecture are predetermined by genetics (Jones, le Noble and Eichmann, 2006). In the zebrafish and mouse, VEGF, Notch and EphrinB2 are involved in mechanisms concerning differentiation into either vessel type, artery or vein, even before blood circulation starts (Hong, Kume and Peterson, 2008; Julius *et al.*, 2008; Swift and Weinstein, 2009; Kume, 2010).

Already angioblasts are committed to become part of the arterial or venous compartment (Kume, 2010). These precursors can be specified towards the arterial fate with the activation of the Notch signaling cascade through VEGF (Lawson *et al.*, 2001, 2003; Lawson, Vogel and Weinstein, 2002). Subsequently, arterial differentiation is engaged through activated EphrinB2 gene expression. On the other hand, differentiation towards the venous fate is acquired by repression of the Notch signaling through the orphan nuclear receptor COUP transcription factor-2, which results in EphrinB4 expression. Those findings are emphasized by studies, which demonstrated that arterial identity is prevented by reduced VEGF levels (Lawson, Vogel and Weinstein, 2002; Visconti, Richardson and Sato, 2002) and that inhibition of Notch stimulates the expression of the venous marker VEGFR-3 in the zebrafish (Lawson *et al.*, 2001).

Additionally, hemodynamics influence arterial-venous differentiation is hemodynamics. Blood flow regulates expression of EphrinB2 and Neuropilin-1 (NRP-1), thereby assisting in the decision between arterial or venous identity (le Noble *et al.*, 2004, 2005).

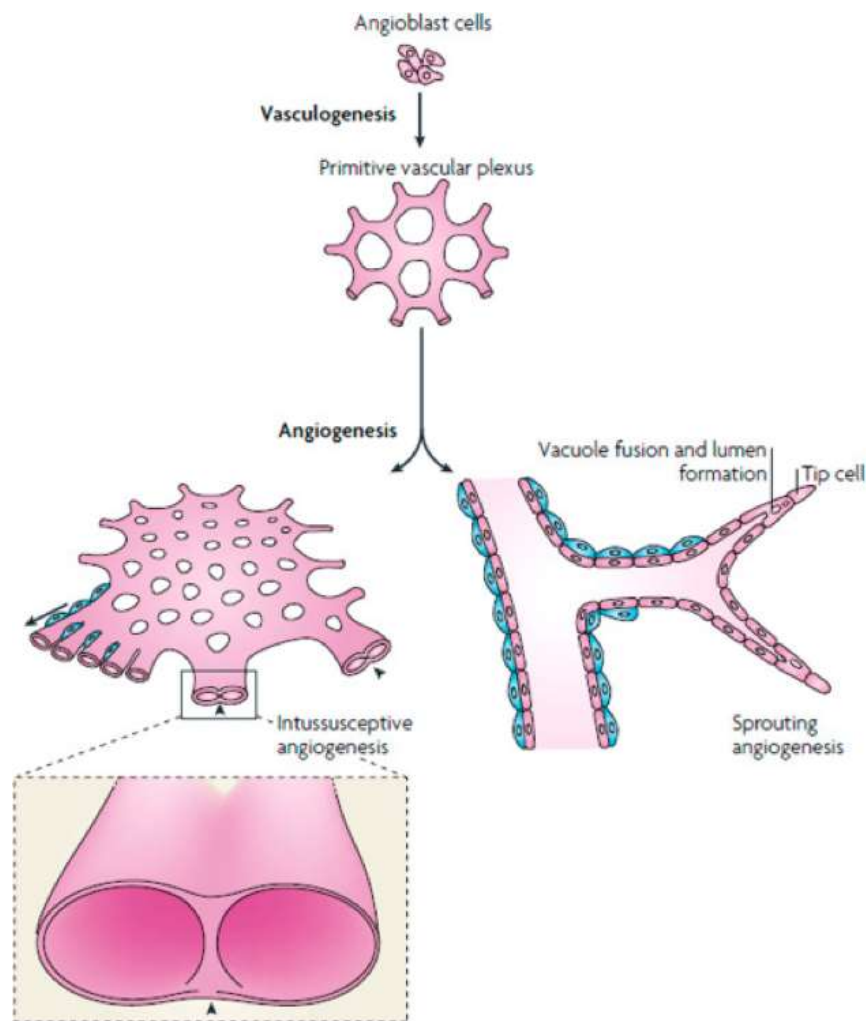


Figure 3-2. Vasculogenesis and angiogenesis. Blood vessels are established *de novo* in a process called vasculogenesis. Angioblasts, precursor cells of the blood and vessel lineage form blood islands, subsequently develop the primitive vascular plexus. Expansion of the vascular labyrinth is achieved by angiogenesis, the formation of blood vessels from already existing ones. There are two angiogenic modes: intussusceptive and sprouting angiogenesis. While the former occurs mainly in capillaries and can be described as splitting of the tubule, the latter is the mode for arteries and veins by which new vascular segments emerge by leading tip cells. Modified from: Kolte, McClung and Aronow, 2016

3.1.6 The vascular system makes difference between health and disease

Deregulated blood vessel development can principally affect any organ and, thus, is associated with various diseases. Excessive amount of blood vessels is related to medical conditions such as arthritis, cancer, obesity or primary pulmonary hypertension (Gimbrone *et al.*, 1972; Carmeliet, 2003). However, excessive regression or pruning of vascular segments is found in hypertensive or diabetic patients (Korn and Augustin, 2015). Accordingly, in numerous medical conditions attenuation of vascular growth is attempted,

for example cancer (Forster *et al.*, 2017) and ailments, when augmentation strategies are required to replace traumatized or degenerative tissue (Young and Schäfer, 2015; Filipowska *et al.*, 2017; Banfi *et al.*, 2018). The knowledge about how a stable and perfused vascular network can be established and its translation to the patient requires still extensive research.

Learning about the development and maintenance of a proper vascular network is crucial. Concerning therapies, a fine regulation of blood vessel growth is needed: increased blood vessel supply benefits regeneration but also CVDs or cancer, while decreasing blood vessel growth is intended to inhibit cancer metastasis or other pathological diseases involving blood vessels.

3.2 The zebrafish vascular system

3.2.1 The zebrafish is a great model organism

The zebrafish is a multifaceted model organism used in many research fields and acquired popularity in the fields of developmental biology, molecular genetics and cancer research as well as in toxicology and drug discovery (Rubinstein, 2003; Parng, 2005; Mione and Trede, 2010; Etchin, Kanki and Look, 2011; MacRae and Peterson, 2015; Letrado *et al.*, 2018; Meyers, 2018). Generation of transgenic and mutant lines as well as overexpression and disease models makes the fish a versatile animal to study (Nasiadka and Clark, 2012; Bradford *et al.*, 2017; Meyers, 2018).

Zebrafish are simple in maintenance and breeding and have a generation time of about 3 months. With one breeding a high number of progeny, which develop *ex utero*, is obtained (Nasiadka and Clark, 2012). Thus, it permits working with many embryos at once that can be easily treated with substances. Fast and transparent development favors *in vivo* and time-lapse imaging. Zygotes can be easily manipulated which allows generation of transgenic or mutant lines with relatively high efficiency.

Physiology and basic anatomical structure, i.e. nervous system and vasculature, is comparable between the zebrafish and humans (Becker and Becker, 2008; Gore *et al.*, 2012). Furthermore, 70% of genes involved in human pathophysiological diseases are similar with those of zebrafish (Santoriello and Zon, 2012).

3.2.2 Development of the zebrafish trunk vasculature

The zebrafish trunk vascular system is characterized by vascular segments, so called intersegmental vessels (ISVs), running from ventral to dorsal between the somites, the developing muscle tissue. On their way they pass the notochord and the neural tube (NT). ISVs are ventrally connected to either the DA or posterior cardinal vein (PCV) and join dorsal of the neural tube by a structure called dorsal longitudinal anastomotic vessel (DLAV) (Isogai *et al.*, 2003; Ellertsdóttir *et al.*, 2010; Wild *et al.*, 2017). The formation of the vascular system in the trunk is described in figure 3-3.

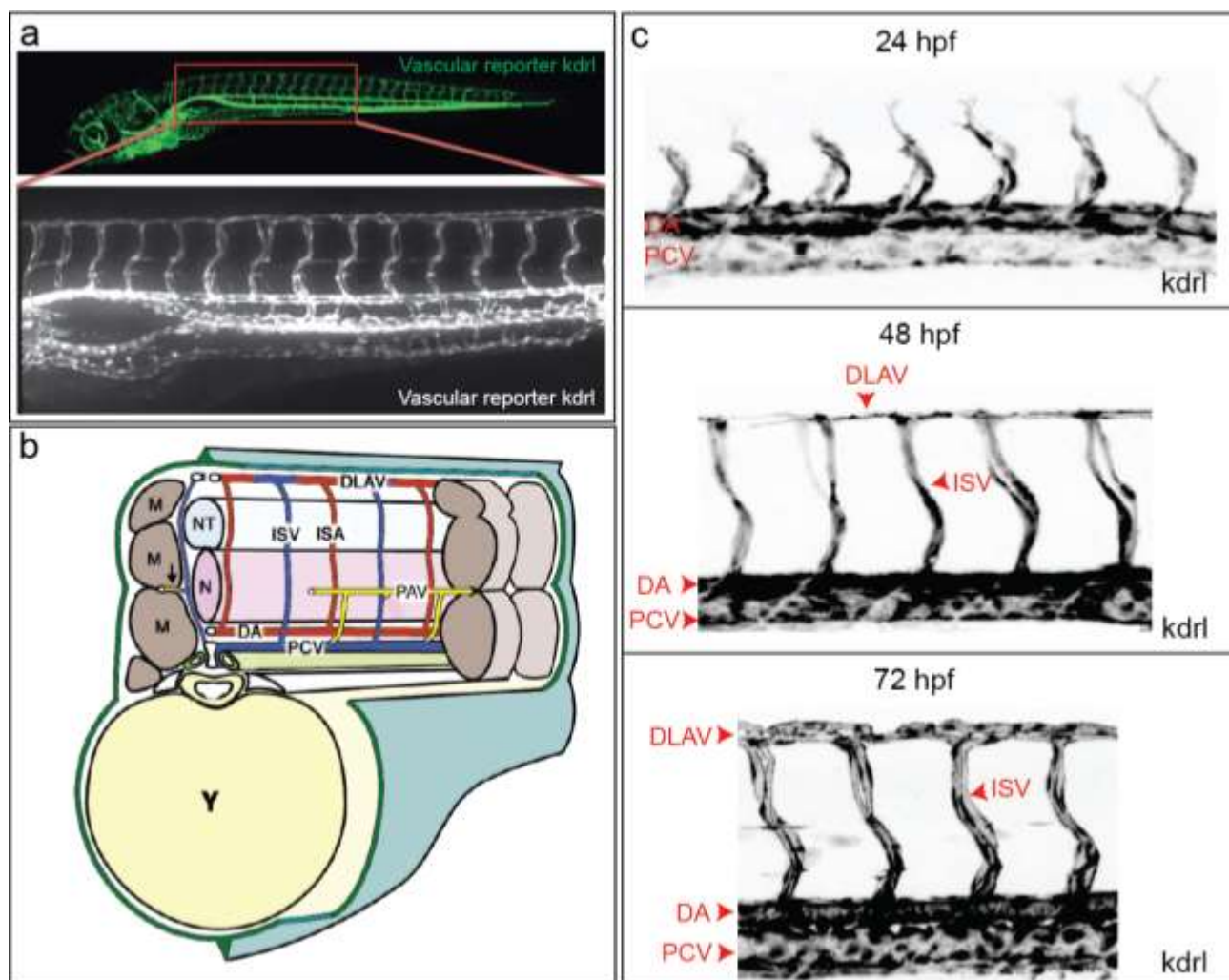


Figure 3-3. Development of the zebrafish trunk vasculature. (a) Depiction of the entire zebrafish embryo transgenic for the blood vessel reporter *kdrl*. The area in the red square illustrates the magnified vasculature of the trunk (Modified from <https://www.flickr.com/photos/nichd/17104754320>). (b) Schematic illustration of the zebrafish trunk anatomy (Modified from Mulligan and Weinstein, 2014). (c) Spinning disc microscopic images demonstrating the development of the zebrafish trunk vascular system visualized by the transgenic reporter *kdrl* from 24 hpf to 72 hpf. DA, dorsal aorta; DLAV, dorsal lateral anastomotic vessel; dpf, days post fertilization; hpf, hours post fertilization; ISA, intersegmental artery; ISV, intersegmental vein (in b); ISV, intersegmental vessel (in

c); M, muscles; N, notochord, NT, neural tube; PAV, parachordal lymphatic vessel; PCV, posterior cardinal vein; Y, yolk.

The zebrafish trunk vasculature is built up in three distinct events, called primary, secondary and tertiary sprouting, as illustrated in figure 3-4 (Isogai *et al.*, 2003; Ellertsdóttir *et al.*, 2010; Wild *et al.*, 2017). Arterial ISVs (aISVs) arise during primary sprouting at around 24 hours post-fertilization (hpf). These vessel segments emerge from the DA and migrate dorsally to form a T-shaped structure. Next, adjacent vessels link to each other, resulting in the DLAV (Isogai, Horiguchi and Weinstein, 2001; Isogai *et al.*, 2003). Sprouting is regulated by Vegfaa expressed in the somites (Ellertsdóttir *et al.*, 2010). Secondary sprouting is defined as the remodeling of aISVs into venous ISVs (vISVs). Blood vessel segments emanating from the PCV at around 32 hpf migrate dorsally and give rise to either vISVs and lymphatic vascular precursors (Isogai *et al.*, 2003; Yaniv *et al.*, 2006). The latter give rise to the parachordal lymphatic vessel. The term 'tertiary sprouting' describes spinal cord vascularization. Vascular segments connect neighboring ISVs horizontally at the level of the neural tube. In the wildtype this phenotype is observed at around 13 days post-fertilization (dpf). However, in some Vegfaa-GOF models it is seen as soon as 4 dpf. Moreover, these sprouts originate mainly from vISVs (Wild *et al.*, 2017).

3.2.2.1 Mechanism of sprout formation: the tip-stalk cell model

A functional vascular network is established by well-regulated extrinsic and intrinsic cues. A tight control and coordination of EC behavior, including those of sprouts, is indispensable for proper expansion and remodeling of the vessel system (Folkman and D'Amore, 1996; Carmeliet, 2003).

The forming sprout can be divided into a tip cell and stalk cells, which are distinct in function and gene expression. A balance between both cell types allows the formation of a functional vasculature (Ruhrberg *et al.*, 2002; Gerhardt *et al.*, 2003; Ruhrberg, 2003). The subdivision is induced by VEGF (Gerhardt *et al.*, 2003; Blanco and Gerhardt, 2013). Tip cells are migrating polarized cells spearheading the forming sprout and eventually anastomose with a neighboring vessel. The 'stem' of the sprouting vessel is made up of stalk cells. They are proliferative, hence responsible for the growth of the sprout, and establish a vascular lumen required for blood circulation (Carmeliet, 2003; Gerhardt *et al.*, 2003; Burri, Hlushchuk and Djonov, 2004; Blanco and Gerhardt, 2013). Non proliferating, quiescent cells are defined as phalanx cells (Geudens and Gerhardt, 2011).

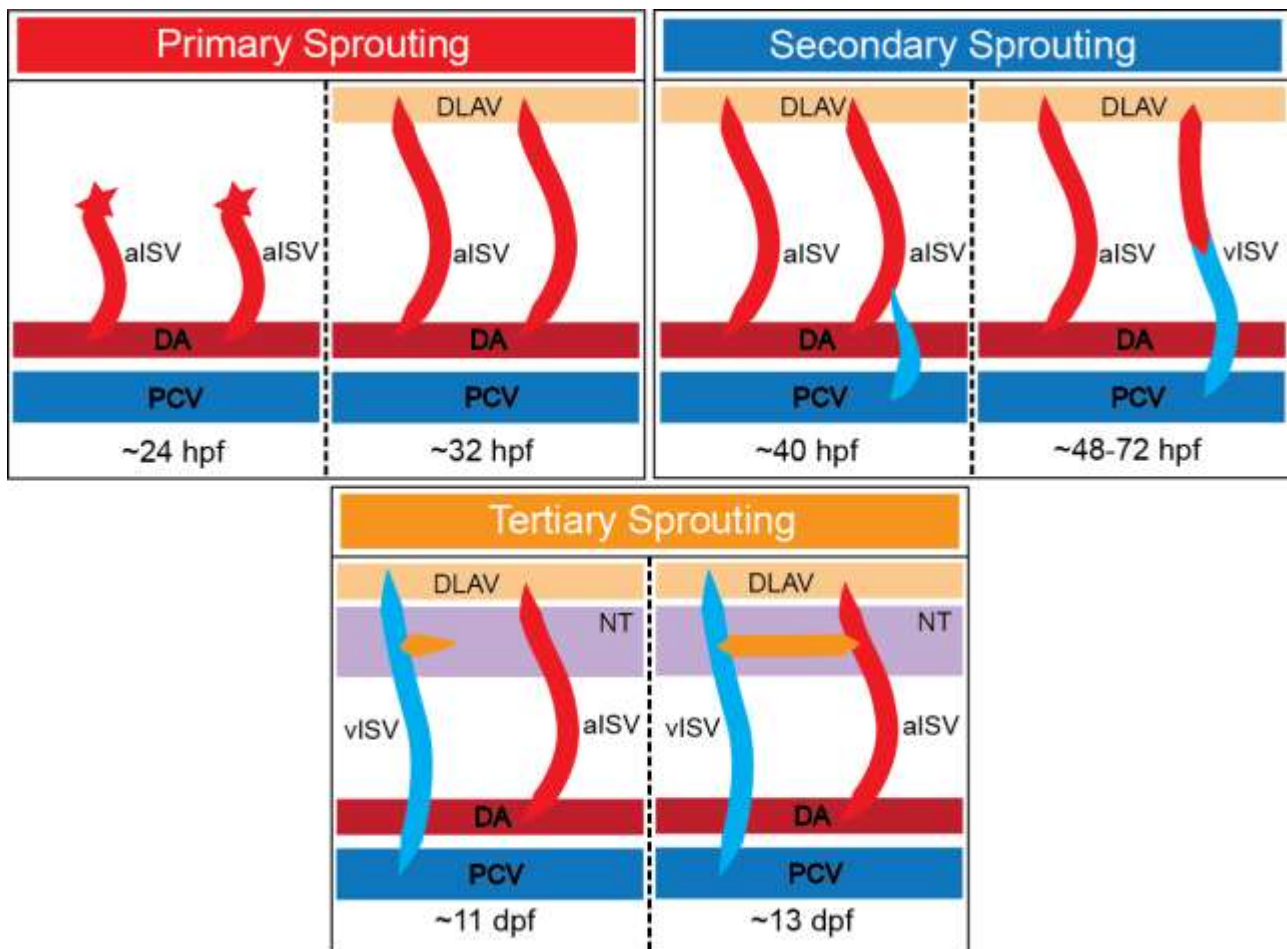


Figure 3-4. The distinct physiological sprouting types establish the vascular network of the zebrafish trunk. In the process of primary sprouting, intersegmental vessels (ISV) of arterial identity (aISV) are formed within the first two days of development. During the following day, a sprout originating from the PCV merges with the aISV, thereby altering the respective arterial flow to a venous one. Around 13 dpf, sprouts at the region of the neural tube emanate from mainly vISVs and establishes a connection to a neighboring vessel. DA, dorsal aorta; DLAV, dorsal lateral anastomotic vessel; dpf, days post fertilization; hpf, hours post fertilization; aISV, intersegmental artery; vISV, intersegmental vein; NT, neural tube; PCV, posterior cardinal vein.

Tip cells express vascular endothelial growth factor receptor (VEGFR)-2, VEGFR-3 and Notch ligand Delta-like 4 (Dll4), Angiopoietin-2, CXCR4 and ESM1 in abundance and are responsive to both angiogenic factors such as VEGF-A and classic guidance factors, including netrin-1 (Gerhardt *et al.*, 2003; Lu *et al.*, 2004; Tammela *et al.*, 2008; Strasser, Kaminker and Tessier-Lavigne, 2010). Stalk cells are enriched in receptors VEGFR-1 and Notch (Phng and Gerhardt, 2009; Strasser, Kaminker and Tessier-Lavigne, 2010). A summary of the tip-stalk cell model with molecules involved in this process is provided in figure 3-5.

How do certain cells become either a tip cell or stalk cell? VEGF-A activates VEGFR-2 in competing ECs, thereby augmenting Dll4 gene expression (Roca and Adams, 2007; Phng and Gerhardt, 2009). Dll4 prevents adjacent ECs from sprout formation through activation of the Notch pathway in these cells. This mode is also called lateral inhibition (Gerhardt *et al.*, 2003; Jakobsson *et al.*, 2010; Herbert and Stainier, 2011). Accordingly, with increasing levels of growth factor, the cell is more likely to acquire a tip cell phenotype and simultaneously impedes its neighboring cells to be selected as such (Hellström *et al.*, 2007; Siekmann and Lawson, 2007; Suchting *et al.*, 2007). In summary, next to other factors, alterations in VEGF gradient or Dll4/Notch signaling in ECs modify the sprouting process and eventually affect the development of the vascular network in the zebrafish model.

3.2.2.2 Vascular guidance cues: which way to go?

Guidance cues direct the developing sprout during migration towards its destination. Developmental structures such as somites and the spinal cord but also tissues with low oxygen such as wounds, ischemic tissue or tumors are considered as sources (Liang *et al.*, 2001; Ferrara, 2005; Haigh, 2008; Wild *et al.*, 2017).

The tip cell migrates a certain way under guidance of various factors attracting or repelling the vascular branch (Cramer, Kay and Zatulovskiy, 2018). Investigations demonstrated that these cells sense their environment for directional cues (Gerhardt *et al.*, 2003; Smet *et al.*, 2009). A study by Phng and colleagues suggested that filopodia are in principle dispensable for sprouting but they might enhance guidance efficacy and pace (Phng, Stanchi and Gerhardt, 2013).

Molecular cues during axon guidance are well studied and evidence exists that their directory function can be transferred to the vascular system (Lu *et al.*, 2004; Larrivéé *et al.*, 2009). The Semaphorins/Neuropilin, Ephrin-Eph, Slits/Roundabout and Netrin/Uncordinated-5 signaling cascades are examples for signaling partners directing not only axons but also blood vessels during physiological or pathological angiogenesis (Klagsbrun and Eichmann, 2005).

Next to molecular guidance cues, blood flow is a player in sprouting events. Hemodynamics might be a necessary condition for sprout formation (Watson *et al.*, 2013).

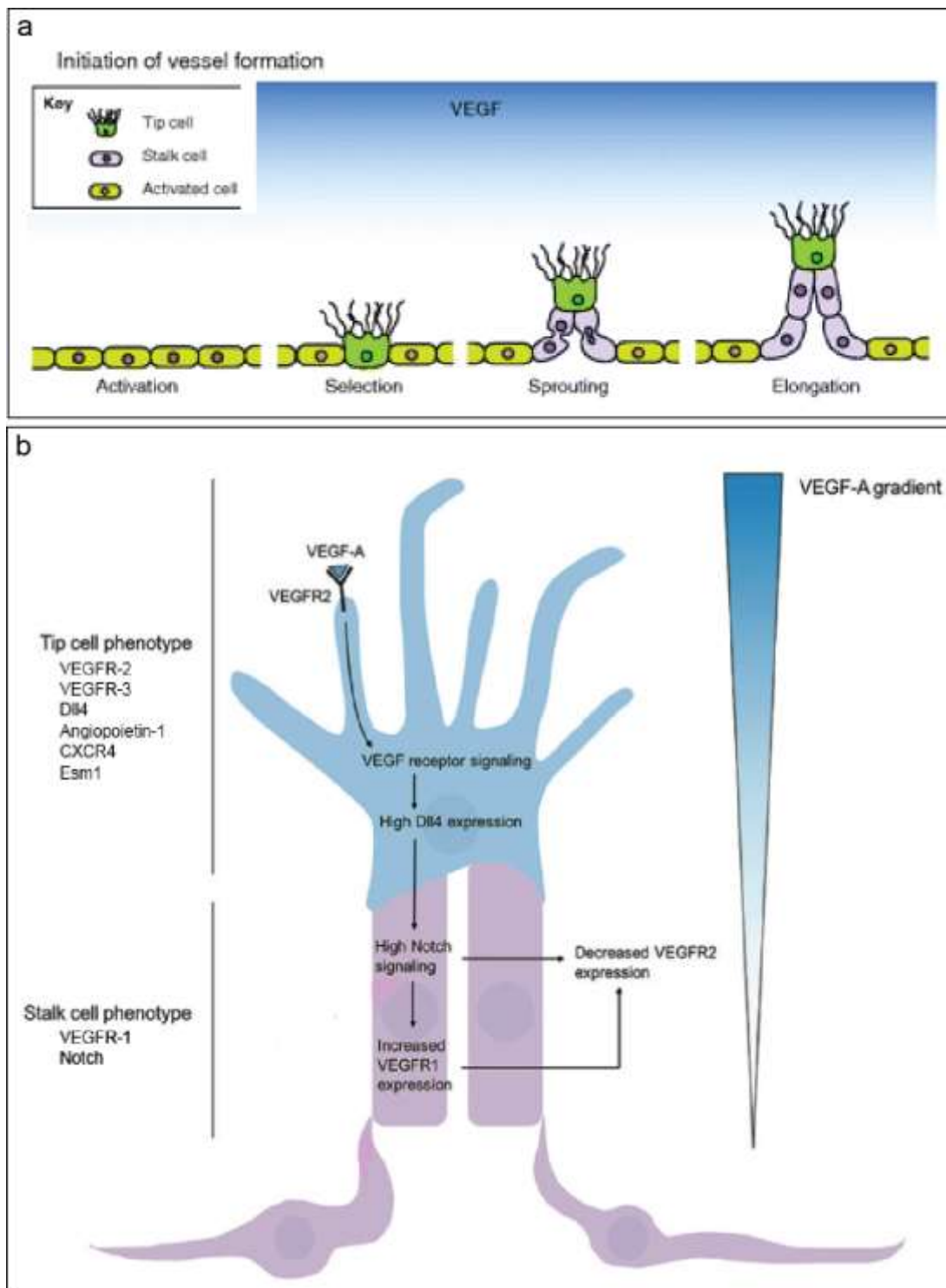


Figure 3-5. The tip-stalk cell model. (a) An EC becomes activated and selected as a tip cell, which is at the front of the developing sprout. Elongation and lumenization of the vascular segment is achieved by proliferation of tip cell adjacent stalk cells (Modified from Geudens and Gerhardt, 2011). (b) Tip cells and stalk cells are distinct in their phenotype and gene expression profiles. The former senses the environment for cues with filopodia and shows increased gene expression for VEGFR-2, VEGFR-3, Dll4, Angiopoietin, CXCR4 and Esm1. Stalk cells express VEGFR-1 and Notch in higher abundance compared to tip cells. The growing sprout is attracted towards increasing VEGF-A concentration (Modified from Gamboa *et al.*, 2017).

3.2.3 Development and function of the zebrafish spinal cord

In the process of neurulation, the neuroectoderm gets specified and remodeled into the neural plate. In most model organisms, neural plate undergoes a folding process to establish a NT which will develop into the brain and spinal cord (Hong and Brewster, 2006; Nyholm, Abdelilah-Seyfried and Grinblat, 2009). In the zebrafish, however, the neural plate forms into a rod-like structure, which develops further into the NT (Nyholm, Abdelilah-Seyfried and Grinblat, 2009).

With maturation of the NT, radial glia cells arise which are progenitors for several types of neurons, oligodendrocytes and astrocytes (Shimojo, Ohtsuka and Kageyama, 2011). Eventually, the spinal cord harbors distinct neuronal cells types for example motoneurons, sensory neurons and interneurons (Bota and Swanson, 2007). The xenopus beta-tubulin promoter *xla.tubb* is specifically active in mature neurons in the zebrafish (Peri and Nüsslein-Volhard, 2008).

3.2.4 Friendship between nerves and blood vessels

3.2.4.1 Similarities between the vascular and neuronal network

The vascular and nervous systems are both highly branched networks and thus share anatomical parallels, in particular at the periphery (Larrivée *et al.*, 2009; Tam and Watts, 2010). Close proximity and similar alignment of nerves and blood vessels let assume a close relationship concerning physical and molecular characteristics. Indeed, larger nerves and the vasa nervorum are physically connected. The other way round, the vascular tone is controlled by innervation of arteries by autonomic nerve fibers (Eichmann and Thomas, 2013). Thus, a close interaction between the two networks ensure a proper development of organs (Larrivée *et al.*, 2009; Tam and Watts, 2010).

Molecular similarities are demonstrated by shared guidance cues through which both the vascular and neuronal patterning is established. Signaling pathways directing not only nerves but also regulate angiogenic processes are Semaphorins, Ephrins, Slit and Netrins with their cognitive receptors (Klagsbrun and Eichmann, 2005).

3.2.4.2 Nerves and blood vessels are well conversant

During growth of the central nervous system (CNS), blood vessels from adjacent tissues get incorporated (Ruhrberg and Bautch, 2013). Angioblasts migrate to the CNS and eventually build up a perineural vascular plexus. Blood vessels ingress into and subsequently

honeycomb the NT during angiogenesis while maintaining the neural architecture. Thus, a regulated cross-talk is suggested (Mukouyama *et al.*, 2005; Ruhrberg and Bautch, 2013; Tata, Ruhrberg and Fantin, 2015). Furthermore, interactions between ECs and neural cells contribute to the blood-brain barrier (Nakao, Ishizawa and Ogawa, 1988; Ruhrberg and Bautch, 2013). Such observations let assume that molecular cues secreted from the nervous system guide vascular sprouts to their destination and vice versa.

In mouse studies was shown that neuronal VEGF is involved in differentiation and patterning of arteries. VEGF from the CNS seems to be indispensable for arteriogenesis (Mukouyama *et al.*, 2005). Moreover, defects in the nervous system might cause failing vasculature (Mukouyama *et al.*, 2002, 2005). In zebrafish, *vegfaa* is secreted by neurons in the spinal cord and guides venous tertiary sprouts in *vegfaa* GOF scenarios (Wild *et al.*, 2017).

The other way round, blood vessels can steer and pattern neurons. In zebrafish, a population of motoneurons comes in close contact to the DA involving the *Vegfc/Flt4* signaling pathway. *Flt4* in the axons benefits guidance towards and subsequent alignment to the *Vegfc* expressing DA (Kwon *et al.*, 2013). Another example are vascular-derived Endothelins. In the mouse embryo was shown that Endothelins direct axons of a subset of sympathetic neurons through Endothelin receptors to the external carotid artery, an intermediate target on the way to their final destination. These findings propose a role of Endothelins in axonal guidance and growth in the developing nervous system, due to which sympathetic neurons differentiate and choose their way through the vascular network to innervate their appropriate end organs (Makita *et al.*, 2008).

Although a bidirectional communication and interaction was described, examples exist in which the neuronal and vascular development is separable. In the zebrafish model, neuronal structures i.e. dorsal root ganglia, neuron clusters and axon tracts in the hindbrain develop even in the absence of blood vessels in an undisturbed fashion (Miller *et al.*, 2010; Ulrich *et al.*, 2011).

In summary, depending on the situation, the neuronal and vascular networks interact with each other to establish a neuro-vascular pattern. However, separable events have also been demonstrated. This knowledge can be exploited for therapeutic approaches.

3.3 The VEGF family – main effectors of vascular guidance

The family of VEGFs has a role in many physiological and pathophysiological processes. Hence, it is of great interest to discern the underlying signaling mechanisms for a future

translation into medicine. An overview of the VEGFs and their receptors is presented in figure 3-6.

3.3.1 The VEGF ligands

VEGFs are secreted glycosylated mitogens, which bind to their receptors as dimers. (Keck *et al.*, 1989; Leung *et al.*, 1989; Peretz *et al.*, 1992; Pötgens *et al.*, 1994; Ferrara, Gerber and LeCouter, 2003; Gabhann and Popel, 2008; Stutfeld and Ballmer-Hofer, 2009). The general structure is conserved between the various members: eight cysteine residues, of which two residues crosslink the monomers by disulfide bridges (Muller *et al.*, 1997). Distinct VEGF variants were identified. These variants are generated due to alternative splicing and proteolytic cleavage. Eventually, they exert different functions in the formation of blood and lymphatic vessels (Muller *et al.*, 1997; Robinson and Stringer, 2001; Lee *et al.*, 2005; Harper and Bates, 2008; Iyer, Darley and Acharya, 2010).

VEGF-A, also known in general as VEGF, was first described as a vascular permeability factor secreted by tumors, which benefitted vascular leakage (Senger *et al.*, 1983; Dvorak, 2006; Ferrara, 2009; Stutfeld and Ballmer-Hofer, 2009). Up to date, it is known about seven VEGF ligands. VEGF-A, VEGF-B, VEGF-C, VEGF-D and the placental growth factor (PlGF) are described in mammals (Roy, Bhardwaj and Ylä-Herttuala, 2006; Ferrara, 2009; Stutfeld and Ballmer-Hofer, 2009). Furthermore, two highly structurally related members, VEGF-E and VEGF-F, were identified. The former is expressed in orf viruses and the latter is present in snake venom (Takahashi and Shibuya, 2005; Roy, Bhardwaj and Ylä-Herttuala, 2006; Stutfeld and Ballmer-Hofer, 2009).

VEGFs bind mainly to VEGFRs, but interactions with other molecules and coreceptors such as heparan sulfate proteoglycans (PGs) and NRPs was evidenced, too (Cébe-Suarez, Zehnder-Fjällman and Ballmer-Hofer, 2006).

In the zebrafish more *veg*f isoforms are present due to genome duplication. *Vegfaa*, *vegfab*, *vegfa*, *vegfb*, *vegfb*, *vegfc*, *vegfd* and *plgf* were identified (Rossi *et al.*, 2016).

3.3.1.1 VEGF-A

VEGF-A is the main ligand of the VEGF family exerting biological function. This glycoprotein has a molecular weight of 46kDa (VEGF-A₁₆₅) and binds as a dimer to VEGFR-1 and VEGFR-2 (Ferrara and Henzel, 1989; Keck *et al.*, 1989; Leung *et al.*, 1989; Peretz *et al.*, 1992; Pötgens *et al.*, 1994; Gabhann and Popel, 2008; Harper and Bates, 2008).

The human VEGF-A gene is located on 6p21.3 and consists of eight exons separated by

seven introns (Houck *et al.*, 1991; Tischer *et al.*, 1991; Vincenti *et al.*, 1996). There exist at least nine subtypes of VEGF-A in the human. They are all splice variants of a single gene and are either freely diffusible or sequestered in the extracellular matrix (ECM) (Houck *et al.*, 1991). The predominant isoforms are VEGF₁₂₁, VEGF₁₆₅ and VEGF₁₈₉, but also VEGF₁₄₅, VEGF₁₄₈, VEGF₁₆₂, VEGF_{165b}, VEGF₁₈₃ and VEGF₁₈₉ exist (Bates *et al.*, 2002; Lange *et al.*, 2003).

Some VEGFs, i.e. of VEGF₁₆₅ and VEGF₁₈₉, have distinct binding capacity to heparin, thus, regulating their bioavailability. Interaction of these isoforms with heparan sulfate PGs in the ECM is thought to provide a pool of biologically active growth factor. Exposure to heparin and heparinases releases the active mitogens more rapidly, whereas proteolysis with subsequent plasminogen activation enables slow liberation from the ECM (Plouët *et al.*, 1997; Takahashi and Shibuya, 2005).

VEGF is expressed in ECs, somites and neurons among other tissues (Freeman *et al.*, 1995; Ferrara and Davis-Smyth, 1997; Melter *et al.*, 2000; Mukoyama *et al.*, 2002; Ruhrberg and Bautch, 2013; Tata, Ruhrberg and Fantin, 2015).

Cells response to low levels of oxygen by increasing VEGF levels. In addition to being a chemoattractant during blood vessel development, VEGF-A also stimulates EC proliferation and tube formation (Risau and Flamme, 1995; Conway, Collen and Carmeliet, 2001; Ruhrberg *et al.*, 2002; Gerhardt *et al.*, 2003; Olsson *et al.*, 2006). In mice and zebrafish, homozygous loss of VEGF-A results in embryonic lethality due to abnormal blood vessel development, emphasizing its indispensability (Carmeliet *et al.*, 1996; Ferrara and Davis-Smyth, 1997; Zhu *et al.*, 2017).

The zebrafish expresses two orthologs for VEGF-A, *vegfaa* and *vegfab*. *Vegfaa* is predominantly expressed in somites and neurons of the spinal cord and is the main isoform regulating the vascular functions known for VEGF-A in other vertebrate models (Rossi *et al.*, 2016; Wild *et al.*, 2017). There are two *vegfaa* isoforms identified in the zebrafish: *Vegfaa*₁₆₅ and *Vegfaa*₁₂₁ (Liang *et al.*, 2001). *Vegfab* seems to be dispensable (Rossi *et al.*, 2016).

3.3.2 The VEGF receptors

The family of VEGF receptors consists of three members: VEGFR-1, VEGFR-2 and VEGFR-3, encoded by FLT1, KDR and FLT4, respectively. This group belongs to the superfamily of type III receptor tyrosine kinases (RTK) (Shibuya *et al.*, 1990; Matthews *et al.*, 1991; Pajusola *et al.*, 1992; Ferrara, 2004; Cébe-Suarez, Zehnder-Fjällman and Ballmer-Hofer,

2006).

VEGFRs share seven extracellular immunoglobulin (Ig) domains and an intracellular split-kinase domain (Herbert and Stainier, 2011; Koch *et al.*, 2011). Upon ligand binding, the receptors form homo- or heterodimers, which leads to conformational changes. Eventually, the receptor-kinase activity is switched on by autophosphorylation of defined tyrosine residues (Olsson *et al.*, 2006).

VEGFR-1 mainly acts as a decoy receptor for VEGF-A, thereby reducing its bioavailability for VEGFR-2. Accordingly, VEGFR-1 functions as a negative regulator of angiogenesis. In addition to VEGF-A, VEGF-B and PlGF bind to this receptor (Hiratsuka *et al.*, 1998; Ferrara, Gerber and LeCouter, 2003; Chappell *et al.*, 2009; Iyer, Darley and Acharya, 2010; Koch *et al.*, 2011).

Many mechanisms and processes in vascular biology involve signaling through VEGFR-2. Cellular and biological functions with respect to survival and proliferation of ECs, vessel permeability and vasculogenesis and angiogenesis are regulated by this receptor. VEGF-A and processed forms of VEGF-C and VEGF-D are known ligands for VEGFR-2 (Ferrara, Gerber and LeCouter, 2003; C  be-Suarez, Zehnder-Fj  llman and Ballmer-Hofer, 2006; Stuttfeld and Ballmer-Hofer, 2009; Koch *et al.*, 2011).

Lymphangiogenesis and formation of early venous structures occurs through VEGFR-2 and VEGFR-3 signaling, induced by binding of VEGF-C and VEGF-D (Tammela *et al.*, 2008; Lohela *et al.*, 2009). First being expressed in all endothelia during development, VEGFR-3 becomes restricted to lymphatic endothelium in the adult, tumor microvasculature and wounds (Tammela *et al.*, 2008).

VEGF isoform, homo- and heterodimerization between the VEGFR family members, co-receptors or affinity to ECM molecules modulate signaling. Participation of PGs and NRPs in VEGFR signaling depend on the VEGF isoform. PGs and co-receptors vary duration and quality of the signaling and aid in formation of a gradient and stabilization of the signaling complex (Olsson *et al.*, 2006).

3.3.2.1 VEGFR-2 – a key player in vascular biology

VEGFR-2 is a highly significant actor in EC biology during development (Shalaby *et al.*, 1995; Carmeliet, 2003; Olsson *et al.*, 2006). Studies by Cort  s and colleagues revealed expression of KDR in the hematopoietic and EC lineage in the early human embryo (Cort  s *et al.*, 1999). Mice deficient for Flk1 (VEGFR-2) do not develop beyond early stages and differentiation towards hematopoietic or angiogenic lineage is disrupted (Shalaby *et al.*,

1995, 1997). These embryos fail in establishing blood islands and consequently blood vessels (Shalaby *et al.*, 1995).

VEGFR-2 activates various signaling pathways and modulation at several levels results in diverse cellular responses (Koch *et al.*, 2011; Koch and Claesson-Welsh, 2012). Biological responses can vary due to the ligand and its isoform, binding of co-receptors, homo- or heterodimerization (Olsson *et al.*, 2006). VEGF-A₁₆₅-mediated VEGFR-2 signaling activates a highly interwoven cascade resulting in proliferation, migration, survival and permeability (Koch and Claesson-Welsh, 2012). These responses ensure development, maintenance and integrity of the three-dimensional tubular structure of blood vessels.

The VEGFR-2 signal is transduced through ERK1/2, Akt or p38 MAPK.. Moreover, a VEGF-A isoform-specific cellular response was evidenced which depends on phosphorylation of distinct cytoplasmic tyrosines (Pan *et al.*, 2007; Kawamura *et al.*, 2008; Koch *et al.*, 2011; Fearnley *et al.*, 2014, 2015; Smith *et al.*, 2016).

In the zebrafish two VEGFR-2 homologs were identified: Kdr (Kdrb) and Kdr-like (Kdrl, Kdra). While the former is the mammalian KDR ortholog, the latter is an additional VEGF receptor not present in mammalian model organisms (Bussmann *et al.*, 2008). Kdrl is the functional equivalent for VEGFR-2 despite being non-orthologous to the mammalian KDR and is expressed in the entire vasculature (Bussmann *et al.*, 2008).

3.3.2.2 Function and role of VEGFR-1 in the development of the vascular system

VEGFR-1 is another significant player in vascular biology. Biallelic loss of VEGFR-1, also known as FLT1, in mice causes abnormal organization of the vascular labyrinth and is embryonically lethal (Fong *et al.*, 1995).

Binding affinity of VEGF-A for VEGFR-1 is about a 10-fold stronger when compared to VEGFR-2 (Park *et al.*, 1994; Hiratsuka *et al.*, 1998; He *et al.*, 1999). Its weak tyrosine kinase activity proposed a scavenger function for VEGF-A (Waltenberger *et al.*, 1994). The transmembrane domains however, recruits VEGF to the membrane. Consequently, VEGF availability for VEGFR-2 is regulated (Hiratsuka *et al.*, 1998, 2005). Accordingly, VEGF-A/VEGFR-2 signaling can be varied by adjusting levels of either VEGFR-1 or its ligands VEGF-B and PIGF.

Next, to its function as a VEGF-A sink, VEGFR-1 could transduce signals upon binding of VEGF-B or PIGF. VEGF-B is mainly active in the heart and skeletal muscle and improves metabolic health, for example insulin resistance in patients with Diabetes mellitus type 2, contributes to cardioprotective mechanisms and counteracts ischemic processes (Olofsson

et al., 1996; Hagberg *et al.*, 2010; Carmeliet, Wong and De Bock, 2012; Kivelä *et al.*, 2014; Rafii and Carmeliet, 2016). Moreover, this ligand was suggested as a survival factor rather than being an player in angiogenesis (Zhang *et al.*, 2009). PlGF is expressed on various cell types (Carmeliet *et al.*, 2001; Fischer *et al.*, 2008). Its loss of insignificant in healthy individuals but becomes relevant in pathological conditions where it is for example involved in angiogenic and inflammatory processes in cancer (Fischer *et al.*, 2008).

Next to the membrane-anchored VEGFR-1 also a soluble form exists. The freely diffusible receptor only carries the extracellular domain of the receptor (Shibuya *et al.*, 1990; Matthews *et al.*, 1991; Terman *et al.*, 1992; Kendall and Thomas, 1993).

In the zebrafish, VEGFR-1 is known as Flt1. Isoforms, function and ligands are analogous to its mammalian counterparts (Hiratsuka *et al.*, 1998; Ferrara, Gerber and LeCouter, 2003; Chappell *et al.*, 2009; Iyer, Darley and Acharya, 2010; Koch *et al.*, 2011; Krueger *et al.*, 2011). *Flt1* reporter lines revealed specific expression in arterial ECs and in a subset of neurons (Bussmann *et al.*, 2010; Krueger *et al.*, 2011; Wild *et al.*, 2017). Loss-of-function (LOF) models prematurely developed hypersprouting at the neuro-vascular interface already at 3 dpf. These ectopic sprouts originate exclusively from vISVs. It is hypothesized that Vegfaa bioavailability for Kdr1 was varied by either missing *flt1* function or stronger neuronal *vegfaa* expression in the spinal cord and thus regulating its vascularization (Wild *et al.*, 2017). Otherwise, the vascular patterning was unaltered. Furthermore enhanced proliferation and increased diameter of ISVs in *flt1* zebrafish mutants was reported (Wild, 2016; Klems, 2017; Wild *et al.*, 2017).

3.3.3 Clinical suitability of VEGFR-2, VEGFR-1 and VEGF-A

Due to their nature, VEGFRs and their ligands are promising candidates for a variety of therapies concerning blood vessels and the nervous system (Shibuya, 2014; Dumpich and Theiss, 2015). Depending on the condition, reinforcement or attenuation of blood vessel growth is attempted. Regeneration of organs upon severe injuries is assisted by VEGF-A, while its inhibition can be deployed for therapies treating cancer or age-related macular degeneration (Harding, 2011; Matsumoto and Ema, 2014). Due to great functional plasticity in vasculature, therapies are prone to side effects (Roodhart *et al.*, 2008). Thus, the treatments value, safety and efficacy have to be pondered against risks.

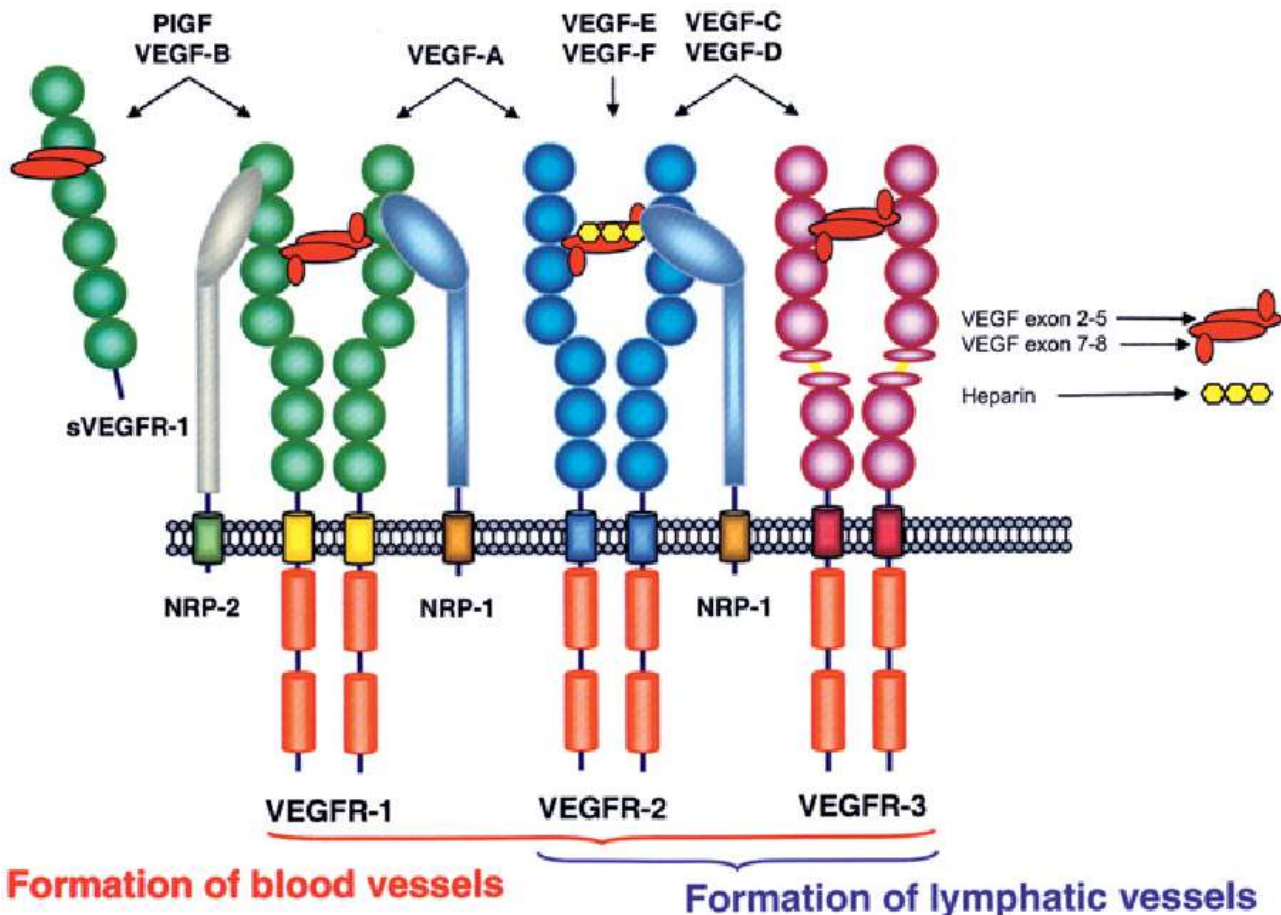


Figure 3-6. VEGFs and their receptors. Six VEGF ligands exist. They bind to one or more of the three members of the VEGFR family. VEGF-B and PIGF exclusively bind to VEGFR-1, while VEGF-A interacts with VEGFR-1 and VEGFR-2. VEGFR-1 can either be membrane-bound or freely diffusible (sVEGFR-1). VEGF-C and VEGF-D signal through VEGFR-2 or VEGFR-3 while VEGF-E and VEGF-F bind to VEGFR-2. The VEGF/VEGFR signaling pathway can be modulated by Neuropilin coreceptors (NRP-1 and NRP-2). Ligand binding to VEGFR-1 and VEGFR-2 regulates vasculogenesis and angiogenesis, whereas VEGFR-3 is mainly involved in lymphangiogenesis. VEGF, Vascular endothelial growth factor; NRP, Neuropilin; PIGF, Placental growth factor. Taken from: Cébe-Suarez, Zehnder-Fjällman and Ballmer-Hofer, 2006.

3.4 Endothelial cell-specific molecule 1

3.4.1 Proteoglycans are important modulators of cellular responses

PGs are significant participants in a variety of cellular processes, for example cell proliferation, adhesion and migration. They are relevant in pathological conditions, such as inflammation, cancer or infection (Perrimon and Bernfield, 2000; Spillmann, 2001; Delehede *et al.*, 2002; Sasisekharan *et al.*, 2002; Sarrazin, Lamanna and Esko, 2011).

PGs are composed of a core protein bearing polysaccharide chains of glycosaminoglycans (GAGs) and are anchored to the cell surface, bound to components of

the ECM or circulating in the blood (Trowbridge and Gallo, 2002; Delehedde *et al.*, 2013). PGs interact with other molecules with either the protein core or their GAG. Interaction partners include soluble signaling effectors, for example growth factors, cytokines and chemokines and structural components of the ECM, such as Fibronectin and collagens as well as membrane-associated proteins, e.g. receptors, integrins (Iozzo, 1998; Gallagher, John T. and Lyon, 2000; Whitelock, Melrose and Iozzo, 2008; Lortat-Jacob, 2009; Myhre and Blobel, 2009; Kim, Turnbull and Guimond, 2011).

Biological functions of PGs are determined by interactions of their glycosaminoglycan (GAG) chains with protein ligands, such as cytokines and growth factors (Trowbridge and Gallo, 2002; Bishop, Schuksz and Esko, 2007). GAGs have repeating disaccharide units of an amino sugar, forming a linear polysaccharide chain, in common. Despite slight variations in the basic sugar backbone, individual GAG chains can be distinguished by subsequent modifications, for example sulfation of dermatan sulfate PGs, which also determines their activity (Taylor and Gallo, 2006).

Heparin, heparan sulfate and dermatan sulfate are GAGs able to modify biological responses. They regulate enzyme activity and may have a role as signaling molecules upon wounding, infection or during tumorigenesis. Bacteria, viral and parasitic virulence factors bind GAGs for attachment, invasion and immune system evasion. GAGs are essential for growth factors, cytokines, and chemokines acting as stabilizers, cofactors, and/or coreceptors (Rostand and Esko, 1997; Schmidtchen, Frick and Björck, 2001; Trowbridge and Gallo, 2002).

3.4.2 Endocan – a distinctive proteoglycan

Endocan is a dermatan sulfate PG secreted by ECs and renal epithelia, especially under inflammatory conditions (Bécharde *et al.*, 2000; Rocha *et al.*, 2014). It is a soluble molecule of 50 kDa circulating in the blood and takes part in a variety of biological processes related to cell adhesion, migration, proliferation and neovascularization (Sarrazin *et al.*, 2006; Kali and Rathan Shetty, 2014).

ESM1, the gene product, encodes for the core protein of Endocan. Subsequent posttranslational modifications with a dermatan sulfate GAG let it be classified as a PG, thus called Endocan (Bécharde *et al.*, 2001). Both components, the protein core and the GAG seem to interact with ECM components, membrane proteins, intracellular molecules and soluble mediators, thus modulating cell differentiation, migration and adhesion (Sarrazin *et al.*, 2010; Delehedde *et al.*, 2013).

Endocan is a distinctive PG: it is one of the few circulating PGs, has a small molecular weight and only one single polysaccharide chain (Sarrazin *et al.*, 2010). The dermatan sulfate chain is covalently linked to Serine₁₃₇ and is negatively charged at physiological pH (Sarrazin *et al.*, 2006; Zhang, 2010).

ESM1 is proposed as a tip cell marker (Abid *et al.*, 2006; Shin, Huggenberger and Detmar, 2008; Rocha *et al.*, 2014; Eilken *et al.*, 2017). More recent studies suggested reported an increased abundance in this cell phenotype, but its expression seems not to be exclusively restricted to those (del Toro *et al.*, 2010; Geudens and Gerhardt, 2011; Rocha *et al.*, 2014).

3.4.3 Endocan and its role in pathological conditions

Endocan is increasingly abundant in cancer, sepsis or obesity and might be essential in inflammation, healing, and tumorigenesis (Lassalle *et al.*, 1996; Scherpereel *et al.*, 2003, 2006; Filep, 2006; Grigoriu *et al.*, 2006; Janke *et al.*, 2006; Sarrazin *et al.*, 2006, 2010; Stéphane *et al.*, 2010; Delehedde *et al.*, 2013).

Endocan levels influence all-cause mortality and events in cardiovascular diseases by modulating the pathogenesis of vascular disorders, inflammation and endothelial dysfunction (Yilmaz *et al.*, 2014). Examples are conditions like hypertension, diabetes mellitus, chronic kidney disease and atherosclerosis (Menon, Kocher and Aird, 2011; Balta *et al.*, 2014; Yilmaz *et al.*, 2014; Arman *et al.*, 2015).

The presence of Endocan in the circulation could provide information about pathological angiogenesis (Sarrazin *et al.*, 2006). *ESM1* is mainly expressed in tip cells during tumor angiogenesis and gene activity seems to be even correlated with invasiveness (Roudnicky *et al.*, 2013). It acts as a proliferation and survival factor in tumor cells (Scherpereel *et al.*, 2003).

In summary, Endocan was suggested as a diagnostic and prognosis marker for disease progression because it is linked to the severity of disorders and outcome of the respective condition (Bechard *et al.*, 2000; Scherpereel *et al.*, 2006; Huang, Tao and Ding, 2009; Hatfield *et al.*, 2011; Balta *et al.*, 2013, 2014; Roudnicky *et al.*, 2013; Kali and Rathan Shetty, 2014). Thus, underlining its importance in pathophysiological events.

3.4.4 VEGF-A signaling and ESM1 expression are linked to each other

Both, VEGF-A and ESM1 are major players during angiogenesis. Accordingly, a link between these two molecules is feasible.

Studies with cell culture reported a dispensability of ESM1 alone but it seems to augment the effects of VEGF-A or VEGF-C (Shin, Huggenberger and Detmar, 2008). Additionally, ESM1 was identified as a downstream target in the VEGF-A/VEGFR-2 signaling cascade, the major signaling pathway for angiogenic processes (Conway, Collen and Carmeliet, 2001; Carmeliet, 2003; Shin, Huggenberger and Detmar, 2008; Rocha *et al.*, 2014; Eilken *et al.*, 2017).

Depending on the isoform, a VEGF-A gradient can be formed, thus shaping the vascular network (Park, Keller and Ferrara, 1993; Rocha *et al.*, 2014). Moreover, the amount of VEGF-A binding to the receptor can be modulated by distinct binding affinities to heparin or proteases (Houck *et al.*, 1992; Ferrara, 2010).

In the *flt1* LOF zebrafish model, *esm1* was upregulated at 4 dpf, at a time point, when spinal vascularization is ongoing. Tertiary sprout formation is not exclusive for *flt1* mutants, but are present in other zebrafish *Vegfaa* GOF models, e.g. von Hippel-Lindau (*vhl*) mutants as well (Wild *et al.*, 2017). It was proposed that in *Vegfaa* GOF scenarios, more *Vegfaa* is available for Kdr1. Consequently, a highly active *Vegfaa*/Kdr1 signaling results in increased angiogenesis visible as ectopic sprouts and *esm1* expression is amplified (Wild *et al.*, 2017). In homozygous *vhl* mutants, *vegfaa*, *flt1*, *kdrl* and *Fibronectin* are intensively expressed (Bluysen *et al.*, 2004; van Rooijen *et al.*, 2011).

3.5 Aim of the work

The present study was aimed to determine the role of *Esm1* in sprouting angiogenesis. *Esm1* was found to be upregulated in *Flt1* deficient fish. Loss of *flt1* caused premature tertiary sprouting from vISV, proliferation of ECs in the ISVs and increased diameter of vISV (Wild, 2016; Klems, 2017). This phenotype was explained with increased *Vegfaa* bioavailability for Kdr1 (Wild, 2016).

First, the spatial and temporal promoter activity and gene expression of the *esm1* during early zebrafish development was determined. Promoter activity was assessed using BAC transgenesis. Gene expression was studied *via* real-time PCR and whole mount *in situ* analysis.

Second, ectopic sprout formation in two *Vegfaa* GOF models, *flt1* and *vhl* mutants, was investigated in dependency of *esm1*. The role of *esm1* and a possible relationship with *Flt1*

in the development of tertiary sprouts was assessed with knockdown and overexpression experiments.

Third, an *esm1* LOF zebrafish model was established. The entire coding sequence was deleted using the CRISPR/Cas9 system. With this model, the effects of *esm1* on the zebrafish trunk vasculature in both wildtype and *flt1* mutants was elucidated.

4 Results

4.1 *Esm1* is expressed during early zebrafish development and levels are increased upon loss of *flt1*.

Previous studies revealed elevated *esm1* levels in *flt1* deficient zebrafish at 4 dpf (Wild et al. 2017). At this stage, hypersprouting at the level of the spinal cord is already well established but still forming. Real-time qPCR analysis should reveal if *esm1* gene expression is augmented as early as ectopic sprout formation begins at 3 dpf in *flt1* mutants and if this observation could be transferred to another Vegfaa GOF model, the *vh1* mutant.

Three clutches with 30-50 embryos from crossings of wildtype (reference), homozygous *flt1*^{ka605} and heterozygous *vh1*^{hu2117/+} adult fish were quantitatively analyzed for *esm1* gene expression at 3 dpf and 4 dpf *via* real-time qPCR. Details about the sampling, qPCR process and data processing are described in section 6.2.3.4.

Esm1 gene expression was significantly increased in *flt1*^{ka605} mutants at both time points examined, while in the pool of *vh1*^{hu2117} mutants with siblings enhanced levels were obtained at only 4 dpf. The results are depicted in figure 4-1. Thus, *esm1* mRNA was present in higher abundance in both Vegfaa GOF models during stages of tertiary sprout formation.

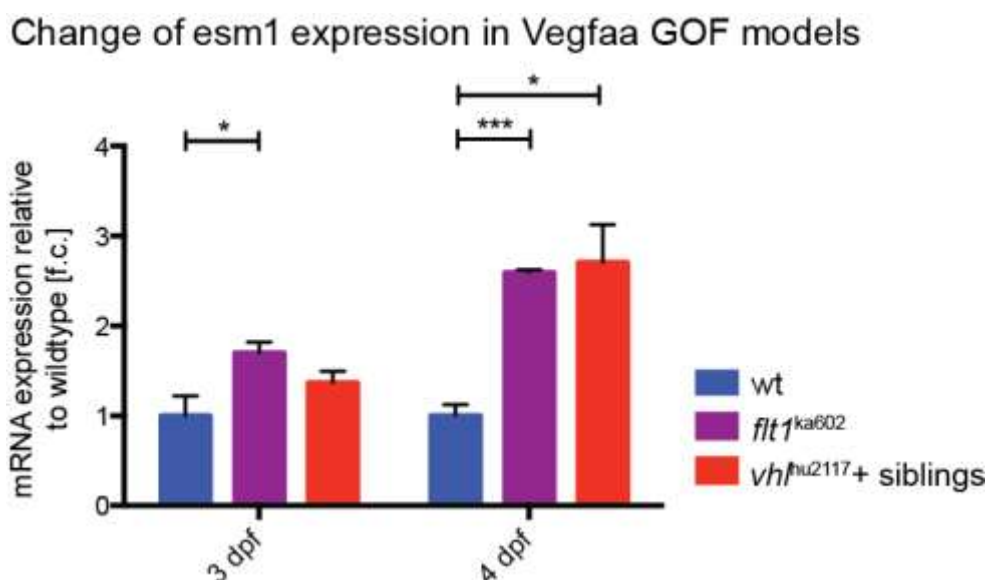


Figure 4-1. *Esm1* expression is enhanced in Vegfaa GOF models. *Esm1* gene expression was analyzed in the wildtype and in Vegfaa GOF models at 3 dpf and 4 dpf using real-time qPCR. Samples were taken from wildtypes, *flt1*^{ka605} mutants and *vh1*^{hu2117} mutants with siblings. dpf, days post fertilization; f.c., fold change; wt, wildtype.

4.2 *Esm1* mRNA is expressed in developing and developed ISVs

Esm1 gene expression was altered upon inactivation of *flt1*, but the identity of expressing cells still remained elusive. Analysis of expression domains with whole mount *in situ* hybridization (WISH) provided insight into this issue.

An *esm1* anti-sense RNA probe complementary bound the sequence from the translation start codon until the translation stop codon in the mRNA. The sense probe served as control. The *esm1* gene and the anti-sense probe target site are illustrated in figure 4-2.

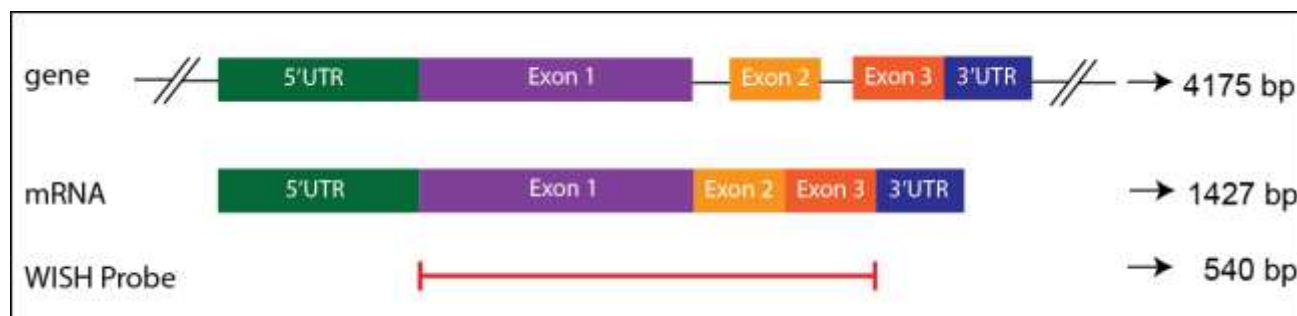


Figure 4-2. Target site of the *esm1* whole mount *in situ* probe. Illustration of where the RNA WISH probe binds complementary to the *esm1* mRNA. The designed probe covers the entire coding sequence. bp, base pairs.

The WISH with the anti-sense probe for the wildtype is presented in figure 4-3d-f and j-l. The red rectangles mark the area magnified in d'-f' and j'-l'. The DA (orange arrowhead in 4-3d') expressed *esm1* at 24 hpf. ISVs in the primary sprouting process (Fig. 4-3d' and e') and when already developed (Fig. 4-3f' and j') were stained from 24 hpf to 56 hpf (red arrowheads). *Esm1* mRNA harboring cells were visible during anastomosis of neighboring ISVs. At stages older than 56 hpf no specific *esm1* expression could be determined (Fig. 4-3k' and l'). A diffuse staining was also observed in embryos treated with the sense probe and should therefore be considered as unspecific background (Fig. 4-3a-c and g-i).

Taken together, *esm1* was specifically expressed during formation of the trunk vascular network, in particular during sprouting of distinct vessels: 24 hpf in the dorsal aorta and from 24 to 72 hpf in ISVs, with a peak from 36 hpf to 48 hpf.

Spatial expression of *esm1* upon loss of *flt1* is presented in figure 4-4. The areas magnified (Fig. 4-4a-f') are indicated in the original picture (Fig. 4-4a-f). At 24 hpf *esm1* mRNA in the DA (orange arrowhead in Fig. 4-4a') was visible. Staining in the ISV during growth of the sprout (Fig. 4-4a' and b') and when already developed (Fig. 4-4c and d') was present from 24 hpf to 56 hpf (red arrowheads). *Esm1* expression at 72 hpf and 96 hpf was not recognized (Fig. 4-4e' and f'). The results indicate a commensurable *esm1* gene expression profile in *flt1* mutants with that in the wildtype.

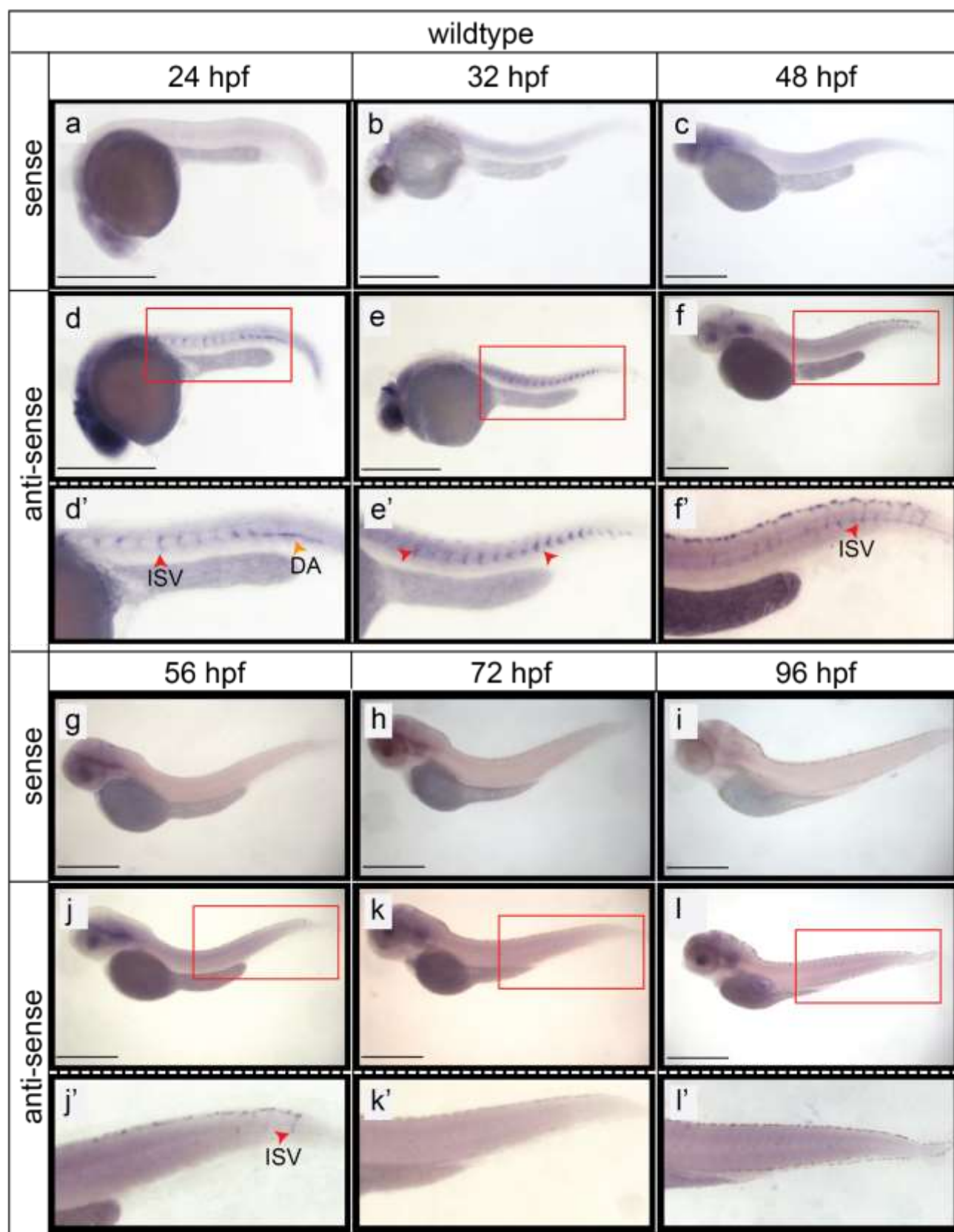


Figure 4-3. Spatial location of *esm1* mRNA in the wildtype. Gene expression was determined using WISH from 24 hpf to 96 hpf. a-c and g-i depict the sense probe. The anti-sense probe is shown in d-f and j-l in which red rectangles indicate the area shown magnified in d'-f' and j'-l'. In early development, the DA was still visible and positively stained (d'; orange arrowhead). *Esm1* mRNA was present developing ISVs (d' and e') and already grown ISVs (f' and j') as indicated by red arrowheads. DA, dorsal aorta; hpf, hours post fertilization; ISV,

intersegmental vessels. Scale bar 1000 μm .

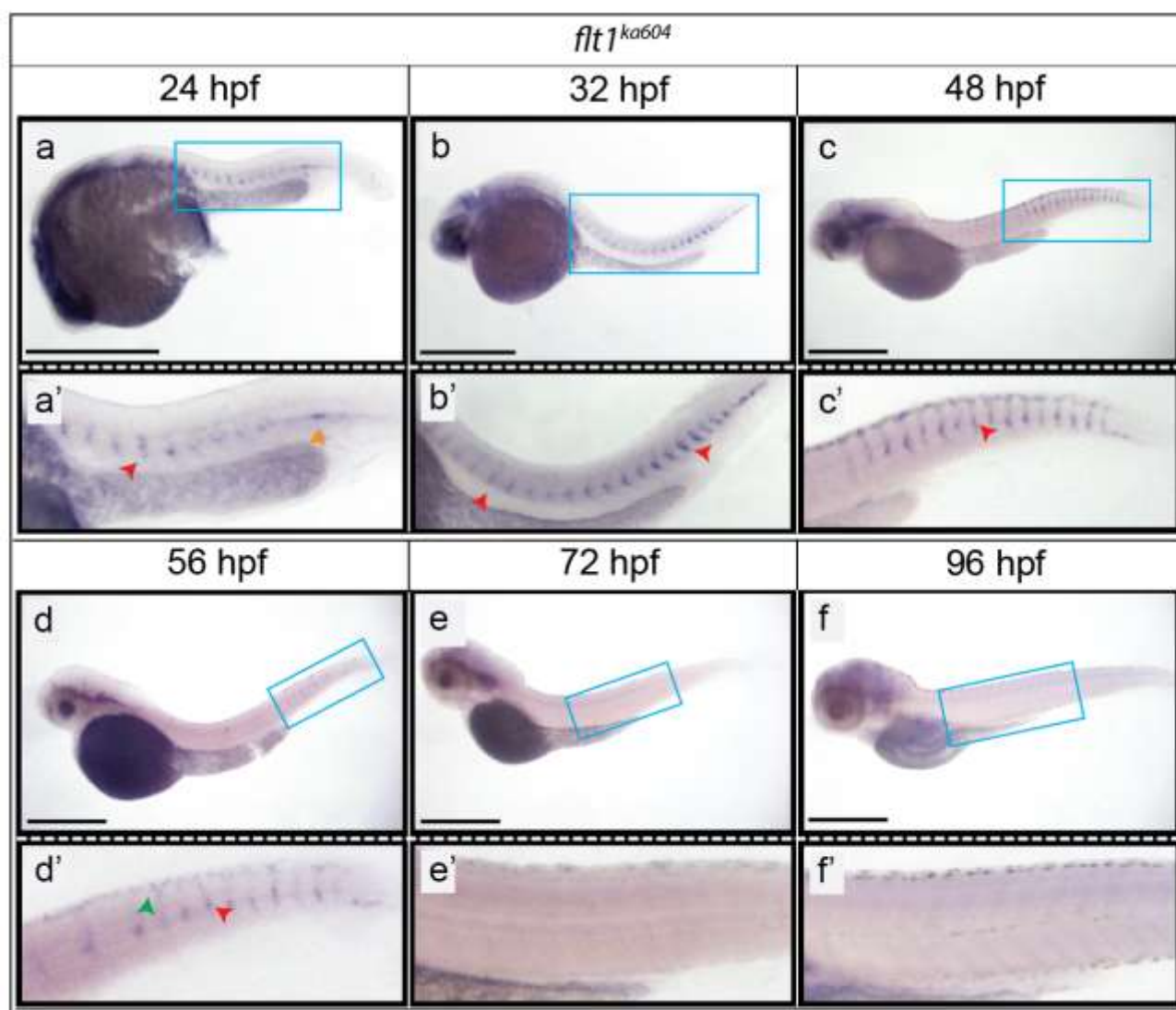


Figure 4-4. Spatial expression of *esm1* mRNA in *flt1* mutants. *Esm1* gene expression in the *flt1^{ka604}* line was ascertained with the anti-sense RNA WISH probe from 24 hpf to 96 hpf with whole mount *in situ* hybridization. Blue rectangles in a-f mark the area depicted magnified in a'-f'. Expression was first seen in the DA (a', orange arrowhead) and then retracts into the developing sprout (a', red arrowhead). With the onset of sprouting, staining was observed in the developing ISVs (a'-d', red arrowheads) and already grown ISVs (c' and d', red arrowhead). hpf, hours post fertilization; ISV, intersegmental vessels. Scale bar 1000 μm .

Thus, independent of *flt1* functionality, the increase of *esm1* levels at 2 dpf as observed by qPCR could not be related to mRNA presence in growing number expression domains, suggesting that either *esm1* expressing cells are cumulated in the positive domains or that individual cells had enriched amount of *esm1*. The absence of signal at 3 dpf and 4 dpf in the WISH although present in qPCR, could be explained by the low sensitivity of this method at these stages.

4.3 *Esm1* promoter activity in the vasculature and cells of the spinal cord

In order to gain a higher resolution and sensitivity for *esm1* expression, another approach next to mRNA visualization *via* WISH was adapted for assessing spatio-temporal activity. *Esm1* promoter activity was investigated to affirm expression to distinctive structures and following it *in vivo*.

A BAC containing a 167kb zebrafish genomic fragment including the *esm1* gene was altered into a promoter reporter construct as described by Bussmann and colleague (Bussmann and Schulte-Merker 2011). The *esm1* gene is encompassed between segments (46 kb upstream and 116 kb downstream). During BAC recombineering, a reporter gene expression cassette (*mCitrine*) was inserted in place of the *esm1* start codon, thereby disabling the *esm1* gene. Furthermore, *tol2* sites were cloned into the BAC for stable integration of the reporter construct into the genome. Consequently, the *tol2* sequences flank the entire genomic fragment in BAC. The generation of BAC reporter construct is described in 6.2.5 and illustrated in figure 6-1. In the promoter activity experiments the construct pTarBAC_Tol2_-46kbEsm1_mCitrine was injected and transgenic embryos referred to as TgBAC(*esm1*:mCitrine). Accordingly, the analyzed embryos were mosaic for the BAC reporter construct.

4.3.1 The *esm1* promoter is active in the endothelium of various regions

Esm1 promoter activity in the vascular network in the wildtype was determined. The signals seen in various regions of embryos are depicted in figure 4-5. pTarBAC_Tol2_-46kbEsm1_mCitrine, the *esm1* BAC reporter construct, was injected into Tg(*kdr*:hsa.HRAS-mCherry)^{s916} wildtype fish. *Esm1* promoter activity was observed in vessels of the brain between 25 hpf and 74 hpf, as indicated by white arrowheads in figure 4-5a. Furthermore, the *esm1* promoter was active in vessels circumferencing the eye at 74 hpf (Fig. 4-5a, yellow arrowhead). Expression of the reporter gene was seen in the heart (white arrowheads) and its outflow tract (yellow arrowhead) from the third to the fourth day of development, shown in figure 4-5b. Signal was visible in the trunk vasculature (entire ISV, DLAV as indicated by white arrowheads) as depicted in figure 4-5c. In addition, an expression domain in the NT at 3 dpf and 4 dpf was observed, suggesting that *esm1* could be expressed by a subset of neurons (yellow arrowhead in figure 4-5c). At 74 hpf and 98 hpf, the reporter gene was expressed in the subintestinal vasculature supplying the intestinal tract (Fig. 4-5d, white arrowheads). These results imply that vessels are a prominent source for *esm1*.

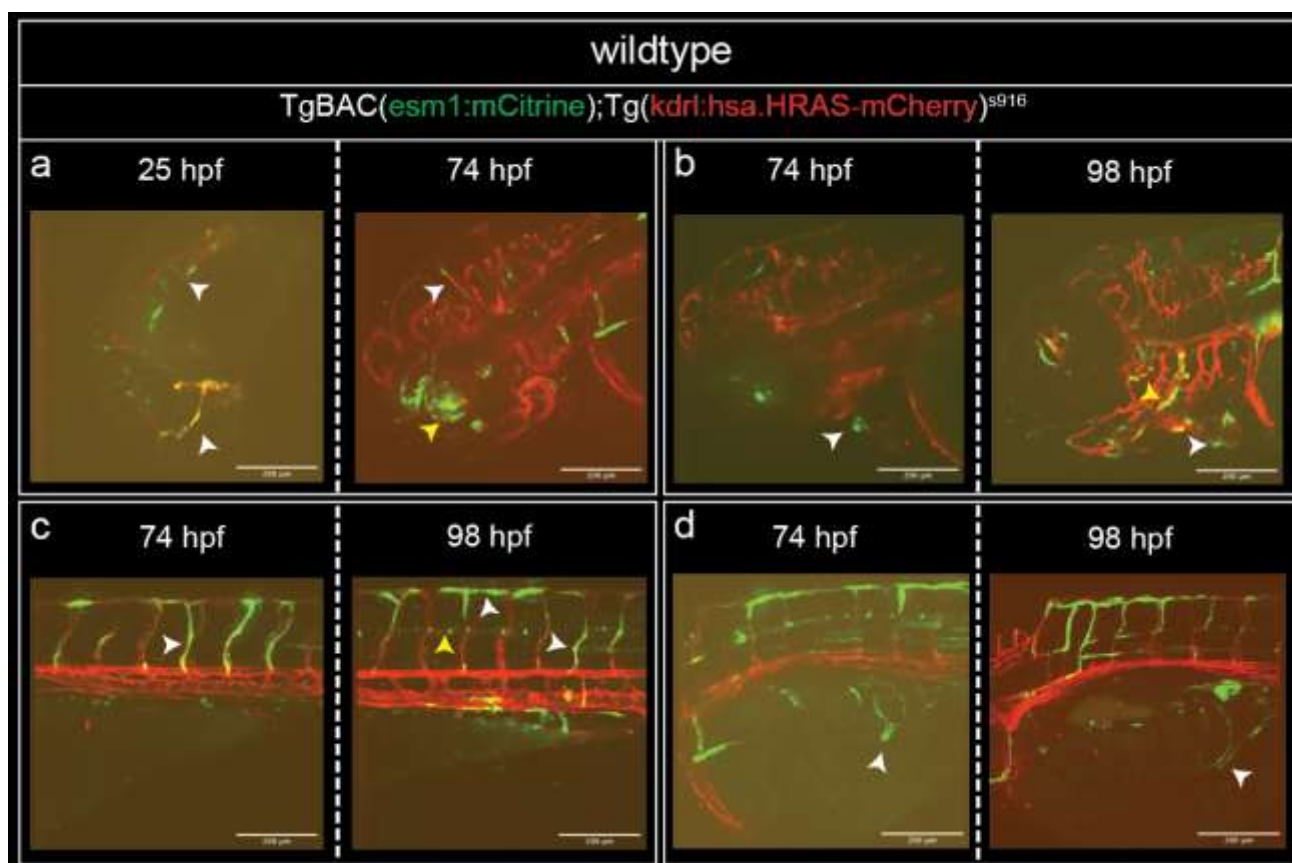


Figure 4-5. *Esm1* promoter activity in the heart and blood vessels. *Esm1* promoter activity (mosaic expression of the pTarBAC_Tol2_-46kb*Esm1*_mCitrine) in the wildtype was observed in the vasculature of the eye and brain from 25 hpf to 74 hpf (a), the heart and its outflow tract (b) as well as vessels of the trunk (c) and intestine (d) from 74 hpf to 98 hpf (white arrowheads). Cells at the level of the spinal cord were also positive for signal (c; yellow arrowhead). The wildtype was in the vascular reporter background Tg(*kdrl:hsa.HRAS-mCherry*)^{S916}. Scale bar 200 μ m.

4.3.2 Active *esm1* promoter in developing and developed trunk vasculature

Esm1 promoter activity was determined in the wildtype from 24 hpf to 96 hpf as shown in figure 4-6. The pTarBAC_Tol2_-46kb*Esm1*_mCitrine plasmid was injected in the one-cell stage into lines transgenic for neuronal Tg(*xla.tubb:DsRed*)^{zf148} or vascular Tg(*kdrl:hsa.HRAS-mCherry*)^{S916}. Fluorescent signal of the reporter construct was observed in the primary aISV sprout (blue arrowheads, Fig. 4-6a and b) and the entire developed ISV (blue arrowheads Fig. 4-6c-e) and remained present in the DLAV (yellow arrowheads in Fig.4-6 b' and c-e). Furthermore, activity of the *esm1* promoter in the DA was visible (Fig. 4-6a and e, white arrowhead).

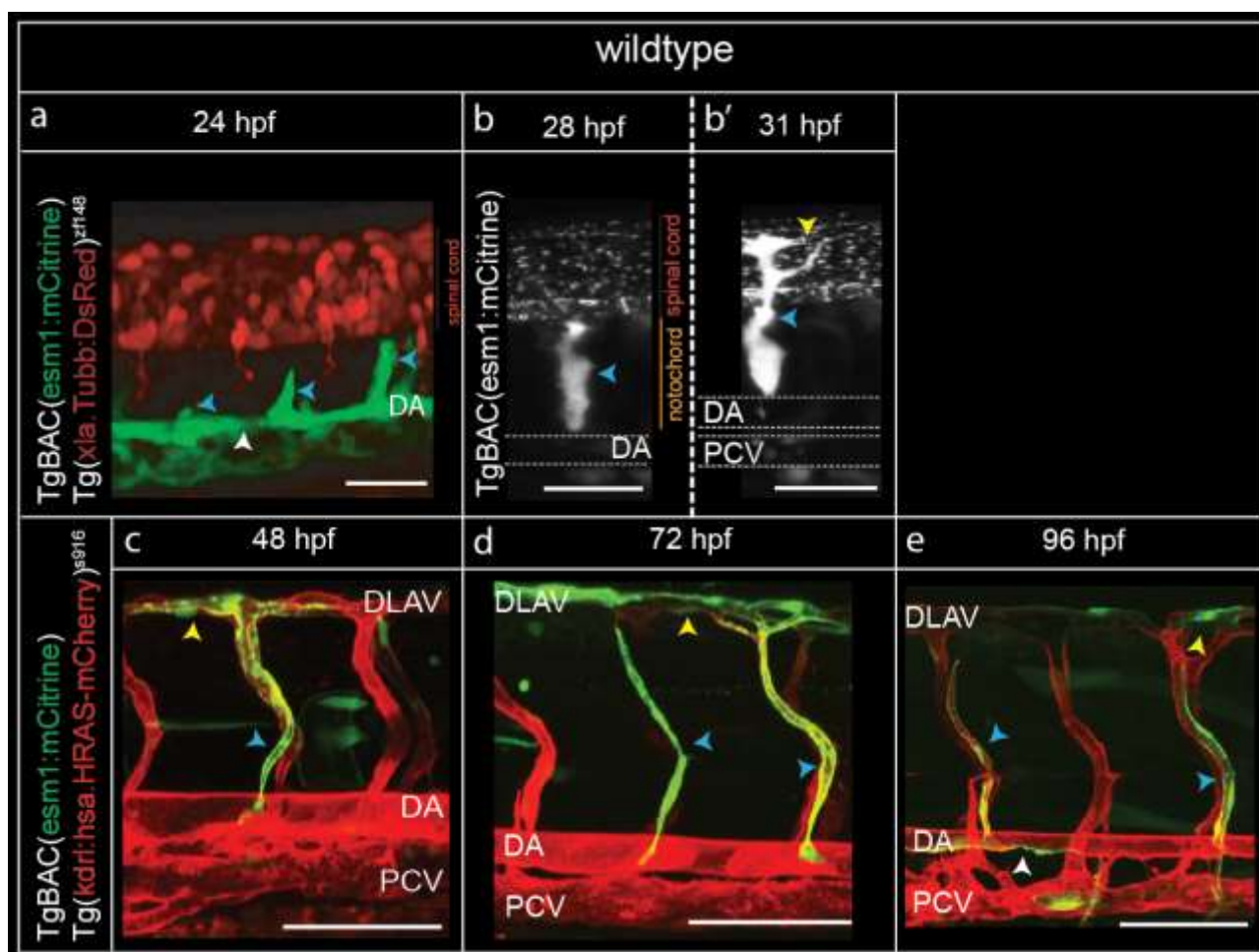


Figure 4-6. *Esm1* promoter activity during development of the trunk vasculature in wildtype. pTarBAC_Tol2_-46kbEsm1_mCitrine was injected into the one-cell stage in wildtype transgenic for the neuronal Tg(*xla.tubb:DsRed*)^{z148} or vascular Tg(*kdrl:hsa.HRAS-mCherry*)^{s916} marker. *Esm1* reporter gene expression was studied from 24 hpf to 96 hpf. The *esm1* promoter was active in the entire growing arterial sprout (blue arrowheads in a and b), in the DA (white arrowhead in a and e), the entire ISV (blue arrowheads in b' and c-e) and DLAV (yellow arrowhead in b' and c-e). DA, dorsal aorta; DLAV, dorsal lateral anastomotic vessels; hpf, hours post fertilization; ISV, intersegmental vessel. Scale bar in a, c-e 100 μ m and in b 50 μ m.

4.3.3 *Esm1* promoter activity in *flt1* mutants is comparable to that in the wildtype and is present in the spinal cord vasculature

Esm1 promoter activity was investigated in the trunk vasculature of *flt1* mutants between 1 dpf to 5 dpf (Fig. 4-7). Mosaic expression of the pTarBAC_Tol2_-46kbEsm1_mCitrine construct in the vascular reporter lines Tg(*kdrl:hsa.HRAS-mCherry*)^{s916} or Tg(*flt1a:nGFP*)^{y7} revealed *esm1* promoter activity in the emerging ISV sprout (Fig. 4-7a white arrowhead), in the developed ISV (Fig. 4-7b and c, blue arrowheads) and DLAV (Fig. 4-7b and c, yellow arrowheads).

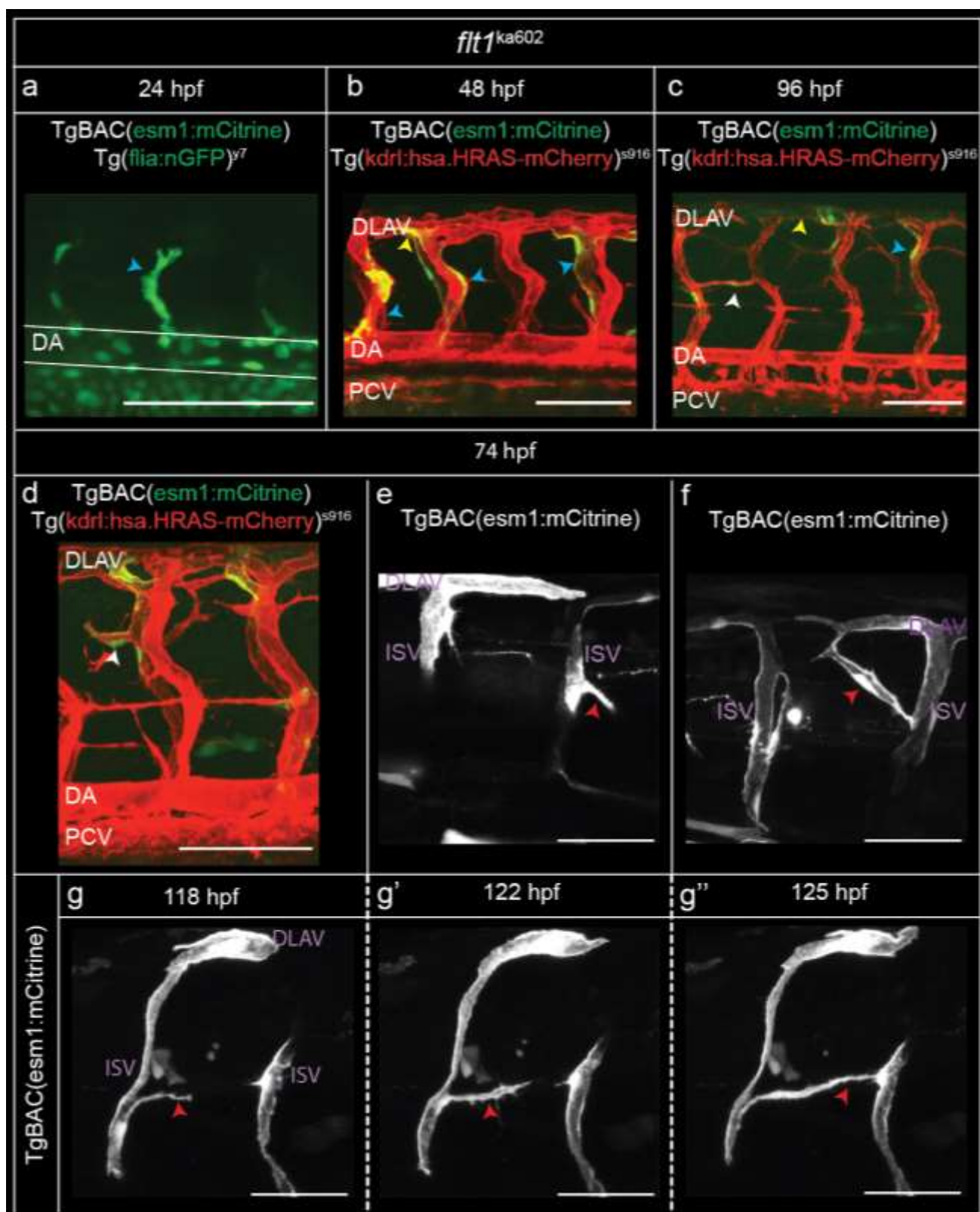


Figure 4-7. The *esm1* promoter is active in *flt1* mutants. pTarBAC_Tol2_-46kbEsm1_mCitrine was injected into the one-cell stage in *flt1* mutant transgenic for the vascular markers (Tg(*kdr*:*hsa*.HRAS-mCherry)^{s916} or Tg(*flia*:nGFP)^{y7}). Embryos were analyzed for transgenesis in the trunk vascular network until 125 hpf. *Esm1* expression in developing and developed ISVs (a-c; blue arrowheads) and DLAV (b and c; yellow arrowheads) was seen. In addition, spinal cord vessels emerging from an ISV (white arrowhead in d; violet arrowheads in e and g) or already connected to a neighboring ISV (white arrowhead in c; violet arrowhead in g'') showed BAC reporter expression. DA, dorsal

aorta; DLAV, dorsal lateral anastomotic vessels; hpf, hours post fertilization; ISV, intersegmental vessel. Scale bar 100 μ m.

Upon loss of *flt1*, zebrafish form ectopic blood vessels originating from vISV at the neuro-vascular interface in the zebrafish trunk in the process of tertiary sprouting. Moreover, *esm1* is upregulated in *flt1* mutants. This knowledge indicates a potential role of *esm1* in tip cells (Wild et al. 2017). *Esm1* promoter activity was observed in the forming (Fig. 4-7 arrowheads in d, e and g) and formed tertiary sprout (Fig. 4-7, white arrowhead in c, red arrowheads in f and g). Accordingly, in addition to ISVs, *esm1* was present in ectopic sprouts in *flt1* deficient zebrafish embryos.

4.3.4 The *esm1* promoter is preferentially active in arterial endothelial cells

As previously shown, the trunk vasculature expressed *esm1*. However, the identity of the respective vessels remained in question. *Esm1* promoter activity in the trunk vasculature of pTarBAC_Tol2_-46kbEsm1_mCitrine injected fish was analyzed in wildtype fish transgenic for the vascular marker Tg(*kdr1:hsa.HRAS-mCherry*)^{s916}. The *esm1* expression pattern was compared to that in lines visualizing arterial, venous or lymphatic endothelium. The results are presented in figure 4-8.

Identity of *esm1* BAC transgenic ISVs was determined at 4 dpf. Mosaic *esm1* BAC expression was seen over the entire aISV, from the DA and reaching into the DLAV (Fig. 4-8a and b, blue arrowheads). *Esm1* promoter activity in vISVs was mainly restricted to the dorsal part (Fig. 4-8a, brown arrowheads), if construct expression was present at all (Fig. 4-8b). Similar observation was made with the main vessels DA and PCV, in which reporter expression was seen mostly in the DA (Fig 4-8b, brown arrowhead) and very seldom in the PCV (Fig. 4-8b, white arrowhead) and connecting vessels (Fig. 4-8b, orange arrowhead). Quantification strengthened this observation when the numbers of aISVs or vISVs with *esm1* promoter activity were divided to sum of both (Fig. 4-8c). Similar observation was made when same measurements were performed for DA and PCV (Fig. 4-8c). Accordingly, *esm1* is preferentially expressed in vessels of arterial identity.

Due to the low occurrence of *esm1* promoter activity in venous vessels, it was compared with the distribution of ECs of either arterial or venous identity in ISVs (Fig 4-8d). Zebrafish embryos transgenic for both the arterial marker *flt1* and venous marker *flt4* showed *flt1* expression in aISVs over the entire length and in the DLAV at 4 dpf. vISVs were not always composed entirely of vECs because in some were still ECs of arterial identity in the dorsal part of the concerning vessel present (white arrowhead, Fig. 4-8d). These results suggest,

that *esm1* is supposedly expressed in ECs of arterial identity.

Comparison of the BAC reporter gene expression in the PCV and connecting vessels with the lymphatic vessel marker *lyve1b* indicated *esm1* promoter activity more likely in lymphatic ECs than cells of exclusively venous identity (Fig. 4-8e).

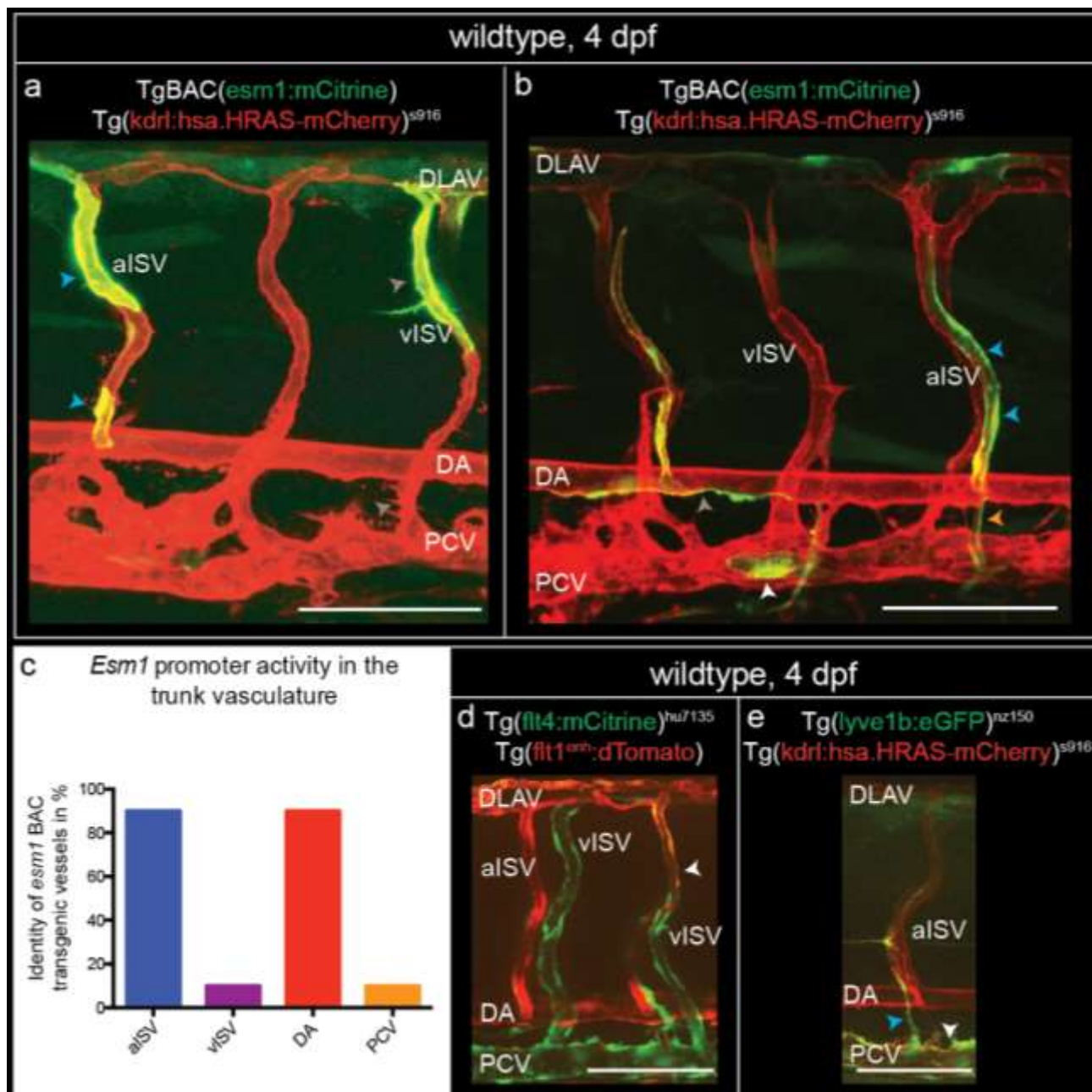


Figure 4-8. The *esm1* promoter is preferentially active in endothelial cells of arterial identity. The BAC *esm1* promoter construct pTarBAC_Tol2_-46kbEsm1_mCitrine was injected into wildtypes and investigated for fluorescence in either arteries or veins in the trunk vascular network at 4 dpf. a and b show the vascular marker *Tg(kdr:hsa.HRAS-mCherry)^{S916}* in red and *esm1* reporter construct expression is visible in green. *Esm1* promoter activity was observed in the entire aISV (blue arrowheads in a and b), in the DA (brown arrowhead in b) and, if present, in the dorsal part of a vISV (brown arrowheads in a). Moreover, the BAC reporter was expressed in the PCV (white arrowhead in b) and its connecting vessels (b, orange arrowhead). c presents a graph which shows quantification of vessels positive for

esm1 BAC reporter gene expression. d depicts the distribution of arterial (red fluorescent *flt1* positive cells) and venous ECs (green *flt4* marker) in ISVs at 4 dpf. Due to supposedly lymphatic cells in b (white and orange arrowheads), its expression was compared with the lymphatic reporter line Tg(*lyve1b:eGFP*)^{nz150} (e, white arrowheads). aISV, arterial intersegmental vessel; DA, dorsal aorta; DLAV, dorsal lateral anastomotic vessels; dpf, days post fertilization; vISV, venous intersegmental vessel. Scale bar 100 μ m.

4.3.5 Neurons of the spinal cord show *esm1* promoter activity

Esm1 promoter activity at the level of the NT was visible. Moreover, previous studies showed that *flt1* is expressed in this expression domain as well (Wild et al. 2017). Mosaic *esm1* BAC reporter construct expression (pTarBAC_Tol2_-46kbEsm1_mCitrine) in neurons of the spinal cord was verified and its expression profile compared with that of *flt1* in the spinal cord as shown in figure 4-9.

First, the *flt1* expression in neurons of the spinal cord at 4 dpf was examined (Fig. 4-9a). The neuronal transgenic line Tg(*xla.tubb:DsRed*)^{zf148} visualizes the spinal cord, whereas a stable BAC reporter line aided in analysis of *flt1* expression. Injection of the *esm1* BAC promoter construct into the neuronal reporter line showed comparable expression in the spinal cord to that of the *flt1* expression (Fig. 4-9b, white arrowheads). In figure 4-9c is presented the spatial location of *esm1* expressing neurons when compared to the vascular marker Tg(*kdr1:hsa.HRAS-mCherry*)^{s916} (white arrowheads).

Conclusively, taking the entire promoter expression profile (predominantly expressed in arterial endothelium and in neurons) of *esm1* into account, it appeared similar to that of *flt1*.

4.4 Altered *esm1* levels influence degree of ectopic sprouting at the neuro-vascular interface in the zebrafish trunk

Flt1 mutants have a hypersprouting phenotype and elevated *esm1* expression (Wild et al. 2017). In the mouse model, ESM1 is considered a tip cell specific gene and is relevant for sprouting (Rocha et al. 2014). Previous data in this work evinced expression domains of *esm1* in the early embryonic stages. Furthermore, *esm1* mRNA levels were significantly increased at 3 dpf and 4 dpf in the *flt1* LOF model; at a time point when ectopic sprouts arise. Apparently, *esm1* is involved in the development of vessels and a relationship between tertiary sprouting and *esm1* was suspected. To test this, *esm1* LOF experiments in wildtype and *flt1* mutants were performed. In addition, the effect of *esm1* overexpression on vascular patterning in wildtype and *flt1* mutants was examined.

Quantification of the spinal cord vascular network was performed as described in section 6.2.12.3.2. This method was applied by colleagues in this lab in previous work (Wild et al.

2017).

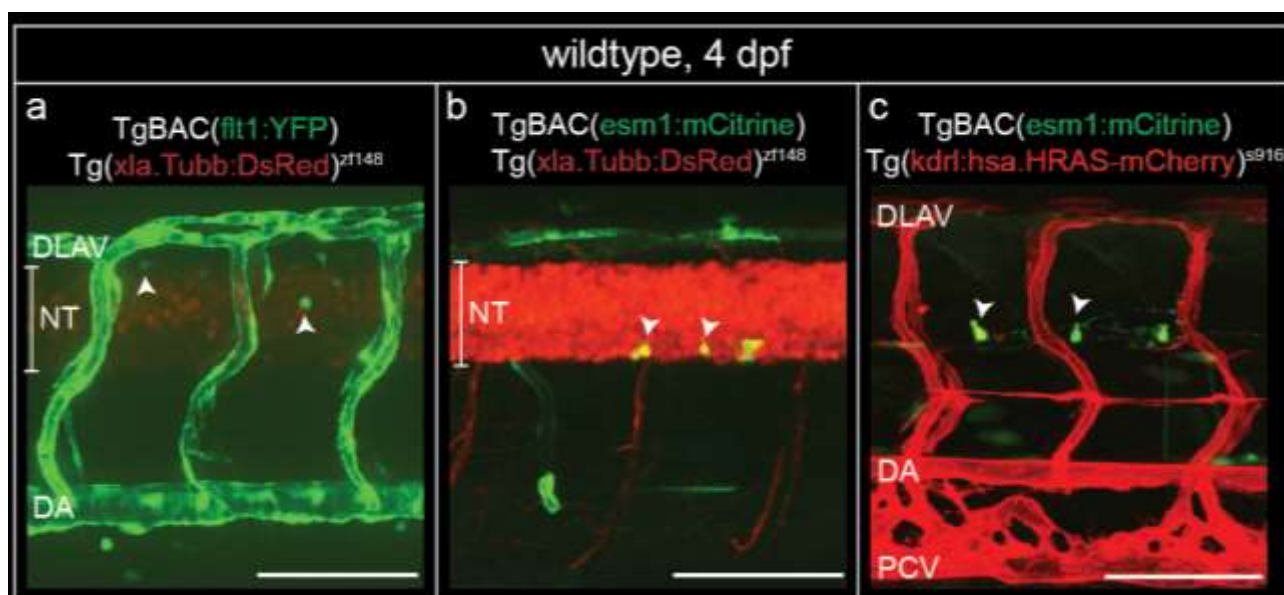


Figure 4-9. Activation of the *esm1* promoter in neurons of the spinal cord. The *esm1* promoter construct pTarBAC_Tol2_-46kbEsm1_mCitrine was injected into wildtypes with either a neuronal (b, *xla.tubb*) or vascular reporter (c, *kdrl*). The observed expression pattern was compared to that found in the arterial specific *flt1* reporter line (a) at 4 dpf. DA, dorsal aorta; DLAV, dorsal lateral anastomotic vessels; dpf, days post fertilization; ISV, intersegmental vessel; NT, neural tube. Scale bar 100 μ m.

4.4.1 Loss of *esm1* rescues hypersprouting in *flt1* mutants

The role of *esm1* during hypersprouting in *flt1* mutants was assessed by several LOF approaches: morpholino mediated knock down of *esm1* and generation of an *esm1;flt1* double knock out zebrafish.

4.4.1.1 Morpholino-induced *esm1* knock down in *flt1* mutants decreases tertiary sprouting

Morpholino (MO)-induced knock down is depicted in figure 4-10. 1 ng of either control or *esm1*-ATG MO was injected into the 1-cell stage embryo and imaged at 4 dpf. Reporter gene expression under *kdrl* promoter enables visualization of the blood vessels and Tg(*xla.tubb*:DsRed)^{zf148} reports mature neurons. Analysis of both segments (Fig. 4-10b) and branching points (Fig. 4-10c) revealed that *flt1* mutants injected with *esm1* targeting MO showed significantly fewer ectopic sprouts when compared to control MO. In contrast, wildtype embryos injected with *esm1* MO did not display any apparent phenotype.

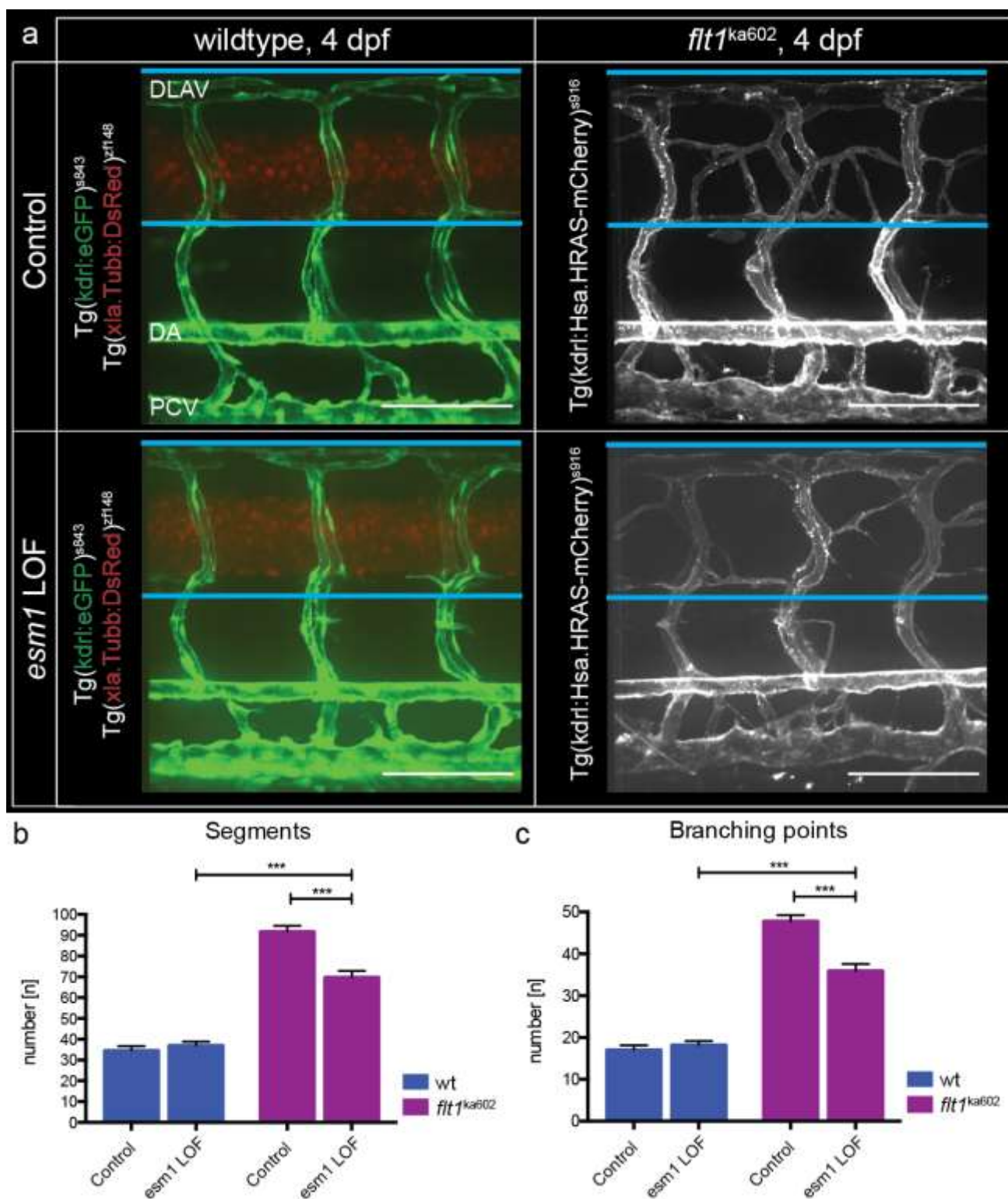


Figure 4-10. *Esm1* knock down in the *flt1* LOF model attenuates tertiary sprouting. (a) Translational knock down (LOF) of *esm1* was achieved by injecting *esm1*-ATG MO into wildtype or *flt1* mutants. The fish lines were transgenic for *kdrl*, a blood vessel specific reporter (DA, DLAV, ISVs, PCV). Additionally, the wildtype visualizes the neural tube (*xla.tubb*). b and c depict quantifications of the vascular network with regard to segments and branching points, respectively. DA, dorsal aorta; DLAV, dorsal lateral anastomotic vessel; dpf, day post fertilization; LOF, loss-of-function; MO, morpholino; PCV, posterior cardinal vein; wt wildtype. Quantification in b and c: mean±s.e.m., normality: D'Agostino & Pearson omnibus, t-test. wt control n=12; wt *esm1* MO n=17; *flt1* control n=16; *flt1* *esm1* MO n=18.

Scale bar 100 μ m.

The MO dosage was verified in *esm1*^{-3721/-3721} mutants. Two concentrations, 1 ng and 3 ng were injected as presented in figure 4-11. Changes in the trunk vasculature could be evaluated and compared to the not injected zebrafish embryos (Fig. 4-11 a) with the vascular reporter Tg(*kdr*:eGFP)^{s843}. Though no side effects were recognized with 1ng MO (Fig. 4-11b), the higher concentration resulted in increased diameter in ISVs (blue arrowhead in Fig. 4-11c) and vessels below the NT, which were otherwise not visible (Fig. 4-11c, white arrowhead).

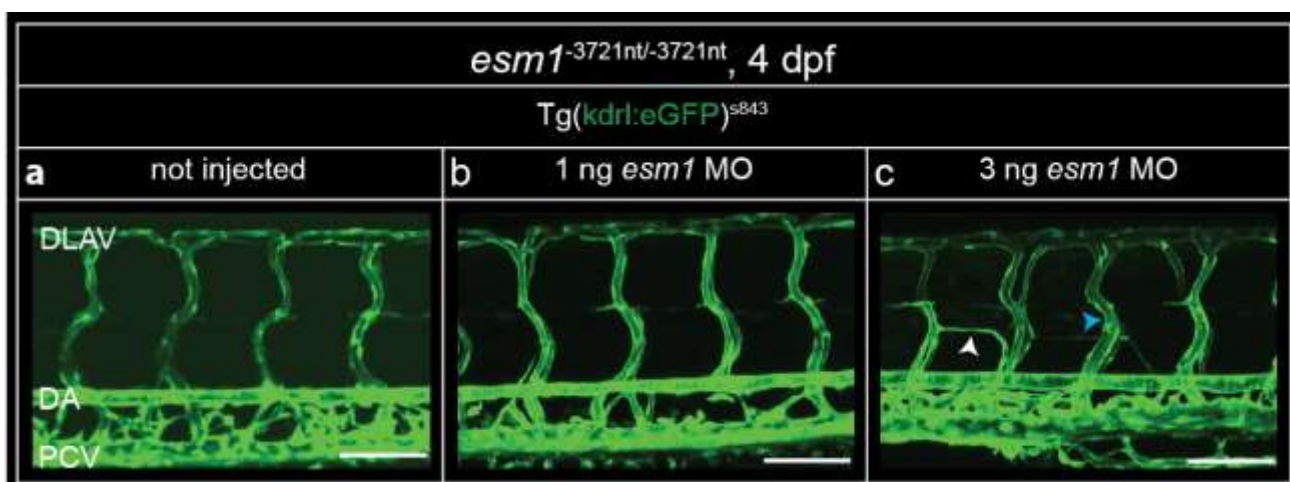


Figure 4-11. Verification of the *esm1* morpholino dosage in *esm1* mutants. 1 ng (b) and 3 ng (c) *esm1* MO was injected into *esm1* mutants with a vascular reporter background (*kdr*) and compared to uninjected control (a) for possible side effects in the vascular system at 4 dpf. 1 ng did not result in phenotypical alterations. Embryos into which 3 ng of MO was introduced showed additional vessels (white arrowhead in c) and ISVs with increased diameter (blue arrowhead in c). DA, dorsal aorta; DLAV, dorsal lateral anastomotic vessel; dpf, day post fertilization; MO, morpholino; PCV, posterior cardinal vein. Scale bar 100 μ m.

4.4.1.2 Generation of *esm1* mutants using the CRISPR/Cas9 approach

The decreased hypersprouting phenotype seen upon *esm1* knock down should be confirmed with a stable *esm1* knock out line. *Esm1* mutants were generated using the CRISPR/Cas9 approach as illustrated in figure 4-12. The *esm1* gene consists of three exons. Computational analysis of protein domains predicted a signal peptide and a cysteine-rich domain. A deletion of the coding sequence was attempted using two sgRNAs targeting the 5' untranslated region (UTR) and 3'UTR, respectively. With this approach neither transcription nor translation will be initiated and compensation due to remaining protein excluded. The presence of a deletion and the genotype was determined with two PCRs, thereby amplifying the wildtype and mutant allele in separate reactions. The mutant amplicon was checked and defined *via* sequencing.

An *esm1* LOF line with a 3721 bp deletion was generated. A detailed description of the generation process is provided in 6.2.9.1.

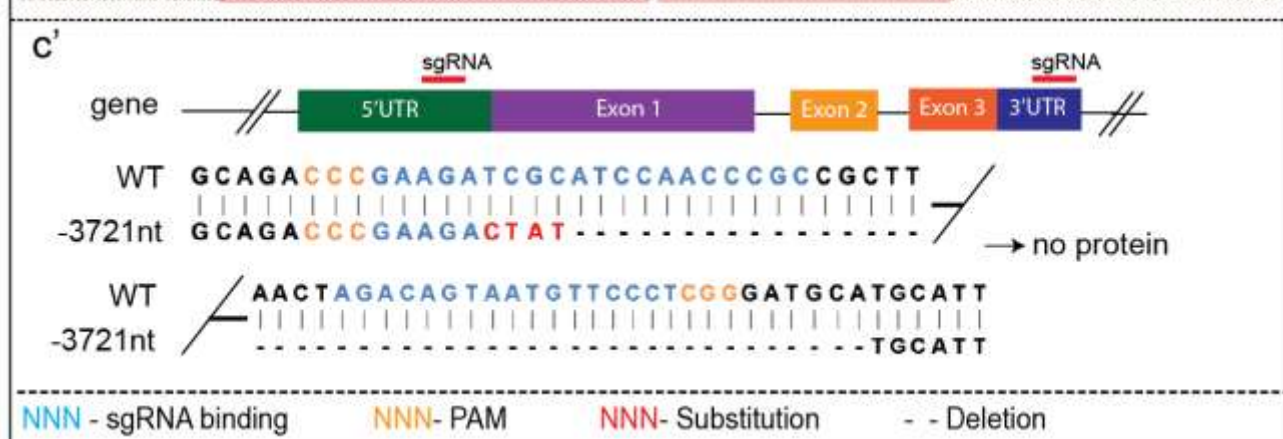
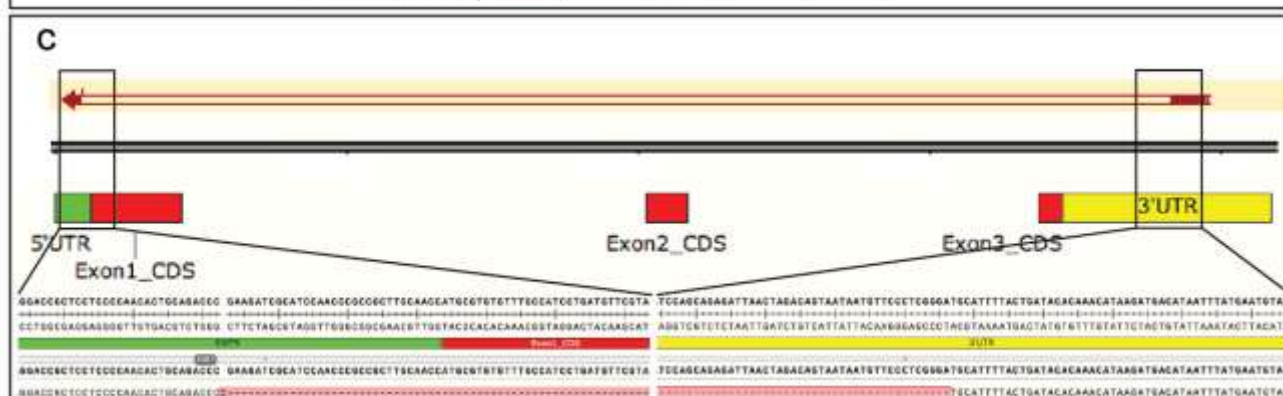
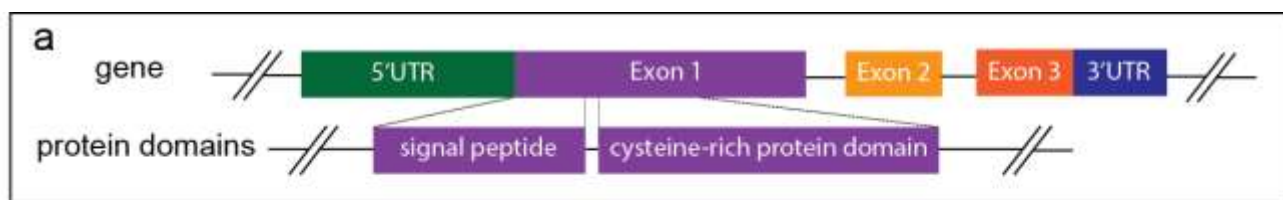


Figure 4-12. Generation and verification of *esm1* mutants. (a) Depiction of the *esm1* gene and its protein domains. The gene consists of three exons. Two protein domains, a signal peptide and a cystein-rich domain, were identified using computational analysis. (b) Mutations were induced using the CRIPR/Cas9 approach with two sgRNAs, which target the 3'UTR and 5'UTR of the *esm1* gene. The genotype (wildtype, heterozygotic or homozygotic) was identified by the size of the amplicons obtained from two Taq PCRs: one for detection of the wildtype allele (548 bp; primer 1 and primer 2) and a second amplifies the mutant allele (243 bp; primer 1 and primer 3). (c) The mutant amplicon was verified and the resulting deletion defined *via* sequencing. The resulting mutation was a deletion of 3721 bp. Thus, the entire coding sequence is missing and consequently no protein was produced. bp, base pairs; UTR, untranslated region.

4.4.1.3 Establishment of an *esm1;flt1* double mutant line

In order to obtain more evidence that *esm1* affects the sprouting phenotype upon loss of *flt1* function, a line was established in which both *esm1* and *flt1* are non-functional. For this, *esm1*^{-3721nt} homozygous mutants were crossed with *flt1*^{ka604} homozygous fish. Consequently, the F0 is heterozygous for both the *esm1* and *flt1* mutant allele and incross resulted in homozygous double mutants (Fig. 4-13).

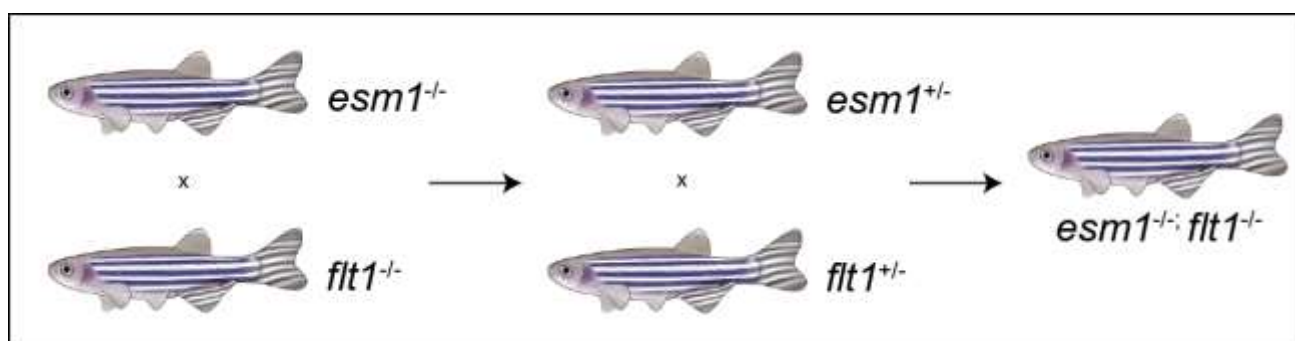


Figure 4-13. Establishing *esm1;flt1* double mutants. Homozygous *esm1* mutants were crossed with animals homozygous for *flt1*. The progeny, heterozygous for both genes, were mated to obtain homozygous mutants for both *esm1* and *flt1*.

The trunk vascular network at the spinal cord level was analyzed in the wildtype, *esm1*^{-3721/-3721}, *flt1*^{ka604} and in the respective *esm1;flt1* double mutant as depicted in figure 4-14. The pattern of the vessels was not altered upon loss of *esm1*. However, loss of *flt1* alone or simultaneously with *esm1* resulted in significant increase of tertiary sprouting when compared to either wildtype or *esm1* mutant. Spinal cord vascularization was with high significance most prominent in *flt1* mutants when collated with the other genotypes.

In summary, the data of the conducted LOF experiments suggests that *esm1* alone does not affect the vascular pattern in the trunk. Loss of *esm1* in *flt1* mutants, however, rescued the hypersprouting phenotype to great extent.

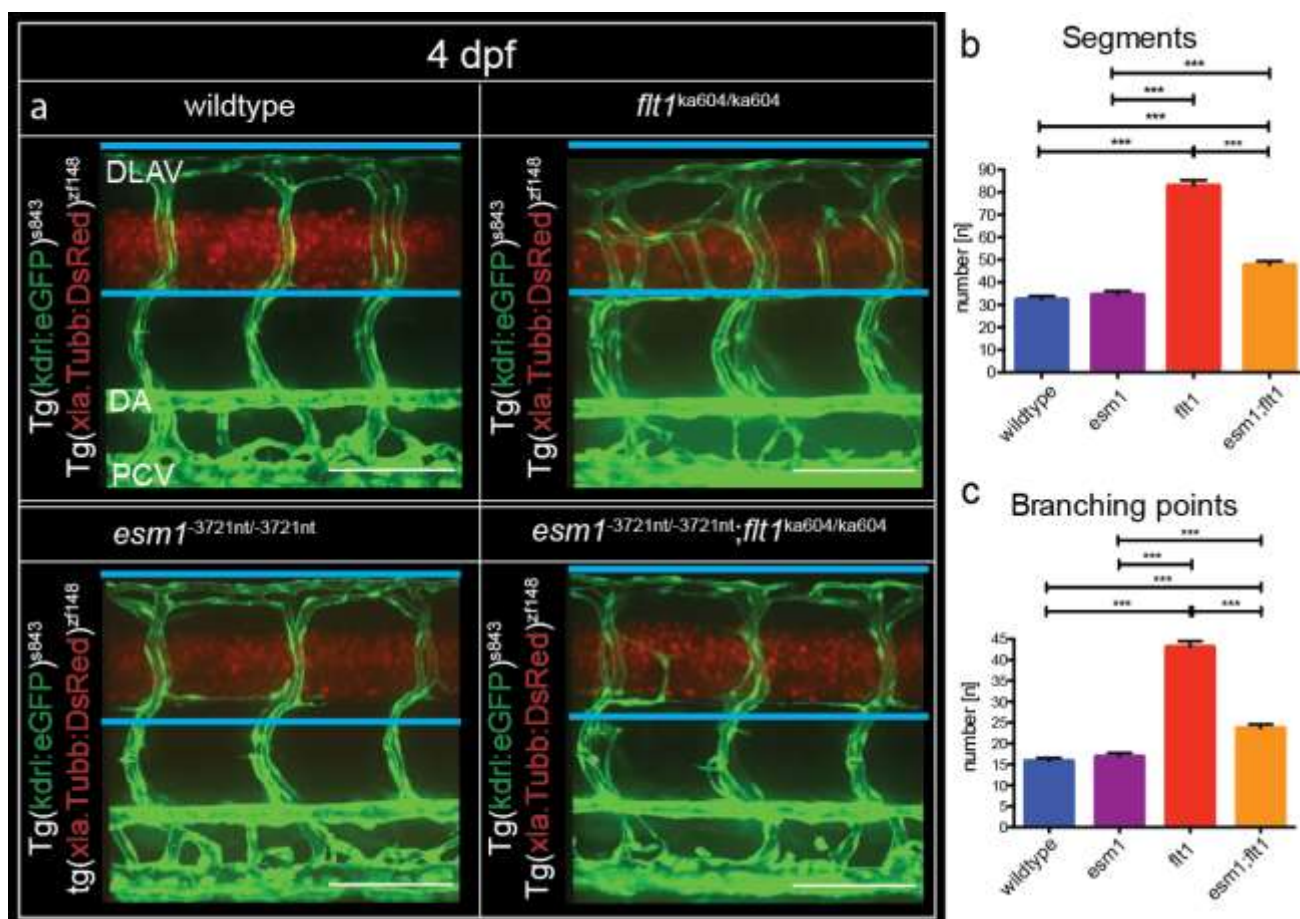


Figure 4-14. Vascular patterning in *esm1* and *flt1* LOF models at the level of the spinal cord. (a) Depiction of the spinal cord vascular network in the wildtype, *esm1* mutant, *flt1* mutant and the *esm1;flt1* double mutant. The fish lines were in a $Tg(kdr:eGFP)^{s843} \times Tg(xla.tubb:DsRed)^{zf148}$ transgenic background, visualizing blood vessels in green and the NT in red. Ectopic sprouting was quantified and presented in b and c, respectively. DA, dorsal aorta; DLAV, dorsal lateral anastomotic vessel; dpf, day post fertilization; PCV, posterior cardinal vein; wt, wildtype. Quantification in b and c: mean \pm s.e.m., normality: D'Agostino & Pearson omnibus, t-test. wt n=28; *esm1* n=30; *flt1* n=27; *esm1;flt1* n=35. Scale bar 100 μ m.

4.4.2 Number of tertiary sprouts is decreased in *esm1* mutants upon *flt1* knock down

If indeed, *esm1* is an essential part of the tertiary sprouting process initiated in the *flt1* mutants, hypersprouting upon induced decreased *flt1* levels should be inhibited in fish with dysfunctional *esm1*. To test this, *esm1*^{sa11057} mutants was used as a model in which *esm1* was inactive. This line had a base pair substitution from C to A in the exon 1, which resulted in a premature stop codon. Thus, transcription stopped after 240 bp and half of the Esm1 protein, including the most relevant cysteine-rich protein domain, was missing. The mutation is illustrated in figure 4-15.

Flt1 levels were decreased in both wildtypes and *esm1*^{sa11057} mutants using a MO based approach. The lines were transgenic for $Tg(kdr:eGFP)^{s843}$ and $Tg(xla.tubb:DsRed)^{zf148}$. Embryos in the one-cell stage were injected with 1 ng of either control of *flt1* MO. The vascular

patterning was assessed at 4 dpf. A control MO served as monitor for any injection effects. *Esm1* knock out zebrafish appeared normal as no aberrant vessel patterning was recognized. *Flt1*-ATG MO targeted knock down significantly increased ectopic sprouting in wildtypes. The same knock down in *esm1*^{sa11057} mutants, also resulted in sprout formation, but to a much lesser extend compared to the wildtype. The results are shown in figure 4-16. In conclusion, *esm1* plays a functional role in tertiary sprouting.

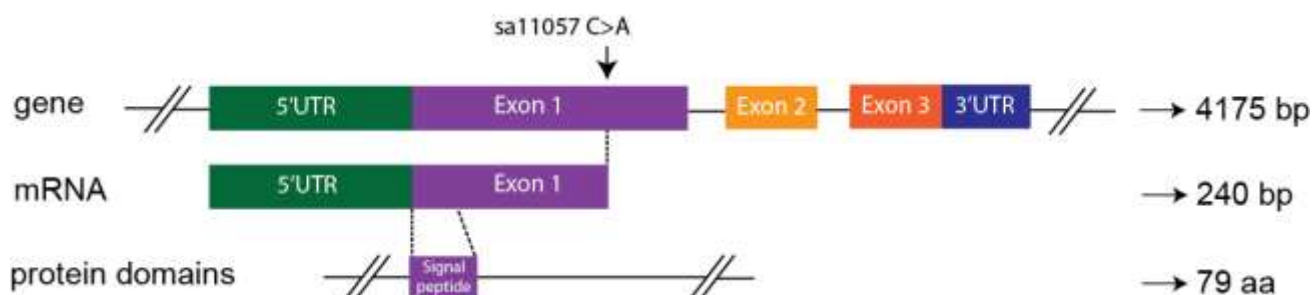


Figure 4-15. Graphical illustration of the mutation in the *esm1*^{sa11057} line. A substitution of a C to an A in exon1 results in a premature stop codon. Only the signal peptide remains in the 79 aa partial protein. A, adenosine; aa, amino acids; bp, base pairs; C, cytosine.

4.4.3 *Esm1* gain-of-function promotes vascular sprouting

The previous experiments showed that loss of both *esm1* and *flt1* results in less tertiary sprouts. Overexpression experiments should reveal, if elevated amounts of *esm1* could enhance hypersprouting at the region of the spinal cord when *flt1* was inactive. These experiments might also give greater insight into a mechanism, how *esm1*, Vegfaa bioavailability and Flt1 are involved with each other.

4.4.3.1 Elevated *esm1* expression under an ubiquitously active promoter results in elevated tertiary sprouting

Overexpression of *esm1* was achieved by injecting the *pCS2+_{esm1}* vector into the one-cell stage zebrafish embryo. This vector contained a cytomegalovirus (CMV) promoter, which was ubiquitously active. As a control, *pCS2+* without any insert was injected. 1 nL of a of 50 ng/μL solution of either plasmid was introduced. The wildtype line was transgenic for both the blood vessel reporter *Tg(kdr:l:eGFP)*^{s843} and neuronal reporter *Tg(xla.tubb:DsRed)*^{zf148} while the *flt1* mutant was transgenic for *Tg(kdr:l:hsa.HRAS-mCherry)*^{s916} only.

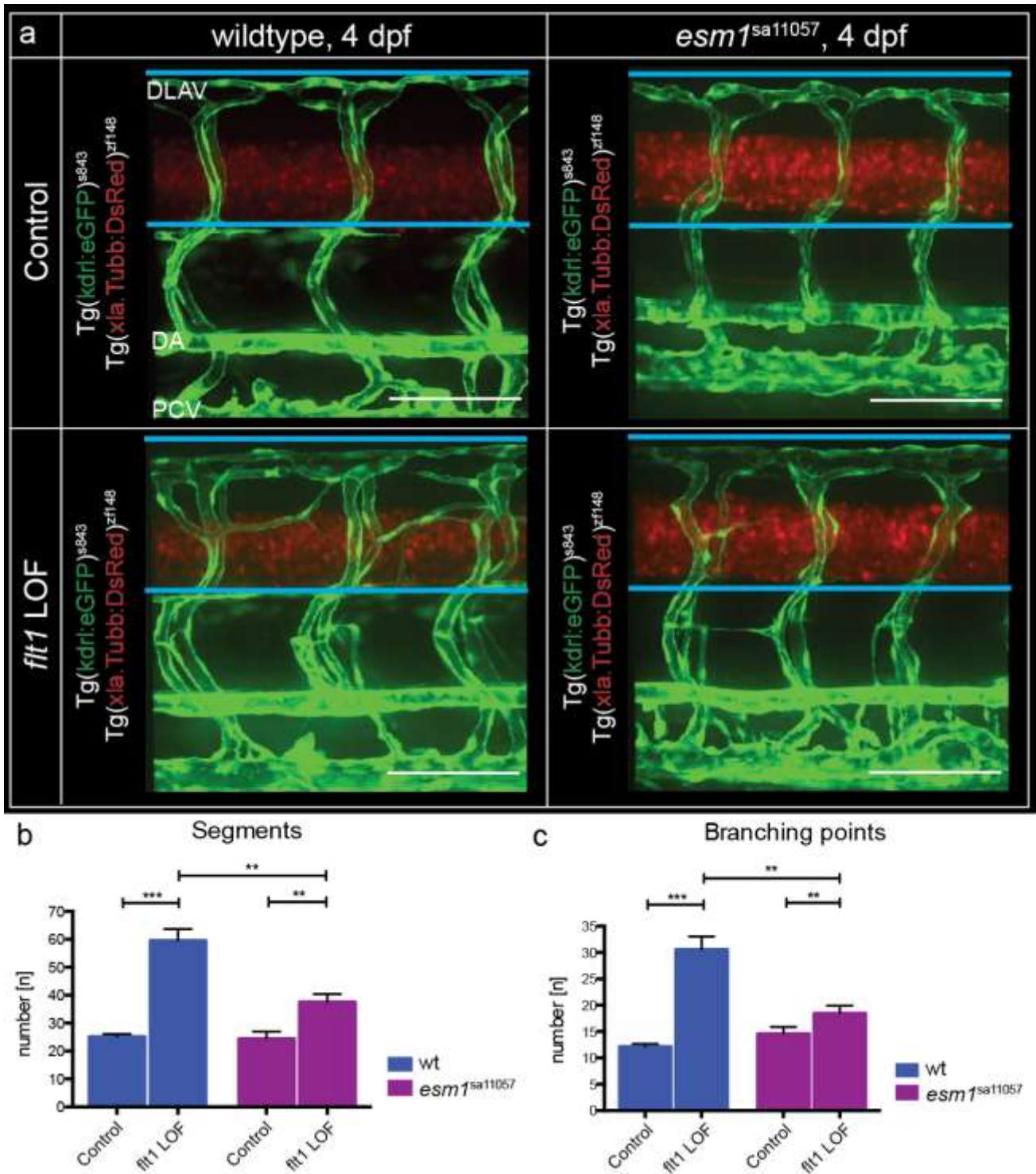


Figure 4-16. Hypersprouting upon *flt1* knock down is less severe in *esm1*^{sa11057} mutants. The effect of decreased amount of *flt1* on tertiary sprouting in *esm1*^{sa11057} mutants at 4 dpf was studied. (a) *flt1* LOF was obtained by injecting *flt1* MO into both wildtype and *esm1*^{sa11057} which have a (*kdr*:eGFP;*xla.Tubb*:DsRed) double transgenic background, with *kdr* being a blood vessel specific reporter (DA, DLAV, ISVs, PCV) and the *xla.Tubb* a neuronal reporter. The number of segments (b) and branching points (c) was measured and thus the degree of tertiary sprouting determined. DA, dorsal aorta; DLAV, dorsal lateral anastomotic vessel; dpf, days post fertilization; LOF, loss-of-function; MO, morpholino; PCV, posterior cardinal vein; wt, wildtype. Quantification in c and d: mean±s.e.m., normality: D'Agostino & Pearson omnibus, t-test, n=12 for wt Control and both *esm1*^{sa11057} groups. n=10 for wt *flt1* MO group. Scale bar 100 μm.

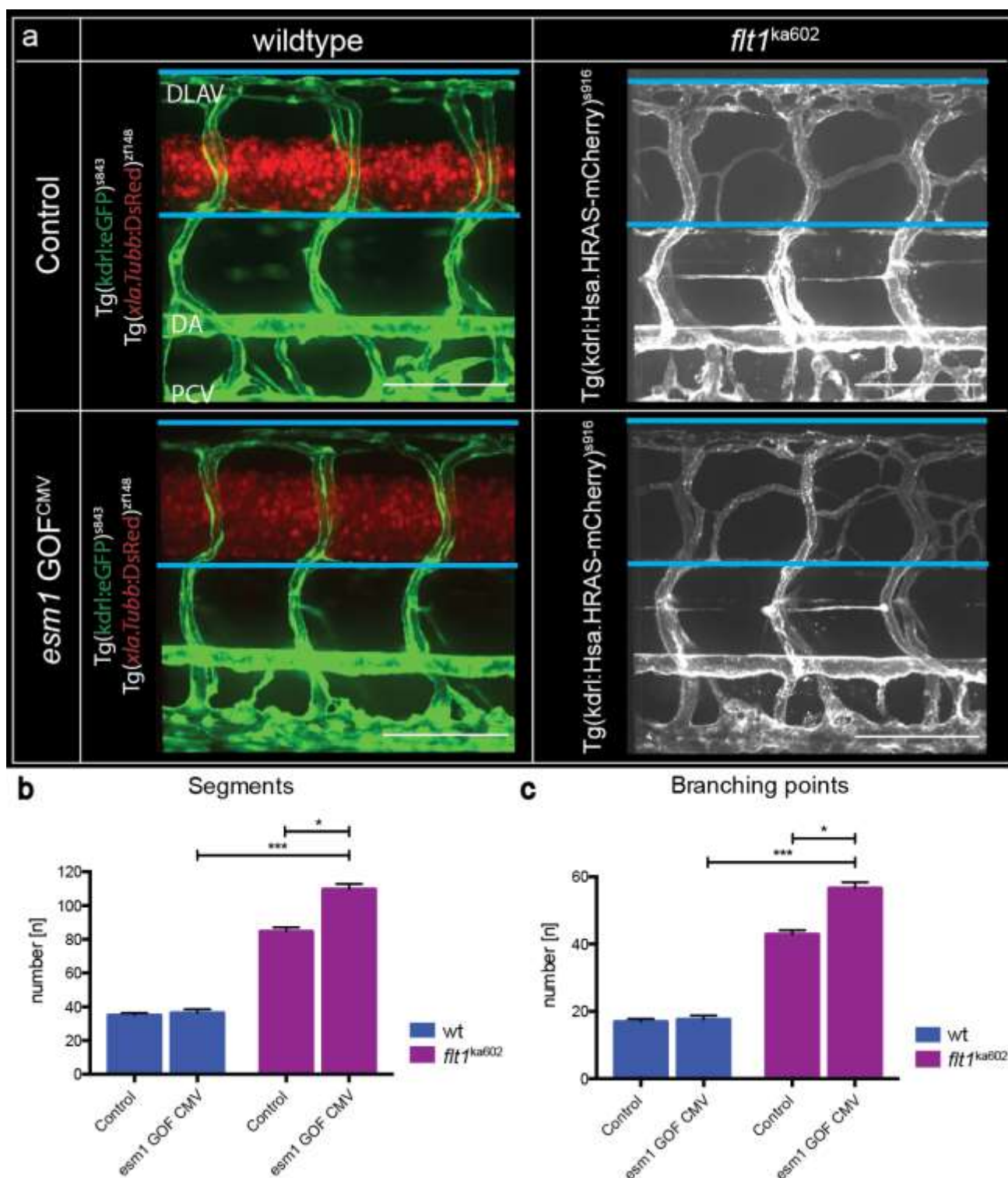


Figure 4-17. Global increase of *esm1* results in augmented tertiary sprouting. The effect of augmented amounts of *esm1* on tertiary sprouting in *flt1* mutants at 4 dpf was studied. pCS2+ was a mammalian expression vector containing the ubiquitously active cytomegalovirus (CMV) promoter. (a) Global *esm1* mRNA expression was obtained by introducing pCS2+_*esm1* (*esm1* GOF CMV) into both wildtype and *flt1* mutants. The wildtype was in a Tg(*kdrI*:eGFP;*xla.Tubb*:DsRed) double transgenic background and the *flt1* mutant line carries the Tg(*kdrI*:Hsa.HRAS-mCherry) transgene. The unmodified pCS2+ plasmid was used as a control. Changes in the vascular network were quantified as illustrated in b and c. DA, dorsal aorta; DLAV, dorsal lateral anastomotic vessel; dpf, days post fertilization; GOF, gain-of-function; PCV, posterior cardinal vein; wt, wildtype. Quantification in c and d:

mean \pm s.e.m., normality: D'Agostino & Pearson omnibus, t-test, n=12 for all groups. Scale bar 100 μ m.

4.4.3.2 *Esm1* overexpression under a blood vessel specific promoter augments number of tertiary sprouts

Unspecific elevation of *esm1* mRNA resulted in a more pronounced hypersprouting and previous data revealed the presence of *esm1* mRNA in blood vessels. Thus, the effects on spinal cord vascularization were tested, when *esm1* was increasingly expressed under the control of the blood-vessel specific *fli1a* promoter. Details about the overexpression construct and its generation are provided section in 6.2.8. and 6.2.8.1.

1 nL of either 0.1% (v/v) DMSO (control) or 50 ng/ μ L of overexpression plasmid *fli1a_eGFP-p2a-esm1;cmlc2:eGFP* (*esm1* GOF^{BV}) solution was injected into wildtypes and *flt1* mutants at the one cell-stage and the effects on the vascular pattern analyzed at 4 dpf. The used fish lines were in a *Tg(kdrt:Hsa.HRAS-mCherry)*^{s916} blood-vessel transgenic background. DMSO injected animals were used as control.

The vascular patterning in the wildtype was not affected when *esm1* was present in higher abundance. Comparable to *esm1* overexpression under the ubiquitously active promoter, tertiary sprouting at the level of the spinal cord was distinctively increased in the *flt1* LOF model, albeit with even higher significance (Fig. 4-18).

4.5 The effects of *esm1* on tertiary sprouting was recapitulated in another Vegfaa GOF model, the *vhl* mutant

Previous data indicate that *esm1* functionality alone does not affect the vascular patterning in the trunk. However, variation of *esm1* levels in the Vegfaa GOF model *flt1* mutants resulted in a correlating change in spinal cord vascularization. Accordingly, alterations in the vascular network at the neuro-vascular interface should be applicable to other Vegfaa GOF scenarios, for example the *vhl* mutant.

Effects of *esm1* in the *vhl* LOF model were examined by MO-induced knock down and blood vessel-specific overexpression at 4 dpf. 1 nL of either 0.1% (v/v) DMSO (control) or 50 ng/ μ L overexpression plasmid *fli1a_eGFP-p2a-esm1;cmlc2:eGFP* (*esm1* GOF^{BV}) solution or 1 ng *esm1*-ATG MO (*esm1* LOF) of was injected and embryos transgenic for *Tg(kdrt:Hsa.HRAS-mCherry)*^{s916}, a blood-vessel reporter, used for analysis.

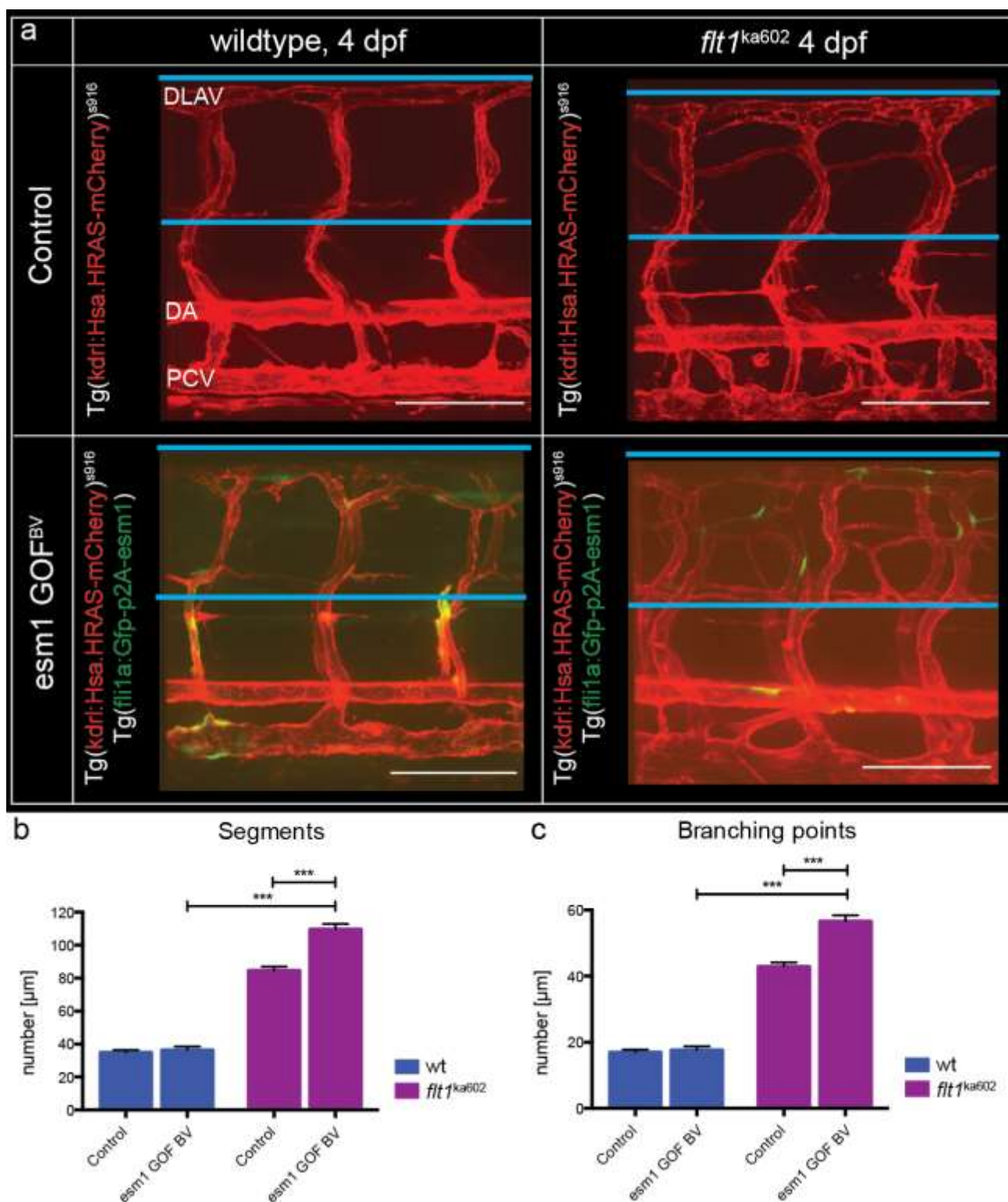


Figure 4-18. *Esm1* overexpressed in blood vessels results in elevated ectopic sprouting. The effect of augmented levels of *esm1* in *flt1* mutants at 4 dpf specifically in the blood vessels on tertiary sprouting was studied. (a) The overexpression construct *fli1a_eGFP-p2a-esm1;cmlc2:eGFP* (*esm1* GOF BV) was injected into *Tg(kdrl:Hsa.HRAS-mCherry)^{s916}* transgenic lines with either a wildtype or *flt1* LOF genotype. The blood vessels were visualized by expression of a fluorescent protein under the *kdrl* promoter (DA, DLAV, ISVs, PCV). DMSO injected animals were used as control. Measurements of the number of segments (b) and branching points (c) was performed and allows visualization of changes in tertiary sprouting. DA, dorsal aorta; DLAV, dorsal lateral anastomotic vessel; dpf; days post

fertilization; GOF, gain-of-function; PCV, posterior cardinal vein; wt, wildtype. Quantification in b and c: mean \pm s.e.m., normality: D'Agostino & Pearson omnibus, t-test, n=14 for all groups. Scale bar 100 μ m.

The effects of *esm1* knock down and overexpression seen in zebrafish with inactive *flt1* could be reproduced in *vhl* mutants as shown in figure 4-19. Translational block of *esm1* resulted in decreased tertiary sprouting while overexpression lead to an increase in spinal cord vascularization. These changes were highly significant.

Summarizing the LOF and GOF experiments suggest that 1) *esm1* has no major effect in wildtype zebrafish embryos, 2) loss of *esm1* rescues hypersprouting in two different Vegfaa GOF models and 3) gain of *esm1* promotes tertiary sprouting. The data suggests, that loss of *esm1* selectively affects the tertiary sprouting process and indicate, that *esm1* plays an active role in sprouting when Vegfaa is present in greater abundance.

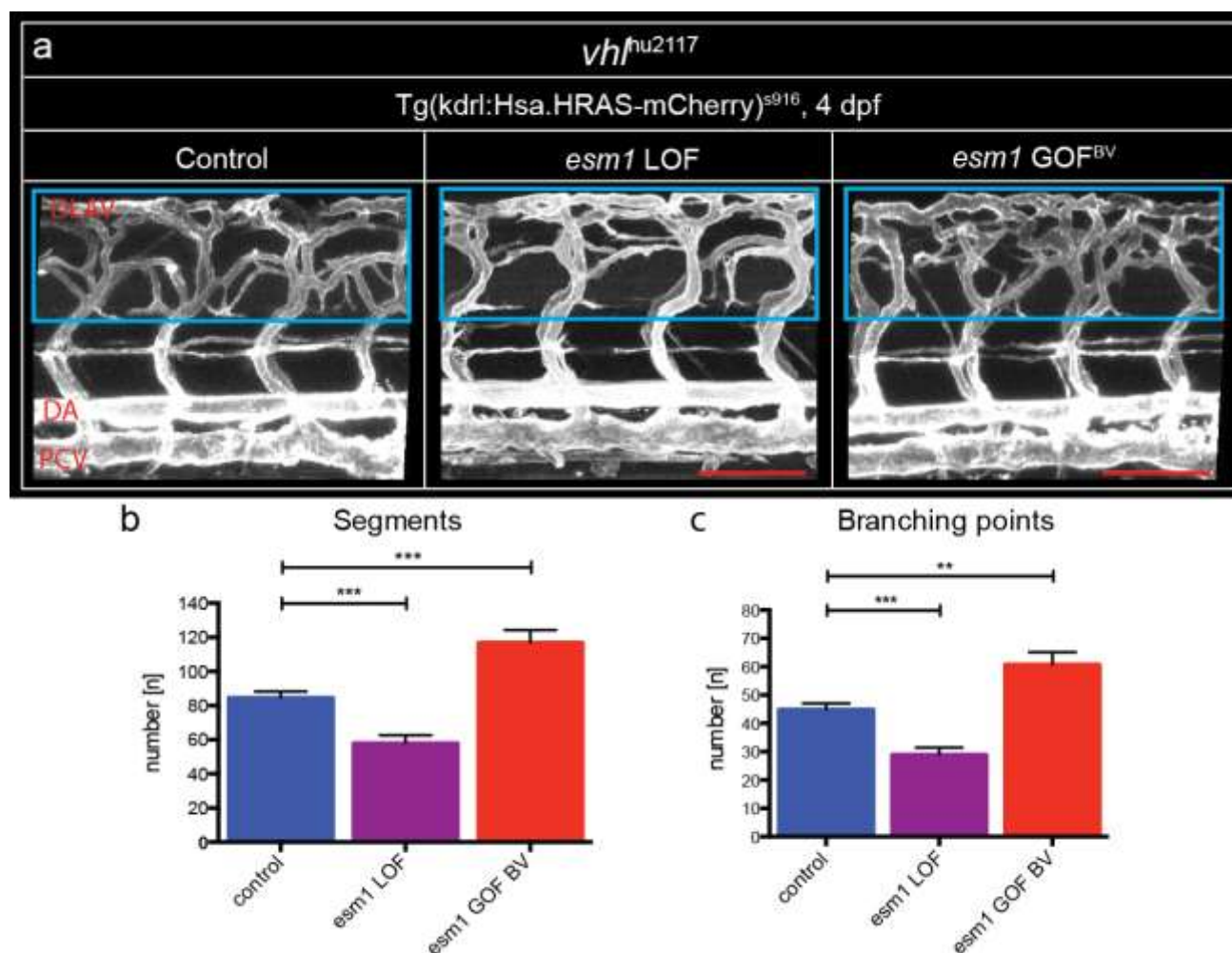


Figure 4-19. *Esm1* levels affect spinal cord vascularization in the *vhl* mutant. (a) *Esm1* levels were either decreased using an ATG MO (knock down) or increased with the blood vessel specific overexpression plasmid fli1a_eGFP-p2a-*esm1* (GOF BV) in the *vhl* mutant. The effects on the vascular network in the spinal cord were analyzed at 4 dpf. Measurements of segments and branching points in the different groups, respectively, is presented in b and

c. DA, dorsal aorta; DLAV, dorsal lateral anastomotic vessel; dpf, days post fertilization; MO, morpholino; PCV, posterior cardinal vein. Quantification in b and c: mean±s.e.m., normality: D'Agostino & Pearson omnibus, t-test. Control n=16; *esm1* MO n=10; *esm1* GOF BV n=5. Scale bar 100 µm.

4.6 The development of the trunk vasculature is not distinctively altered upon loss of *esm1*

The results of the gene expression and the various LOF and GOF scenarios prompt an effect of *esm1* on the zebrafish trunk vasculature. Previous data let assume an effective role of *esm1* only with increased abundance of Vegfaa. A closer look into an *esm1* related phenotype was intended with a LOF model.

The vascular pattern was analyzed in the *esm1*^{-3721/-3721} mutant line transgenic for the vascular specific reporter Tg(*kdr*:eGFP)^{s843} from 1 dpf to 4 dpf (Fig. 4-20). In this line the entire coding sequence was deleted. Consequently, no protein was translated and possible compensation mechanisms prevented at the best possible. Compared to the wildtype, no change in the vascular architecture was observed. Primary sprouts at 1 dpf developed into functional ISVs and DLAV and secondary sprouting successfully formed vISVs. *Esm1* mutants were devoid of tertiary sprouts. Thus, the loss of *esm1* alone seemed to have no effect on the vascular patterning in the zebrafish trunk.

The vascular network in the trunk showed no distinctive phenotype upon loss of *esm1*. Next, an effect of *esm1* on an individual ISV was investigated by following parameters: diameter, length and nuclei (Fig. 4-21). Vessel morphology was observed in the reporter Tg(*kdr*:eGFP)^{s843}. The parameters were ascertained in 2 dpf, 3 dpf and 4 dpf old *esm1*^{-3721/-3721} zebrafish embryos and contrasted to the wildtype. The measurement procedures are described in 6.2.12.3.1. No morphological changes were perceptible according to any parameter at 2 dpf. Following significant changes were found at later stages: at 3 dpf, aISVs in *esm1* mutants were longer. At the same time point, more nuclei were present in both aISVs and vISVs. In 4 dpf old embryos, diameter was decreased in aISVs while vISVs were shorter and harbored a more nuclei. Variations in diameter and length affect vascular resistance, while the number of nuclei permits statements about cell number, such as were determined at 3 dpf and 4 dpf.

Thus, a physiological role of *esm1*, to some extend even distinctive to aISVs and vISVs, could be assumed. Furthermore, this data let suppose an inhibiting effect of *esm1* on cell proliferation, especially on vISVs. Further investigations have to validate this observation.

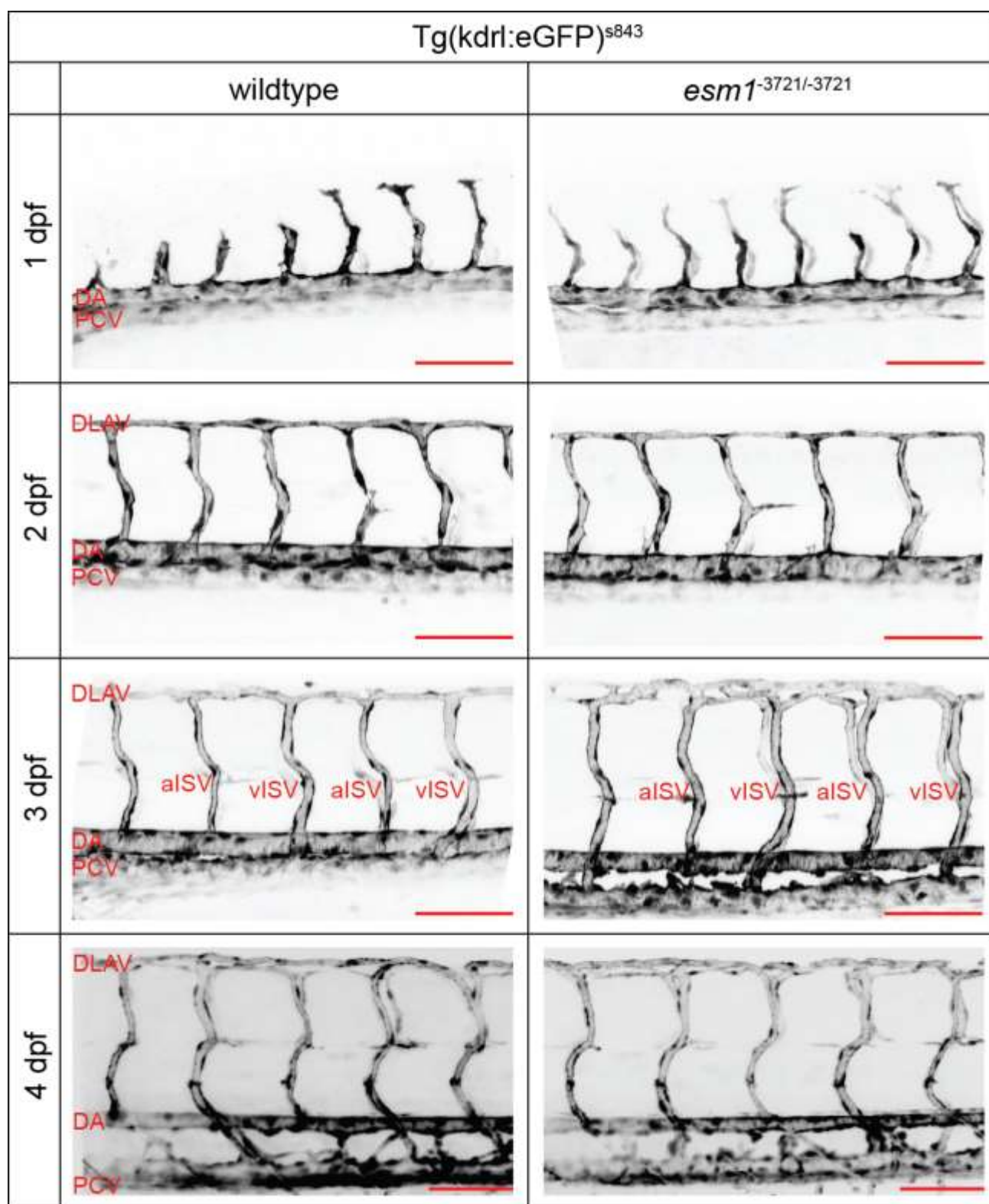


Figure 4-20. The trunk vascular pattern in *esm1* zebrafish mutants was not altered during early development. The arrangement of the trunk vascular network in *esm1*^{-3721/-3721} mutants was compared to that of wildtype zebrafish embryos from 1 dpf to 4 dpf. The fish were in the vascular reporter Tg(*kdr*:eGFP)^{s843}. aISV, arterial intersegmental vessel; DA, dorsal aorta; DLAV, dorsal lateral anastomotic vessel; dpf, days post fertilization; PCV, posterior cardinal vein; vISV, venous intersegmental vessel. Scale bar 100 μ m

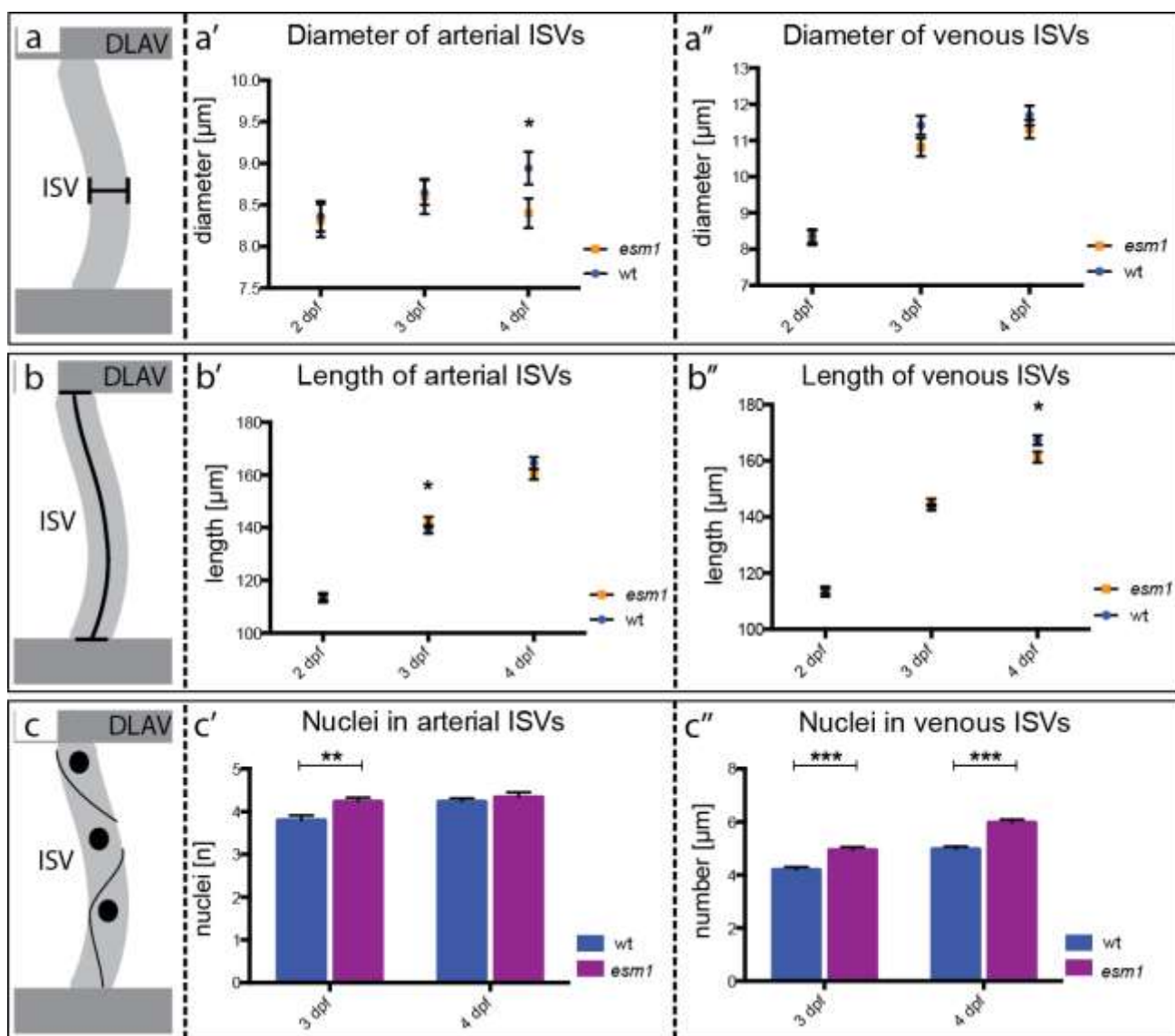


Figure 4-21. Trunk vessels show a mild phenotype in *esm1* knock out fish. The diameter (a), length (b) and the number of nuclei present in ISVs were determined. DA, dorsal aorta; DLAV, dorsal lateral anastomotic vessel; dpf, days post fertilization; ISV, intersegmental vessel; PCV, posterior cardinal vein; wt, wildtype. Quantification: mean \pm s.e.m., normality: D'Agostino & Pearson omnibus, t-test. For each parameter investigated: wildtype and *esm1*^{3721/-3721} mutant at 2 dpf and 3 dpf: n=30; wildtype 4 dpf n=29; *esm1*^{3721/-3721} mutant n=30.

5 Discussion

Esm1 is one of the most upregulated genes during the process of tertiary sprouting in *flt1* deficient zebrafish (Wild *et al.*, 2017). *ESM1* was formerly described as a tip cell marker and competitor for VEGF-A binding on Fibronectin, thus as a putative regulator of VEGF-A bioavailability (Shin, Huggenberger and Detmar, 2008; Rocha *et al.*, 2014). These data point to an important role of *Esm1* in angiogenic processes. In the model organism zebrafish, the expression of *esm1* in the embryo was not published until now. Moreover, functional data on this molecule is sparse in general and unpublished in the model organism zebrafish. In here, it has been shown that *esm1* is predominantly expressed in the developed and developing vasculature with probable specificity to arterial ECs as well as a subset of neurons in the spinal cord. On functional basis, *esm1* is proposed as a necessary but not sufficient factor for vascular patterning at the neuro-vascular interface in the zebrafish trunk in dependency of *Vegfaa*. Furthermore, the data let assume an anti-proliferative effect of *esm1* on endothelial cells.

5.1 Gene expression pattern of *esm1*

The dynamic expression pattern of *esm1* was studied with three approaches from the first until the fourth day of development. 1) qPCR was used to semi-quantitatively investigate alterations in *esm1* gene expression in two *Vegfaa* GOF models at 3 dpf and 4 dpf. In this time window tertiary sprouting starts and is still ongoing. 2) WISH was used to study mRNA location allowing allocation of distinct expression areas and changes in expression domains during development. However, WISH is not quantitative. Compared to other methods, the sensitivity is rather low, making it likely that low-level expression areas are overseen. Furthermore, this method strongly relies on specificity of the probe and minimization of background because in general the development of the staining reaction is usually stopped as soon as the signal to noise ratio appears optimal. 3) Fluorescent reporter gene analysis of *esm1* promoter activity visualized individual *esm1* expressing cells and might unveil putative expression domains overseen in WISH. However, this method relies on the fact that the promoter construct used contains, indeed, all relevant regulatory elements. Furthermore, the high sensitivity of this strategy allows detection of even low levels of *esm1* expression. The stability and accumulation of the fluorescent reporter protein venture overseeing reduction of expression levels.

5.1.1 *Esm1* gene expression is enhanced in Vegfaa GOF models

qPCR data obtained during this work and literature showed increased *esm1* gene expression with the beginning and onset of spinal cord hypersprouting in Vegfaa GOF models at 3 dpf and 4 dpf. The data let conclude an enhanced *esm1* gene activity upon binding of Vegfaa to Kdr1. In other models was shown an upregulation of *ESM1* expression upon binding of VEGF-A to VEGFR-2 (Conway, Collen and Carmeliet, 2001; Carmeliet, 2003; Shin, Huggenberger and Detmar, 2008; Rocha *et al.*, 2014).

ESM1 is present in tip cells in higher abundance. This knowledge can be transferred to tip cells spearheading the ectopic sprout zebrafish embryos with inactive *flt1* or *vhl* (Abid *et al.*, 2006; Rocha *et al.*, 2014; Eilken *et al.*, 2017). Indeed, promoter activity in the entire tertiary sprouts was detected, however, the overexpression in tip cells has to be tested with quantitative ISH or a stable reporter line.

Taken together, the data substantiate an activation of *esm1* gene expression through the Vegfaa/Kdr1 signaling pathway during angiogenesis also in the zebrafish model.

5.1.2 *Esm1* is expressed in the vasculature of zebrafish embryos

Gene expression profiles about *ESM1* in general are sparse. Literature described presence of *ESM1* gene activity in ECs of mouse retinas and lymph vessels, in continuous cell lines of ECs (e.g. HUVEC and HEK) and various kinds of tumors, e.g. glioblastoma and bladder (Lassalle *et al.*, 1996; Sarrazin *et al.*, 2006, 2010; Shin, Huggenberger and Detmar, 2008; Maurage *et al.*, 2009; Delehedde *et al.*, 2013; Roudnicky *et al.*, 2013; Rocha *et al.*, 2014; Yang *et al.*, 2015; Eilken *et al.*, 2017). In zebrafish, expression of *esm1* was so far is unknown but was expected to be present in ECs during phases of major growth of the organism as it happens during early zebrafish development. Therefore, this thesis provides the first detailed expression analysis in the zebrafish model.

WISH revealed presence of *esm1* mRNA predominantly in the developing vasculature. The pattern in the DA and developing IVS were commensurable to that characterized in blood vessel markers, such as *kdr1* or *fli1a* (Herbert, Cheung and Stainier, 2012; Pociute, Schumacher and Sumanas, 2019). Comparison of the most dorsal signal alludes remaining gene activity in cells of the DLAV, but this expression domain has to be proven with sections (Childs *et al.*, 2002; Kwon *et al.*, 2012; Novodvorsky *et al.*, 2015). However, contrasting to other vascular marker genes, expression of *esm1* decreased after 2 dpf and becomes undetectable in WISH. The data connote a relation of *esm1* to the development of the trunk vasculature because the gene is active at time points where the ISVs are growing or are

already developed. Activation of *ESM1* gene expression in ECs of both lymphatic and retinal blood vessels downstream of the VEGF-A/VEGFR-2 signaling cascade, the major signaling pathway for angiogenic processes, was described (Shin, Huggenberger and Detmar, 2008; Rocha *et al.*, 2014; Eilken *et al.*, 2017).

Surprisingly, in WISH no staining was visible in older stages. Since *esm1* transcription was verified at day three and four in qPCR, this might be due to methodological reasons. Either the probe did not reach into the deeper tissues with increasing size or signal became weaker with ongoing development. Either, the WISH protocol could be optimized for both increasing embryo size and the probe or another probe target site should be considered. However, first *in situ* on sections could be performed with the already available probe to confirm the observed domains and possibly identify additional expression areas.

On cellular level, as demonstrated by reporter gene analysis, the *esm1* promoter was predominantly active in endothelium. Next to the trunk vasculature, the reporter construct was active in vessels of the brain, eye and intestine as well as the heart and its cardiac outflow tract. Studies with primary cell culture of healthy and tumor material of various tissues and mouse retinal endothelium identified *ESM1* expression in these anatomical regions, however, under conditions where the gene is overexpressed (Abid *et al.*, 2006; Shin, Huggenberger and Detmar, 2008; Rocha *et al.*, 2014).

ESM1 is known as a tip cell marker due to its high abundance in such but is not exclusive for this cell phenotype (del Toro *et al.*, 2010; Geudens and Gerhardt, 2011; Rocha *et al.*, 2014). In this thesis, no accumulation of *esm1* in the tip cells, neither during development of the trunk vasculature in wildtype or *flt1* mutant embryos nor in forming ectopic sprouts in the *flt1* LOF model, was observed. This might be due to methodological problems including low resolution of WISH and the accumulation of GFP in the reporter fish, but could also reflect differences between vertebrate species (mouse vs. zebrafish).

Wildtype and *flt1* mutants showed analogous *esm1* expression pattern at 1 dpf and 2 dpf, which is in accordance to literature. An effect of deficient *flt1* on the architecture of the trunk vascular network until the second day of development was excluded (Wild, 2016; Klems, 2017; Wild *et al.*, 2017). Promoter activity in the trunk at 3 dpf and 4 dpf was unaltered in *flt1* deficient zebrafish embryos. Additionally, ectopic sprouts also showed reporter gene expression. These data confirm a vessel specific expression of *esm1* in the zebrafish model.

In summary, *esm1* is expressed in the vasculature during ongoing zebrafish development but most importantly in the developing and established trunk vascular network.

5.1.3 *Esm1* is active preferentially in arterial endothelial cells and subset of neurons

Esm1 activity in a subset of neurons was revealed. Furthermore, *esm1* seems to be most likely expressed in EC of arterial identity. The specificity of *esm1* expression in these anatomical region should be confirmed with a stable reporter line. The expression domains are quite similar to that found in a BAC *flt1* reporter line, where *flt1* is active in a subset of neurons and a marker for arterial ECs (Wild, 2016; Wild *et al.*, 2017). Also, neurons and somites are sources for the ligand Vegfaa (Rossi *et al.*, 2016; Wild *et al.*, 2017). It could be hypothesized, that secretion of *Esm1* by arteries and neurons might regulate bioavailability of Vegfaa for either receptor, Flt1 or Kdrl, by establishing a Vegfaa gradient. Similarities between *esm1* and *flt1* expression pattern could be coincidental or *esm1* could be an artery specific modulator of Vegfaa response.

The proposed *esm1* gene expression in lymphatic vessel should be validated with a stable reporter line.

5.1.4 BAC transgenesis as an alternative tool to study gene expression

A BAC harbors a genomic fragment, which is up to 300kb in size (Bussmann and Schulte-Merker, 2011; Beil *et al.*, 2012). The generation of a reporter line has many benefits when compared to mRNA localization *via* WISH. First, studies can be performed *in vivo*, and thus even enables time-lapse imaging. Second, embryos undergo much less treatments and do not need to be fixed. Third, BAC transgenesis is much more sensitive to detection and the construct can basically be in any cell of the embryo. Also, studies can be performed, even when the promoter regions are still unknown. On the other hand, drawbacks of this approach have to be considered. First, transgenesis is inefficient in general and thus the low probability of germ line transmission, as well. Second, the recombineering process to obtain a BAC reporter construct is elaborate. Third, the BAC is unspecifically integrated into the genome, even multiple times (Beil *et al.*, 2012).

The BAC CH211-66D12 was identified and recombineered as described by Bussmann and colleagues (Bussmann and Schulte-Merker, 2011). This way, a reporter construct for *esm1* promoter activity was obtained. The size of the sequences upstream and downstream of the *esm1* gene let assume a high coverage of its promoter. A promoter is a DNA segment on which proteins assemble to form a pre-initiation complex for transcription. This DNA sequence specifies transcription start sites (TSS) and be up to several thousand base pairs upstream of the TSS (Juven-Gershon *et al.*, 2008; Bai and Morozov, 2010; Yella, Kumar and Bansal, 2018). In eukaryotes, promoter DNA segments are classified as core promoter,

proximal promoters and distal promoter: the first are distinctively positioned in relation to the TSS; the second are sequences of 500bp relative to the TSS; the last are further away and include enhancer, silencer and insulator sequences (Carninci *et al.*, 2006; Sandelin *et al.*, 2007; Lenhard, Sandelin and Carninci, 2012; Yella, Kumar and Bansal, 2018). Accordingly, the probability that the entirety of the *esm1* promoter, which is still unknown for *esm1*, is contained within the BAC is high and thus this molecular tool is suitable for the studies performed during this project. However, disadvantages of this method has to be kept in mind, and alternative approaches for generation of transgenic lines could be applied, such as knock-in of a reporter gene *via* CRISPR/Cas9 or introducing a construct carrying a core promoter sequence only (Beil *et al.*, 2012).

The expression profile in the trunk vasculature found by BAC transgenesis was in accordance with that of the WISH. Thus, the chosen BAC seems to be reliable. Moreover, the fluorescent signals were overlapping with that of the vascular reporter *kdrl*. Because injected embryos were analyzed not all cells become transgenic due to mosaic distribution of the reporter construct. Thus, expression is not present in the entire structure, and eventually not in the entire embryo.

5.2 Esm1 alone does not influence the vascular architecture in the trunk

Alteration of *esm1* expression did not result in any detectable changes in the patterning of vessels in the zebrafish trunk. The number of segments or branching points was unchanged in GOF and LOF models. Furthermore, the development of the trunk vasculature in *esm1* knock out zebrafish embryos was not distinctively altered from 1 dpf to 4 dpf. Thus, *esm1* is neither sufficient nor necessary for primary and secondary sprouting. Accordingly, at these stages *esm1* should be considered as a vascular specific marker gene with unknown function. This is consistent with literature stating that in cell culture loss of *ESM1* alone does not result in a phenotype (Shin, Huggenberger and Detmar, 2008).

5.3 Esm1 has minor effect on ISV morphology and endothelial cell proliferation

In zebrafish embryos with inactive *esm1* some minor changes in morphological parameters affecting vascular resistance were observed. Vascular resistance is related to blood pressure and blood flow. Indeed, *ESM1* is associated with hypertension, but is predominantly known as a marker for cardiovascular conditions rather than affecting blood pressure (Celik *et al.*, 2015; Sun *et al.*, 2019). Further studies have to be performed to reveal if these variations have considerable effect on zebrafish physiology or if they compensate

each other in some way and if these effects can be related to EC identity. Moreover, it has taken into consideration that these morphological changes might be attributed to pronounced effects of another molecule when *esm1* is missing.

Increased number of cells in aISVs and vISVs upon loss of *esm1* let assume an inhibitory effect on cell proliferation. While VEGF-A is known to potentiate cell proliferation, binding partners of dermatan sulfate PGs, the family to which Endocan belongs to, include ECM components which also have proliferative effect on ECs (Boilly *et al.*, 2000; Trowbridge and Gallo, 2002; Olsson *et al.*, 2006). It is likely, that the proliferative effects observed in the *esm1* mutants can be attributed to an interaction partner in the ECM, for example fibroblast growth factor, rather than an effect on Vegfaa signaling because Vegfaa bioavailability was to be unaltered. Additional studies have to be performed to elucidate this issue.

5.4 Spinal cord vascularization is modulated by Esm1 when Vegfaa/Kdr1 signaling is highly active

The role of *esm1* in angiogenesis was analyzed in GOF and LOF experiments. Until now, a potential function of *esm1* on the trunk vascular system in the zebrafish remained elusive.

With regard to *esm1* LOF experiments, putative unspecific site effects of antisense morpholino and alleged compensatory effects of genetically disrupting *esm1* masking inactivation phenotypes had to be considered. Therefore, both approaches, morpholino based translational block and genetic deletion of *esm1*, were used in parallel. Any phenotype arising by both LOF approaches has to be considered as specific. Concerning GOF experiments, plasmid injections of *esm1* under the control of either an ubiquitously expressed or blood vessel specific promoter yield mosaic overexpression.

Augmenting Vegfaa bioavailability in zebrafish was achieved by deficiency of *flt1* or *vhl* resulting in a hypersprouting phenotype at 3 dpf and 4 dpf. They are models for physiological spinal cord vascularization around 13 dpf. Different approaches were applied to proof a relationship between Vegfaa bioavailability and *esm1*: 1) *Esm1* knock down in fish deficient for *flt1* or *vhl*. 2) *flt1* knock down in *esm1*^{sa11057}. 3) Ubiquitous and blood vessel specific overexpression of *esm1* in *flt1* or *vhl* LOF models. 4) *esm1;flt1* double mutants. It could be hypothesized that with low *esm1* levels, Vegfaa bioavailability for Kdr1 decreases and consequently, ectopic sprouting is diminished. The other way around overexpression of *esm1* increased spinal cord vascularization in Vegfaa GOF models. Changes in the vascular network ventral of the neural tube were not observed. Accordingly, only the degree of tertiary sprouting seemed to be affected. The angiogenic process appeared unaffected because no

variations in both segments and branching points were recognized. It would be interesting to investigate, if *esm1* mutants develop hypersprouting at the neuro-vascular interface at 13 dpf, when it occurs under normal condition. These data could be confirmed even more by establishing a stable *esm1* GOF line and *esm1;vhl* double mutants.

Previous studies in cell culture and in the mouse model revealed enhanced *ESM1* levels during angiogenesis, which is requirement in the formation of tertiary sprouts (Shin, Huggenberger and Detmar, 2008; Rocha *et al.*, 2014; Eilken *et al.*, 2017). This thesis showed in two scenarios of increased Vegfaa bioavailability that *esm1* is a major player in establishing the trunk vascular pattern. Indeed, ectopic sprouting was largely decreased upon deficiency of either *flt1* or *vhl* when *esm1* levels were low. As proposed by Wild *et al.*, with loss of *flt1* or *vhl* function, more Vegfaa is available to bind to Kdr1 and results in a highly active Vegfaa/Kdr1 signaling. Subsequently, angiogenesis occurs, ectopic sprouts are formed and *esm1* becomes upregulated (Wild *et al.* 2017). Relating to this hypothesis, *ESM1* was described a downstream target VEGF-A/VEGFR-2 signaling cascade, thus encouraging this hypothesis (Conway, Collen and Carmeliet, 2001; Carmeliet, 2003; Shin, Huggenberger and Detmar, 2008; Rocha *et al.*, 2014; Eilken *et al.*, 2017).

Loss of *flt1* or expression of *vegfaa* in neurons of the spinal cord enable formation of ectopic sprouts (Wild *et al.*, 2017). Simultaneous expression of *esm1* and *vegfaa* in neurons might be substantial. With close spatial relation, Esm1 could modulate Vegfaa bioavailability with high efficiency and indirectly regulate angiogenesis at the level of the spinal cord (Fig. 5-1a). The performed *esm1* overexpression experiments substantiate the hypothesis.

A potential analogy between *flt1* and *esm1* concerning gene expression in arterial ECs and neurons could indicate an alleged governing effect of Esm1 on *flt1* positive cells concerning Vegfaa signaling transduction. However, reproducibility of the knock down and overexpression experiments in *vhl* mutants let assume that action of Esm1 is attributed to the higher abundance of Vegfaa rather than to the absence of *flt1*. Upon biallelic *vhl* inactivation, *vegfaa*, *flt1* and *kdrl* are simultaneously upregulated (Bluyssen *et al.*, 2004; van Rooijen *et al.*, 2011). As shown in this work, *esm1* is another gene with increased activity upon loss of *vhl* function. Accordingly, *vhl* mutants simulate a Vegfaa GOF scenario and do not represent an alternative for inactive *flt1*. The findings let propose a competition between Esm1 and Vegfaa for binding an ECM molecule. Thus, release of Vegfaa, capable of binding to Kdr1, into the ECM is modulated.

5.4.1.1 Reliability of morpholino experiments

In this project, a translational knock down was achieved using morpholino. This approach has many benefits. Morpholinos are stable, able to target the region of interest (splice variant knock down or translational knock down) and can easily be introduced into the egg cell by microinjection. Nonetheless, disadvantages come along with this method. Growth of the organism results in dilution of the morpholino and thus, the effect milder over time. Furthermore, reported morphant phenotypes were absent in the respective mutant (Law and Sargent, 2014; Kok *et al.*, 2015; Rossi *et al.*, 2015; Joris *et al.*, 2017). Thus, morpholinos have to be used in a moderate concentration and the results taken with caution. Its side effects can be evaluated by introducing the morpholino into the corresponding mutant. Alternative approaches, for example altered CRISPR/Cas9 method, in which no breaks are induced but spatially inhibits translation, should be considered (Liu *et al.*, 2016).

In the performed experiments a control morpholino was used to exclude any effects from injection. Next to that, the concentrations were always the same and moderately low. *Flt1* knock down was performed in previous studies. According to that, the concentration was already determined and their side effects analyzed in the corresponding mutant (Krueger, 2012; Wild *et al.*, 2017). Similarly, side effects concerning the *esm1* morpholino were evaluated in this work. The concerning experiments were performed with a reasonable amount of morpholino.

5.5 Esm1 affects binding efficiency of Vegfaa to Kdr1

Endocan and VEGF-A are present in the ECM and in literature a relationship between these molecules with a common ECM component was proposed (Trowbridge and Gallo, 2002; Rocha *et al.*, 2014). In the following two scenarios are proposed, how Esm1 and Vegfaa work together to affect ectopic sprouting in the zebrafish trunk: 1) Esm1 fosters binding of Vegfaa to Kdr1 through an ECM component. 2) Vegfaa and Esm1 rival for an ECM component and more Vegfaa is liberated upon presence of its competitor (Fig. 5-b). In both scenarios, angiogenesis is encouraged. Thus, the mode of action could be as follows (Fig. 5-1c): in the wildtype, binding of Esm1 and Vegfaa to a common ECM component is balanced. With loss of Esm1, more Vegfaa will remain bound in the ECM, thus Vegfaa/Kdr1 signaling will be less active and consequently the vascular patterning unaltered. In Vegfaa GOF scenarios, Vegfaa is present in high abundance. Accordingly, bioavailability of Vegfaa for Kdr1 is increased and angiogenesis is driven as seen by emerging ectopic sprouts. Furthermore, *esm1* is overexpressed to increase Vegfaa/Kdr1 signaling. However, when

Vegfaa is present in excess and *esm1* is deficient, sprouts will still be formed but in less efficient manner.

In the wildtype, *flt1* is artery specific while *vhl* is ubiquitously expressed and thus it has to be tested if an exclusive expression of *esm1* in arterial ECs is of any importance at all or if it aids in the formation of a Vegfaa gradient from a vISV to an aISV (Fig.5-1a).

Depending on the isoform, a biochemical gradient of freely diffusible VEGF-A could develop that might probably be altered by ESM1 through a common binding partner in the ECM, such as Fibronectin, as illustrated in figure 5-1a (Park, Keller and Ferrara, 1993; Rocha *et al.*, 2014). Thus, affecting sprouting of blood vessels. *Fibronectin* is increasingly expressed in *vhl* mutants and is proposed as a common binding partner for Vegfaa and Endocan (Trowbridge and Gallo, 2002; Bluysen *et al.*, 2004; van Rooijen *et al.*, 2011; Rocha *et al.*, 2014). Further studies should provide proof to confirm rivalry over Fibronectin or if other contestants can be identified.

ESM1 could dose the amount of freely available VEGF-A in the ECM. In cell culture and mouse models distinct binding affinities of VEGF-A to heparin or proteases was described, thus modulating the amount VEGF-A for receptor binding (Ferrara, 2010). Binding to VEGF-A occurs through heparan sulfate PGs (Houck *et al.*, 1992).

While direct binding of ESM1 to growth factors and cytokines is feasible, VEGF-A is an unlikely binding partner (Trowbridge and Gallo, 2002). ESM1 is a PG interacting through its dermatan sulfate chains and while VEGF-A binds heparin sulfate PGs. Furthermore, dermatan sulfate chains in ESM1 allow binding to positively charged molecules while charge of VEGF-A depends on the splicing form (Ferrara, 2010). Another possibility is protease-induced VEGF-A liberation independent of heparin (Park, Keller and Ferrara, 1993). This knowledge encourages the hypothesis of a common binding partner in the ECM rather than direct binding.

5.6 Using Esm1 for treating vascular conditions in medicine

Any therapies aimed directly at the VEGF-A/VEGFR-2 signaling cascade are closely tied to severe side effects (Roodhart *et al.*, 2008). Consequently, alternatives for fine regulation of blood vessel growth are needed. A feasible approach is the use of indirect regulators of VEGF-A bioavailability for VEGFR-2, such as ligands for the decoy receptor VEGFR-1 or, as revealed in this study, ESM1. Due to the blood vessel specificity and its relation to VEGF-A, ESM1 could be exploited in strategies for augmenting or alleviating blood vessel growth. ESM1 might thus be suitable for application in tumor or regenerative therapies.

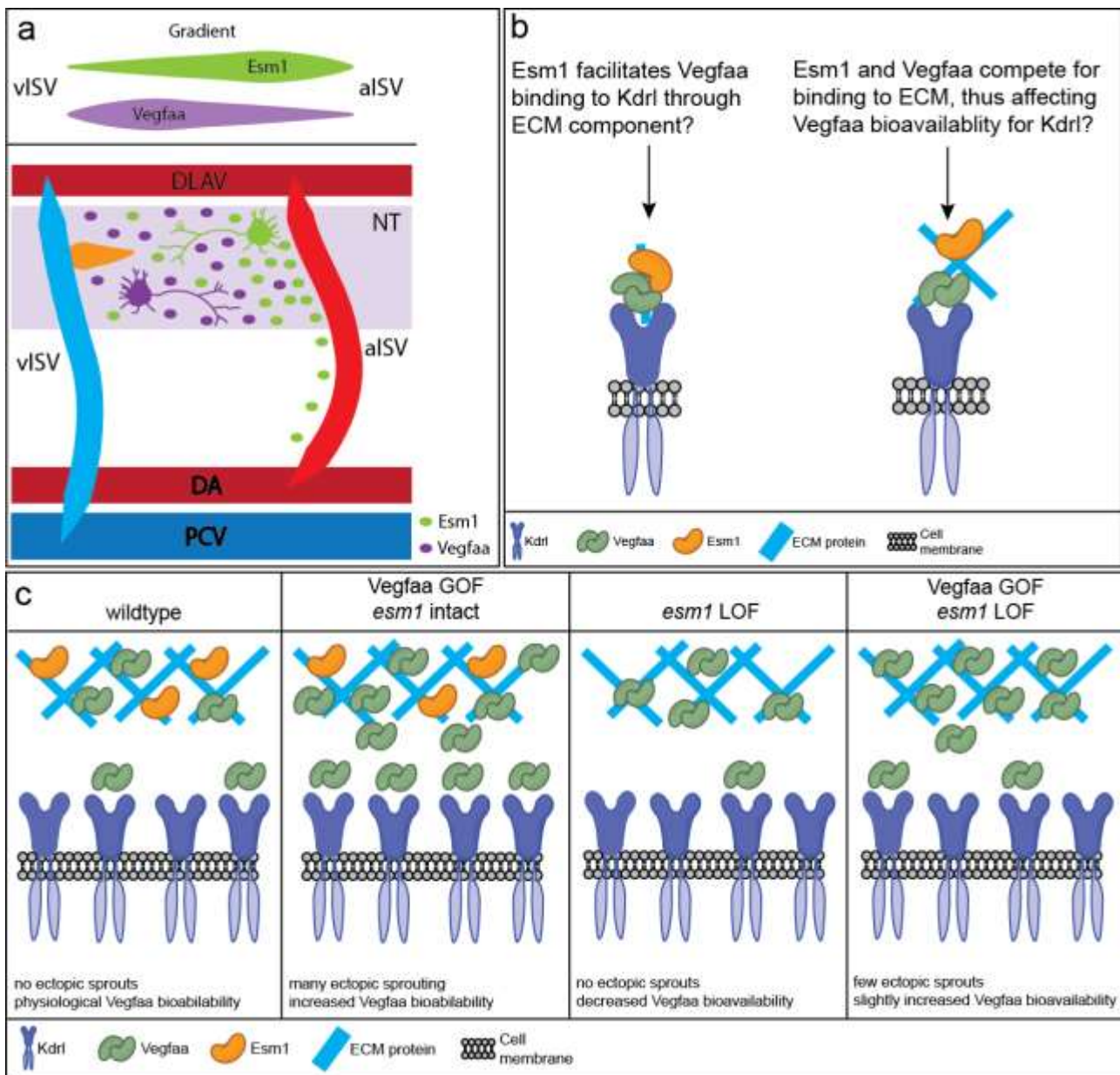


Figure 5-1. Hypothesis how Esm1 modulates bioavailability of Vegfaa for Kdr1. (a) Esm1 forms a trend affecting a Vegfaa gradient and thus aiding in formation a vascular segment. (b) Two scenarios could of a relationship between Esm1 and Vegfaa are reasonable: Either Esm1 facilitates binding of Vegfaa to Kdr1 through an ECM component or Esm1 and Vegfaa rival over binding to an ECM component, thus liberating Vegfaa for Kdr1 binding. (c) Mode of action how a possible competition between Esm1 and Vegfaa over binding to an ECM molecule could regulating binding of Vegfaa to Kdr1.

6 Material and Methods

6.1 Material

6.1.1 Transgenic and mutant zebrafish lines used

The lines Tg(*kdr*:EGFP)^{S843} (Jin *et al.*, 2005), Tg(*kdr*:hsa.-HRAS-mCherry)^{S916} (Hogan *et al.*, 2009), Tg(*xla.Tubb*:DsRed)^{zf148} (Peri and Nüsslein-Volhard, 2008), Tg(*fli1a*:nGFP)^{y7} (Kulik *et al.*, 2002), Tg(*flt1^{enh}*:tdTomato), Tg(*flt4*:mCitrine)^{hu7135}, TgBAC(*flt1*:YFP)^{hu4624} (Bussmann *et al.*, 2010) and *vh*^{hu2117} (van Impel *et al.*, 2014) and were published elsewhere. The lines *flt1^{ka602}* and *flt1^{ka604}* were generated in this lab in previous work (Wild *et al.*, 2017). Details about the lines are listed in table 6-1 and 6-2.

Table 6-1. Zebrafish transgenic reporter lines

Transgenic line	Marked Cells/Tissue	Publication
Tg(<i>fli1a</i> :nGFP) ^{y7}	Green fluorescent nuclei of EC and NCCs in green	Kulik <i>et al.</i> , 2002
Tg(<i>flt1^{enh}</i> :tdTomato)	Labeling of non-neuronal, arterial vascular endothelium with red fluorescent protein.	Bussmann <i>et al.</i> , 2010
Tg(<i>flt4</i> :mCitrine) ^{hu7135}	Yellow fluorescence of venous ECs	Bussmann <i>et al.</i> , 2010
Tg(<i>kdr</i> :eGFP) ^{S843}	Green cytosol of blood vessels cells	Jin <i>et al.</i> , 2005
Tg(<i>kdr</i> :hsa.-HRAS-mCherry) ^{S916}	Red fluorescent labeling of EC membranes	Hogan <i>et al.</i> , 2009
Tg(<i>lyve1b</i> :eGFP) ^{z150}	Labeling of lymphatic vessels with green fluorescent protein.	Okuda <i>et al.</i> , 2012
Tg(<i>xla.Tubb</i> :DsRed) ^{zf148}	Mature neurons labeled with red fluorescent protein	Peri and Nüsslein-Volhard, 2008
TgBAC(<i>flt1</i> :YFP) ^{hu4624}	arterial endothelium and <i>flt1</i> ⁺ specific labeling with yellow reporter protein	Bussmann <i>et al.</i> , 2010

Table 6-2. Zebrafish mutant lines

Mutant line	Mutation	Publication
<i>esm1</i> ^{sa11057}	point mutation in exon 1, premature stop codon	this work
<i>flt1</i> ^{ka602}	5 bp deletion in exon 3, frame shift mutation.	Wild <i>et al.</i> , 2017
<i>flt1</i> ^{ka604}	14 bp deletion in exon 3, frame shift mutation.	Wild <i>et al.</i> , 2017
<i>vh1</i> ^{hu2117}	point mutation in exon	van Rooijen <i>et al.</i> , 2011

6.1.2 Solutions and buffer

In table 6-3 recipes for preparation of solutions and buffers are listed.

Table 6-3. Composition of solutions and buffer

Solution	Composition
Base solution (50x)	1.25M NaOH; 10mM EDTA; pH 12
Cas9 working buffer (1x)	20mM HEPES; 15 mM KCl; pH 7.5
E3 medium (60x)	34.8g NaCl; 1.6g KCl; 5.8g CaCl ₂ •2 H ₂ O; 9.78g MgCl ₂ •6 H ₂ O; in 2l H ₂ O
Egg water (10x)	7.5ml 60mg/ml (w/v) sea salt stock solution; 2.5ml 0.1% methylenblue solution; in 500ml ddH ₂ O
Hybridization mix	50% (v/v) formamide; 5× SSC; 0.1% (v/v) Tween-20; 50µg/ml of heparin; 500µg/ml of RNase-free tRNA
IPTG solution	200 mg/ml dissolved in dH ₂ O
LB-agar	20g LB medium in 1l H ₂ O; 1.5% (w/v) agar-agar
LB-media	20g LB in 1l H ₂ O
Loading buffer (5x)	0.5% (w/v) orange G; 50% (v/v) glycerol; 25mM EDTA; pH 8.0
MAB-T (1x)	1x maleic acid buffer; 0.1% (v/v) Tween-20
Maleic acid buffer (5x)	58g maleic acid; 43.5g NaCl; 37.5g NaOH in 1l dH ₂ O, pH 7.5
Neutralization solution (50x)	2M Tris-HCl; pH 5

NTMT	0.1M Tris-HCl pH 9.5; 0.1M NaCl; 1% Tween-20; 50mM MgCl ₂
PBS (10x)	800g NaCl; 20g KCl; 144g Na ₂ HPO ₄ · 2H ₂ O; 24 g KH ₂ PO ₄ ; add up to 10l
PBT (1x)	1x PBS, 0.1% (v/v) Tween-20
Pronase solution	1mg/ml in egg water
PTU (10x)	304mg 1-phenyl-2-thiourea (PTU); 16.66ml E3 stock solution (60x); add to 1l with ddH ₂ O
RNAse A solution	100ng/μl RNAse A in RNase buffer
RNase buffer	HEPES 0.1M pH 7.5; NaCl 0.15M; 0.1% Tween-20
SOC medium	20mM MgCl ₂ ; 20mM MgSO ₄ ; 20mM glucose in ddH ₂ O
SSC (20x)	175.3g NaCl; 88.2g trisodium citrate; add up with ddH ₂ O to 1l; pH 7.
TAE buffer (1x)	20mM Tris-base; 10mM acetic acid; 0.5mM EDTA; pH 8.0
Tricaine (25x)	0.4g Tricaine; 2.1ml 1M Tris pH 8.5; add to 100 ml with ddH ₂ O
X-Gal solution	2% (w/v) X-Gal in DMSO

6.1.3 Enzymes, chemicals and kits

Enzymes are listed in table 6-4. Commercial kits are summarized in table 6-5.

Table 6-4. Enzymes

Enzyme	Provider/Manufacturer
Cas9 nuclease	Integrated DNA Technologies
GoTaq DNA Polymerase	Promega
LR Clonase II plus	Thermo Fisher Scientific
Phusion HS II DNA Polymerase	Thermo Fisher Scientific
Restriction enzymes	Promega
RNA Polymerases	Roche Life Science, Thermo Fisher Scientific
T4 DNA Ligase	Promega
Thermosensitive alkaline phosphatase	Promega

Table 6-5. Commercial kits

Product/Kit	Manufacturer
Dig RNA Labeling Kit (SP6/SP7)	Roche Life Science
GoScript™ Reverse Transcription Kit	Promega
mMessage MACHINE SP6 ULTRA transcription Kit	Thermo Fisher Scientific
Monarch DNA Gel Extraction Kit	New England Biolabs
Monarch PCR & DNA Cleanup Kit	New England Biolabs
Plasmid DNA purification NucleoBond® Xtra Midi kit	MACHEREY-NAGEL
QIAprep Spin Miniprep Kit	QIAGEN
RNeasy Mini Kit	QIAGEN

6.1.4 Oligonucleotides

Primer for genotyping, real-time PCR and cloning were purchased from Eurofins Genomics and morpholino were acquired from Gene Tools. Primer sequences are listed in table 6-6 and 6-7 respectively. Details about morpholino sequences are summarized in table 6-8.

Table 6-6. Primer sequences for real-time qPCR or genotyping

Primer name	Primer sequence (5'-3')
Esm1_3'UTR_rev	ATGGGATGCCATATCTGTGAACT
Esm1_5'UTR_fw	CTGAGCCGCTTCATTCCTG
Esm1_E1_rev	TTATGCTTTAAATGTAGCACTCGAT
Flt1_E3_fw	CAGCTCAACACACACAGTATTGTTTTA
Flt1_E3_rev	ACACCTGAAGCATCTTACCTGTGA
Vhl_fw	AGTCACGTACACAGTCTTTCTCTCC
Vhl_rev	AACGCGTAGATAGCAATTTACCAA
zesm1_E2- E2/3_rev	AACCCACTTCATTACCTGCTT CA
β-actin_fw	CTCTTACCTCAGTTACAATTTATA
β-actin_rev	TTCTGTCCCATGCCAACCA

Table 6-7. Primer sequences for construct cloning

Primer name	Primer sequence (5'-3')	Purpose
amp_HA1_Cntrl_fw	CTGAGATAGGTGCCTCACTG	BAC
amp_HA1_Cntrl_rev	ACATTTCCCGAAAAGTGG	BAC
BAC Esm1 HA1 Cntrl fw	CTGAGCCGCTTCATTCCTG	BAC
BAC Esm1 HA2 Cntrl rev	ATTTGTCCGGGCAATTCACG	BAC
Esm1_HA1_mCitrine_fw	TCCTCCCCAACACTGCAGACCCGAAGATCGCAT CCAACCCGCCGCTTGCAACCATGGTGAGCAAG GGCGAGGAG	BAC
Esm1_HA2_Kan_rev	GTCTCTCCAAAAACACCATCAGTACGAACATC AGGATGGCAAACACACGTCAGAAGAACTCGTCA AGAAGGCG	BAC
Esm1cds_fw	TG CGT GTG TTT GCC ATC CTG ATG TTC GTA CTG AT	ISH
Esm1cds_rev	TCA GCG AGG GGT GAG GAA ATT GCG AGC GGA GGC CC	ISH
kanR_HA2_Cntrl_fw	TCCTCGTGCTTTACGGTATC	BAC
mCitrine_HA1_Cntrl_rev	GGACACGCTGAACTTGTGG	BAC
pCS2+_Esm1cds_fw	GCGGGAATTGGATCCATGCGTGTGTTTGCCATC CT	OE
pCS2+_Esm1cds_rev	CTAGTGATTCTCGAGTCAGCGAGGGGTGAGGA AAT	OE
pTarBAC_HA1_Cntrl_fw	CTGTCAAACATGAGAATTGGTC	BAC
pTarBAC_HA1_iTol2_fw	GCGTAAGCGGGGCACATTTTCATTACCTCTTTCT CCGCACCCGACATAGATCCCTGCTCGAGCCGG GCCCAAGTG	BAC
pTarBAC_HA2_Cntrl_rev	GAGAGCCTTCAACCCAGTC	BAC
pTarBAC_HA2_iTol2_rev	GCGGGGCATGACTATTGGCGCGCCGGATCGAT CCTTAATTAAGTCTACTAATTATGATCCTCTAGA TCAGATC	BAC

BAC, BAC recombineering; ISH, in situ hybridization; OE, overexpression

Table 6-8. Morpholino

Morpholino	Target	Sequence (5'-3')	Amount used
Control	none	CTCTTACCTCAGTTACAATTTATA	1 ng
Esm1	ATG of <i>esm1</i>	ACATCAGGATGGCAAACACACGCAT	1 ng
Flt	ATG of <i>flt1</i>	ATATCGAACATTCTCTTGGTCTTGC	1 ng

6.1.5 Tools for mutant generation

crRNAs, tracrRNA and Cas9 nuclease were purchased from Integrated DNA Technologies. crRNA sequences are shown in table 6-9.

Table 6-9 crRNA target sequences used for CRISPR/Cas9 mutagenesis

Target gene	crRNA sequence (without PAM)
Esm1_3'UTR	AGACAGTAATAATGTTCCCT
Esm1_5'UTR	GCGGGTTGGATGCGATCTTC

6.1.6 Plasmids

For some experiments, some plasmids were already available for various purposes. Those are listed in table 6-10. Plasmids cloned during this work are summarized in table 6-11.

Table 6-10. Plasmids generated elsewhere

Plasmid	Purpose	Manufacturer or provider
BAC CH211-66D12	BAC Recombineering	BACPAC Resources
p3E_polyA	Gateway cloning	Gift from Kawakami K, NIG, Japan
p5E_fli1a	Gateway Cloning	Janna Krueger; Max Delbrück Center Berlin, Germany
pCR8GW-iTol2-amp	BAC Recombineering	Bussmann and Schulte-Merker, 2011
pCS2+	Mammalian overexpression	Seyfried, S; Max Delbrück Center Berlin, Germany
pCS2+_mCitrine_kanR	BAC recombineering	Bussmann and Schulte-Merker, 2011
PCS2FA	tol2 transposase mRNA	Kwan <i>et al.</i> , 2007

pDestTol2CG2	Gateway cloning	Gift from Kawakami K, NIG, Japan
pGEM-T Easy	TA-Cloning	Promega GmbH, Mannheim, Germany
pME_eGFP-p2a_Smal	Gateway cloning	Wild <i>et al.</i> , 2017
pRedET	BAC Recombineering	Bussmann and Schulte-Merker, 2011

Table 6-11. Plasmids generated in this work

Plasmid	Purpose
pCS2+_esm1	Overexpression
pDest_fli1a_eGFP-p2a-esm1cds	EC specific overexpression
pGEMT_esm1cds	In situ hybridization
pME_eGFP-p2a-esm1cds	Overexpression

6.1.7 Online tools and softwares

Sequences were found in genome browsers and then employed for virtual cloning, genotyping and finding target sequences for knockdown or mutagenesis applications. Furthermore, word processing, image editing, graphical illustration as well as biostatics software were exerted for proper description of findings. A summary of is presented in table 6-12.

Table 6-12. Online tools and softwares used

Product	Description	Provider/Source
Adobe Illustrator CS6	Graphical illustration	Adobe Systems
Adobe Photoshop CS6	Image editing	Adobe Systems
ChemDraw Professional	Graphical illustration	PerkinElmer Informatics
Crispor	sgRNA target finding	Tefor Infrastructure
Fiji	Image editing and processing	Open source
GraphPad Prism	Biostatics	GraphPad Software
Microsoft Office	Word processing, spreadsheet and presentation	Microsoft

NCBI Primer Blast	Primer sequence finding tool	National Center for Biotechnology Information
NCBI pubmed	Publication database	National Center for Biotechnology Information
SnapGene	DNA sequence analysis and virtual cloning	GSL Biotech
UCSC Genome Browser	Genome browser	University of California Santa Cruz

6.2 Methods

6.2.1 Ethics statement

Zebrafish maintenance and experiments were performed according the German animal protection standards and were approved by the Government of Baden-Württemberg, Regierungspräsidium Karlsruhe (Akz: 35-9185.81/G-11/19 and 35-9185.82/A-17/19).

6.2.2 Zebrafish methods

6.2.2.1 Maintenance of zebrafish embryos and prevention of melanization

Female and male zebrafish were placed into a breeding tank overnight (o/n). In this tank the fish share the same water and see each other but were physically separated. In the morning the partition was removed so that the fish could mate. Fertilized zebrafish eggs were collected after spawning and then kept at 28°C in 1x egg water.

If experiments required transparent larvae, embryos were transferred into 1x E3 medium containing 0.2mM 1-phenyl-2-thiourea (PTU), which disturbs the melanization pathway by inhibiting tyrosinases (Whittaker, 1966).

For analysis of embryos before hatching, the chorion was removed either manually using forceps or enzymatically by incubation in pronase solution

6.2.2.2 Microinjections

Zebrafish eggs were collected directly after spawning and placed into an injection ramp. The ramp was casted by dissolving 2% (w/v) agarose in egg water. The solution was poured into a 90mm petri dish and a mold placed into the still liquid agarose. Microinjection needles

were prepared from 1mm capillary tubes with filaments (World Precision Instruments) pulled in a needle puller (Sutter Instruments Co.).

The embryos were injected at the one-cell-stage. 1nl of injection mixture was released into the cell by applying pressure with a gas microinjector. Morpholino were injected into the yolk, whereas for mutagenesis and transgenesis experiments the solution was injected into the egg cell.

6.2.3 Molecular biological methods

6.2.3.1 Polymerase chain reaction

Polymerase chain reactions were performed with either GoTaq® DNA Polymerase (Promega) or Phusion Hot Start II DNA Polymerase (Thermo Fisher Scientific) in case proof-reading was required. The first was chosen for genotyping and the latter for cloning purposes. Conditions for the amplification reaction were taken from the manufacturers' instructions.

6.2.3.2 Agarose gel electrophoresis

The separation of nucleic acids as well as analysis of the size of DNA fragments was analyzed with agarose gel electrophoresis.

Loading buffer was added to the sample. The mixture was then loaded on a 1% (w/v) agarose gel and run in 1x TAE buffer at 100V. Visualization of nucleic acids was accomplished by addition of Midori Green Advance (Nippon Genetics) staining solution into the gel as suggested by the provider and subjecting it to UV-light.

6.2.3.3 RNA extraction and first-strand cDNA synthesis

Dechorionated embryos were collected at the desired embryonic stage and then shock-frozen in liquid nitrogen with as less surplus medium as possible. Afterwards, they were stored at -20°C until use.

Purified total RNA of the zebrafish embryos fish was obtained using the RNeasy Mini Kit (Qiagen). The extraction was performed according to the manufacturers' manual.

First-strand cDNA was synthesized using the GoScript™ Reverse Transcription Kit (Promega) as described in the instruction of the manufacturer. Between 250-500ng RNA was used as template for the reverse transcription process. For cloning purposes Oligo-dT

primer were chosen, whereas for real-time qPCR analysis a mixture of Oligo-dT and random Hexamer primer were set in in the reaction.

6.2.3.4 Gene expression analysis by real-time qPCR

One sample batch consists of 30-50 embryos. Three batches per time point were collected, RNA extracted and cDNA synthesized.

For real-time qPCR analysis cDNA samples were mixed with SYBR® Green PCR Master Mix (Thermo Scientific). The reaction was conducted in the CFX Connect real-time PCR detection system (Bio-Rad). Gene expression was analyzed with the primer pairs *zesm1_E2- E2/3_fw/rev* and β -actin_fw/rev, respectively.

All *esm1* expression data was first normalized to the housekeeping gene β -actin. Afterwards, the data of the mutants was normalized to the mean of the wildtype sample of 3 dpf and 4 dpf, respectively.

6.2.3.5 Conventional cloning

All restriction enzymes, TSAP and the T4 DNA Ligase were purchased from Promega.

Linearization of plasmids was required for either cloning purposes or *in situ* probe synthesis. The enzyme was added to a mixture of buffer, recommended by the provider, 1-2 μ g plasmid and dH₂O. The reaction was performed at the enzyme-specific temperature for 60-90min.

Restriction digests result in phosphorylated plasmid ends. Hence, vector backbones were dephosphorylated with thermosensitive TSAP to prevent re-circularization of the plasmid. 2 μ l 10x restriction buffer, 2 μ g plasmid, 2 μ l TSAP were added into a total reaction volume of 20 μ l. The reaction was incubated at 37°C for 15min and afterwards stopped at 74°C for 15min. Next, the DNA was loaded onto an agarose gel and isolated with the Monarch® DNA Gel Extraction Kit (New England Biolabs).

The vector and the insert were ligated with the T4 DNA ligase according to the instruction of the manufacturer.

PCR products are blunt-ended and require the addition of 3' A-overhangs with the Taq DNA Polymerase. A-tailing was achieved by mixing purified PCR product, 0.2mM dATP, 1x PCR buffer, 1U GoTaq DNA polymerase (Promega). The volume was adjusted to 20 μ l with dH₂O and the reaction was incubated at 72°C for 20min.

6.2.3.6 Bacterial transformation

Chemocompetent JM109 cells or One Shot TOP10 Chemically Competent (Thermo Fisher Scientific) *E. coli* cells were used for transformation. The first served for re-transformations and products of standard cloning procedures and the latter for transformation of Gateway reactions.

DNA was added to the cells and the suspension kept on ice for 30min. Subsequently, bacteria were heat-shocked at 42°C for 45s and immediately cooled down on ice again for 2min. The heat shock permeabilizes the cell membrane, thereby enabling access of DNA into the cell. The bacteria were added to SOC-medium without antibiotics and then allowed to regenerate for 1h at 37°C under agitation at 225rpm. Next, the cells were plated onto LB agar plates and incubated o/n at 37°C. For clone selection, the plates were supplemented with the respective antibiotic.

The pGEMT vector allowed Blue/White selection. For this, agar plates were prepared in advance of spreading the cells. 4µl of IPTG solution and 40µl of the X-Gal solution were distributed over the surface of the LB agar plate. The cells were put onto the plates when the solutions were absorbed for 30min.

6.2.3.7 DNA preparations

For plasmid preparation either minicultures (4ml) or midicultures (100ml) were used. For this, the liquid LB medium supplemented with the appropriate antibiotic was inoculated with a single colony and let grown o/n at 37°C under agitation at 300rpm. Afterwards, the culture was harvested and the plasmid purified with the Qiaprep Spin Miniprep Kit (Qiagen) or Plasmid DNA purification NucleoBond® Xtra Midi kit (MACHEREY-NAGEL).

PCR products with a single band were isolated using the Monarch® PCR & DNA Cleanup Kit (New England Biolabs). PCR reactions resulting in multiple products were loaded on an agarose gel and the band of interest was cut out with a sterilized scalpel under a transilluminator and cleaned up with the Monarch® DNA Gel Extraction Kit (New England Biolabs).

The procedures for extraction, isolation and purification of nucleic acids were performed according to the respective instructions of the provider.

6.2.3.8 *In vitro* transcription

In situ probes and tol2 transposase mRNA were transcribed *in vitro*. Prior to *in vitro* transcription, the plasmids were linearized with the adequate restriction enzyme. A summary

of the RNA polymerase needed for transcription and the enzyme chosen for vector linearization is given in table 6-13.

RNA probes for whole mount *in situ* hybridization (WISH) were generated with the Dig RNA Labeling Kit (SP6/SP7) (Roche Life Science). tol2 transposase mRNA was generated from the pCS2FA plasmid (Whittaker, 1966) with the mMessage MACHINE SP6 ULTRA Transcription Kit (Thermo Fisher Scientific). Transcription was carried out according to the manufacturers' manual of the respective kit.

Table 6-13. mRNA generation from different plasmid

mRNA	RNA Polymerase	Enzyme for linearization
Esm1_cds WISH probe (AS)	SP6	Apal
Esm1_cds WISH probe (S)	T7	SpeI
tol2 transposase	SP6	BstBI

6.2.4 Staining methods

6.2.4.1 Whole mount *in situ* hybridization

Zebrafish embryos were collected at the desired developmental stage. Dechorionized embryos were fixed in 4% (w/v) PFA either for 2h at room temperature (RT) or o/n at 4°C. Following three washing steps with 1x PBT for 5 min, the fish were dehydrated in an ascending series of ethanol (25%, 50%, 75% (v/v) in 1xPBT), after which long-time storage in 100% ethanol at -20°C is possible. With the start of the WISH process, the embryos were rehydrated by subjecting them to a series of decreasing ethanol concentration until they are again in 1x PBT. The dehydration and rehydration permeabilizes the tissue, an important step for the procedure, which was further increased by transfer of the fish into acetone for 7min at -20°C. The embryos were then fixed again in 4% PFA for 20min and incubated in hybridization mix. After this pre-hybridization step, the embryos were put in RNA probe/hybridization mix solution and hybridization was allowed o/n at 62°C. Subsequently, formamid was removed in a descending series of hybridization mix in 2x SSC at the hybridization temperature down to 0.2x SSC at RT. Single stranded RNA was digested with incubation in RNase A (Thermo Fisher Scientific) solution for 45min. Next, the fish were washed in 1x MAB-T. The pH of the solution was regulated by addition of 37.5g NaOH and adjusted to pH7.5. Afterwards, non-specific antibody binding was prevented by incubation

of the embryos in 2% (w/v) Blocking Reagent in 1x MAB-T for 2 to 3h. Next, the fish were incubated with alkaline phosphatase-conjugated antibody anti-digoxigenin-AP, Fab fragments (Roche) o/n at 4°C. The antibody was used in a dilution of 1/4000 in blocking solution. The embryos were prepared for the subsequent staining reaction by following washing steps: 4 times in 1xMAB-T for 30min, twice for 15min in NTMT. For color development, BM-Purple (Roche), a colorimetric alkaline phosphatase substrate, was added to the fish and the reaction allowed to proceed in the dark at 37°C.

6.2.5 BAC Recombineering

A BAC was recombineered into a reporter construct to enable analysis of endogenous *esm1* expression using BAC transgenesis.

Identification of a suitable BAC, the recombineering and transgenesis process was performed as proposed by the group of Schulte-Merker (Kwan et al. 2007). The UCSC genome browser helped with the identification of the BAC CH211-66D12 (BACPAC Resources) in a pTarBAC2.1 backbone. The clone was confirmed for the *esm1* gene with the primers BAC Esm1 HA1 Cntrl fw/rev in a colony PCR. Positive clones were transformed with the pRedET vector. This vector carries genes for the homology- directed repair system, which are essential for the subsequent recombineering steps.

The transgenic insertion of the BAC was enabled due to the *tol2* transposon system. Accordingly, the first recombineering step was the integration of *tol2* sites into the BAC backbone. For this, a PCR product amplified from the plasmid pCR8GW-itol2-amp (kindly provided by S. Schulte-Merker) with the pTarBAC_HA1_iTol2_fw and pTarBAC_HA2_iTol2_rev primer was recombineered into the BAC. The insertion was checked with a PCR targeting the left *tol2* site and the right *tol2* site. The primers pTarBAC_HA1_control_fw and amp_HA1_control_rev amplified the former, whereas the primer pair amp_HA2_control_fw and pTarBAC_HA2_control_rev confirmed the latter site.

In the second recombineering step the reporter gene mCitrine was inserted 3' of the ATG of *esm1*. pCS2+_mCitrine_kanR (kind gift from S. Schulte-Merker) plasmid was used as a template from which a PCR product with the primers *esm1*_HA1_mCit_fw and *esm1*_HA2_kanR_rev was generated. Successful recombineering was confirmed with two PCRs: the first using the primer pair *esm1*_HA1_control_fw and Citrine _HA1_control_rev, and a second with kanR_HA2_control_fw and *esm1*_HA2_control_rev.

The BAC CH211-66D12 was recombineered as described by Bussmann and colleagues (Bussmann and Schulte-Merker, 2011) as illustrated in figure 4-5. The BAC contains a

zebrafish genomic fragment of 167kb in size. The *esm1* gene is sandwiched between 46kb upstream and 116kb downstream sequences. Alteration of the BAC into a reporter construct, which can be stably transposed into the genome, required the recombination of *tol2* sites and a reporter gene (*mCitrine*). The expression cassettes for the *tol2* sites and the reporter gene are flanked by homology arms, which are required for homologous recombination into the BAC. After recombination of the *mCitrine* gene, the translation start site of *esm1* gene in the genomic fragment will be missing. The construct was injected into the one-cell stage together with *tol2* mRNA and the embryos developed until the desired stage. Eventually, the *mCitrine* gene was expressed upon activation of the *esm1* promoter.

6.2.6 Cloning of pGEMT_ *esm1* cds

pGEMT_ *esm1* cds plasmid was cloned for the purpose to obtain a vector which carries the *esm1* coding sequence. The resulting vector served as a template for WISH RNA probe generation and for further re-cloning purposes.

The PCR product was obtained *via* Phusion PCR with the primer pair Esm1cds_fw/rev. The PCR product was purified and, after A-overhangs were added to the ends, cloned into the pGEMT-vector (Promega) using the TA-cloning system.

6.2.7 Cloning of pCS2+_ *esm1* cds

The pCS2+_ *esm1* cds plasmid was cloned for the execution of overexpression experiments. The vector contains a cytomegalovirus promoter for ubiquitous expression of the gene of interest.

The PCR product was obtained *via* Phusion PCR with the primer pair pCS2+_Esm1cds_fw/rev for which the pGEMT_ *esm1* cds served as a template. An adapter sequences were included into the primers, which contain restriction sites. Both the amplicon and the plasmid pCS2+ were digested with the restriction enzymes BamHI and XhoI. Afterwards, the plasmid pCS2+_ *esm1* cds was obtained using conventional cloning.

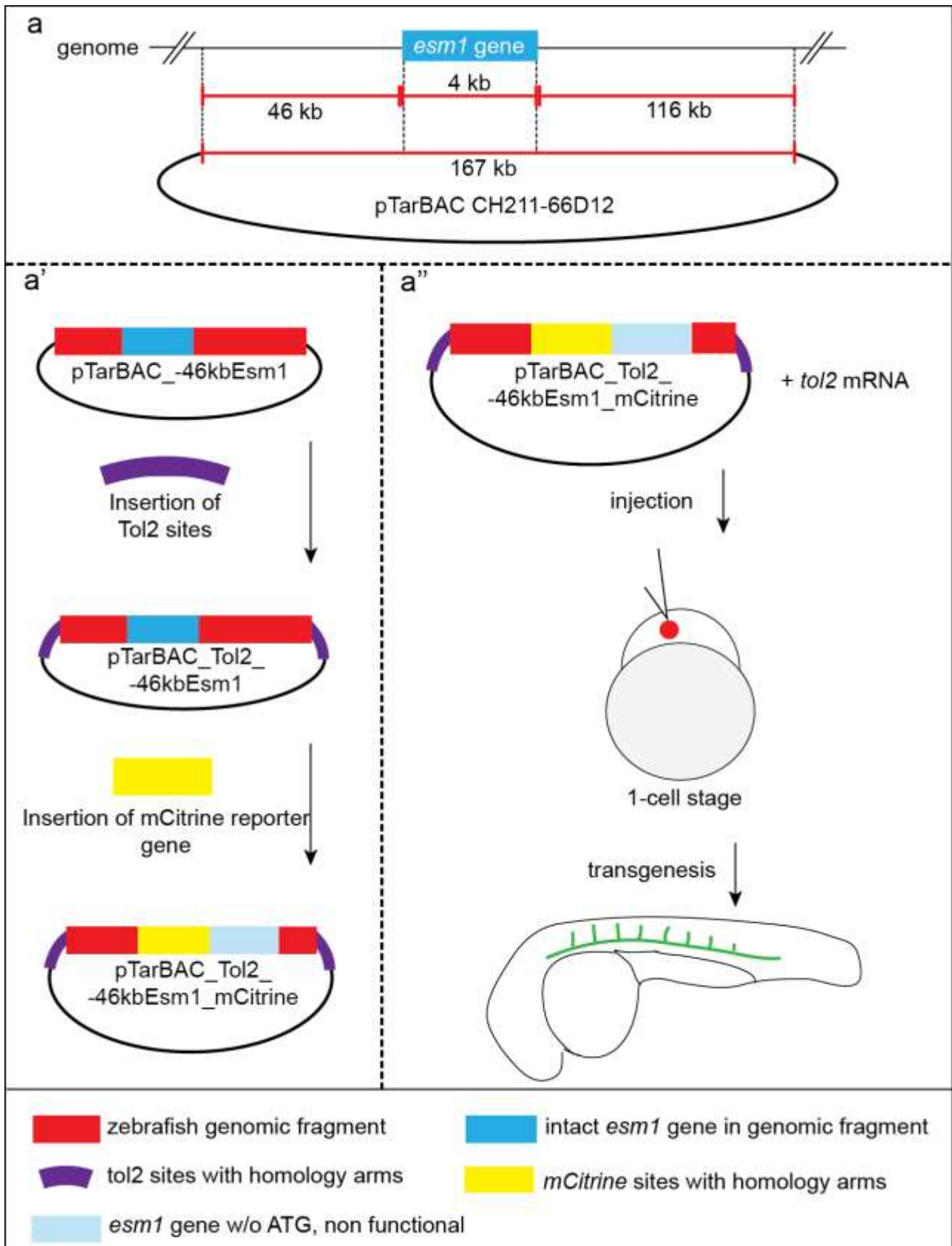


Figure 6-1. Illustration of the BAC recombineering process and establishing transgenesis for studying promoter activity. (a) Unmodified BAC clone, pTARBAC_CH211-66D12, which harbors a fragment of the zebrafish genome containing the *esm1* gene flanked by sequences 46kb upstream and 116kb downstream. (a') BAC

recombineering process as described in Bussmann and Schulte-Merker, 2011. Tol2 sites and the reporter gene *mCitrine* were recombineered into the BAC. The former is needed for insertion into the genome, and the latter encodes for a fluorescent protein, which is expressed upon promoter activation. Homology arms flanking the sequence to be inserted allow homologous recombination. During the homologous recombination step with *mCitrine*, the ATG of the *esm1* gene becomes deleted. (a'') the final construct gets injected into the zygote at the one-cell stage. Simultaneous introduction of the BAC with *tol2* mRNA allows stable integration of the reporter construct into the zebrafish genome and thus increased transgenesis efficiency. kb, kilo base pairs.

6.2.8 Cloning of pME_eGFP-p2a-esm1cnds

This vector was generated with the purpose of easy identification of transgenic cells. The pGEMT-*esm1* plasmid was used as template for a Phusion PCR and was performed with the primers *eGFP-p2a-esm1cnds_fw* and *eGFP-p2a-esm1cnds_rev*. The primers contain a EcoRV and XhoI restriction sites, to render the PCR product and vector compatible for cloning. The PCR product was digested with EcoRV and XhoI, whereas the vector pME_eGFP-p2a-SmaI was cut with SmaI and XhoI. Subsequent purification, modification and ligation of the plasmids were performed in the manner of conventional cloning.

6.2.8.1 Generating *fli1a_eGFP-p2a-esm1cnds* using the Gateway system

The multisite Gateway technology enables quick and efficient assembly of a gene-like sequence in a Tol2 transposon backbone using the Tol2Kit system. This cloning method is site-specific and based on recombination events. Clonase II plus (Thermo Fisher Scientific) was used according to the manufacturers' instruction. In the reaction p5E_ *fli1a*, pME_eGFP-p2a-*esm1cnds*, p3E_polyA and pDestTol2CG2 were recombined with the LR Clonase II plus.

The construct *fli1a_eGFP-p2a-esm1cnds* enables *esm1* overexpression under the control of the blood vessel specific *fli1a* promoter, specific for blood vessels. The *fli1a:eGFP-p2a-esm1* construct harbors two transgenesis markers. The *cmhc2:eGFP* reporter gene in the destination vector pDestTol2CG2 allowed the identification of transgenic fish by a green fluorescent heart and thus assessment of the overall transgenesis success. The *eGFP-p2a* system allows tracing of single *esm1* overexpressing cells. Upon activation of the *fli1a* promoter, the *eGFP-p2a-esm1* fusion gene is expressed specifically in the endothelium. Subsequent to its translation, the protein is split at the p2A site. Accordingly, Gfp and Esm1 are present within in the same cell but can act separately. The eGFP renders the *esm1*-overexpressing cell visible (Fig. 4-15).

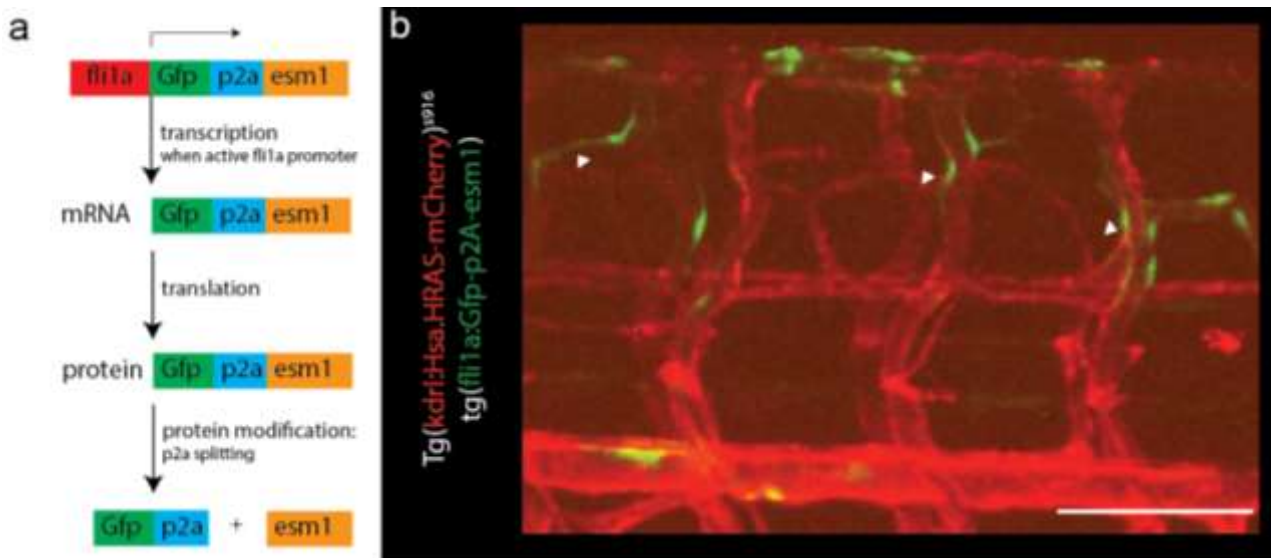


Figure 6-2. The eGFP-p2a system. A gateway expression vector *fli1a_eGFP-p2a-esm1;cmlc2:eGFP* was cloned which allows to select for two transgenesis markers: the cardiac myocyte specific *cmlc2:GFP* transgene to screen for the overall transgenesis efficiency and the eGFP-p2a system to screen for overexpressing cells. eGFP-p2a-esm1 is under the control of the blood vessel specific *fli1a* promoter. (a) Graphical illustration of the eGFP-p2a system. When the *fli1a* promoter is active, the fusion protein eGFP-p2a-esm1 is transcribed and translated. Next, the protein is cleaved at the p2a site. Thus, the eGFP and Esm1 proteins are present in the same cell as individual proteins, whereas the first aids in visualization of an *esm1* overexpressing cell. (b) Microscopic spinning disc image illustrating green fluorescent *esm1* overexpressing cells (white arrowheads). Scale bar 100 μ m.

6.2.9 Generation and verification of *esm1* and *esm1;flt1* mutants

6.2.9.1 Generation of mutants

The mutants were generated using the CRISPR/Cas9 system (Kwan *et al.*, 2007). Target sites were determined using the genome browser UCSC and crRNA sequences found with the Crispor tool.

Target specific Alt-RTM CRISPR-Cas9 crRNA and guiding Alt-RTM CRISPR-Cas9 tracrRNA were purchased from Integrated DNA Technologies. 3 μ M crRNA and 3 μ M tracrRNA in Nuclease-Free Duplex Buffer (Integrated DNA Technologies) were heated to 95°C for 5min to allow annealing of both components to single guide sgRNA. Next, Alt-R® S.p. Cas9 Nuclease V3 (Integrated DNA Technologies) protein was diluted with Cas9 working buffer to a working concentration of 0.5 μ g/ μ l. Subsequently, the two sgRNAs and the diluted Cas9 protein were mixed in a ratio of 1:1: 2 and incubated at 37°C for 10min. 1nl of the sgRNA/Cas9 suspension was injected into the one-cell stage zebrafish embryos.

F0 generation was raised to adulthood and checked for mutations by genotyping.

Individuals positive for mutations were outcrossed with a wildtype to identify germline transmission founder fishes. If germline transmission was given, heterozygous fish were obtained by outcross of the F0 individual with a wildtype. Adult fish of the F1 generation were genotyped and heterozygous animals were incrossed to obtain a F2 generation. Homozygous animals in the F2 generation were again ascertained by genotyping.

sgRNA^{Esm1_5'UTR} targets upstream and sgRNA^{Esm1_3'UTR} binds downstream of the *esm1* coding sequence. As both sgRNAs were injected at once, the entire coding sequence was deleted. The resulting line has a deletion of 3721nt.

The *esm1;flt* double mutant line was established by crossing homozygous *esm1*^{-3721nt/-3721nt} mutants with *flt1*^{ka604/ka604} homozygous fish. The resulting animals were heterozygous for each mutation. The *esm1*^{+/-3721nt} *flt1*^{+/-ka604} line was incrossed and the progeny genotyped for *esm1*^{-3721nt/-3721nt}; *flt1*^{ka604/ka604} double homozygous individuals.

During the process, both, the *esm1* mutants and *esm1;flt1* mutants were screened for Tg(*kdr*:eGFP^{s843}; *xla.Tubb*:DsRed^{zf148}) double transgenesis. Accordingly, the established lines carry a blood vessel and a neuronal reporter.

6.2.10 Genotyping

The genotype of adult fish was determined *via* fin biopsy and germline transmission was identified on embryos.

Genomic DNA was isolated *via* the HotSHOT (Hot Sodium Hydroxide Tris) method (Hwang et al. 2013). 30-60µl 1x Base solution was added to the tissue and subsequently boiled for 20min at 95°C. Next, the suspension was neutralized with 1x Neutralization solution and centrifuged. 1-5 µL of supernatant were used as template in a Taq PCR.

The deletion of 3721nt in the *esm1* gene mutant was verified by amplification with the primer pair Esm1_5'UTR_fw and Esm1_3'UTR_rev. Due to the relative distance of 3972nt in the wildtype, an amplicon was very unlikely to appear. Indeed, no visible PCR product was detectable. The amplicon from the mutant, instead was expected to contain 243bp, and was easily detectable and verified by sequencing. Heterozygous and homozygous animals were distinguished with a second PCR. In the wildtype a region of 548bp was amplified with the primers Esm1_5'UTR_fw and Esm1_E1_rev. However, this region does not exist in the *esm1* homozygous individuals due to the deletion and accordingly, no PCR product was visible on the gel.

Adult individuals of the zebrafish mutants used in this thesis (*esm1*^{sa11057}, *flt1*^{ka602}, *flt1*^{ka604} and *vhl*^{hu2117}) were genotyped using fin biopsy. Details about the lines are presented in table

6-2 and primers for genotyping are listed in 6-5.

6.2.11 Microscopy

Living embryos were either imaged with the Leica TCS SP8 confocal inverted microscope (20x or 40x objectives); Leica TCS SP5 confocal microscope (10x or 20x objectives) or with the Carl Zeiss Spinning Disk Microscope (10x and 25x objectives). Time lapse images were performed with the confocal microscope at 28.5°C. Prior to *in vivo* imaging the embryos were anesthetized with 1x Tricaine (Sigma- Aldrich) and incubated for a few seconds in 25x Tricaine solution before they were fixed in the desired position. Therefore, the fish were positioned in microscopy dishes (MatTek) with 0.7% (w/v) low-melting NuSieve GTG Agarose (Lonza) in E3 medium. After the agarose hardened, 0.7x Tricaine in PTU was added to keep up anesthesia during the imaging.

Images of WISH stainings were acquired with a Leica MZFLIII microscope and a QICAM 12-Bit color camera (QImaging). Morphologically and malformed embryos were excluded from analysis.

6.2.12 Computational methods

6.2.12.1 Genome browsers, in silico analyses, computational analyses

Genomic, mRNA and protein sequences, with which were worked with in computational studies, were found in the genome browsers NCBI and UCSC.

Primers were designed *in silico* with the online tool NCBI Primer Blast. *In silico* cloning, which was applied for example for restriction enzyme cloning, Gateway cloning and T/A cloning, was performed with the SnapGene software.

6.2.12.2 Image processing

Fiji was used for image processing. This program enables the generation of z projections as well as merge and separation of channels in multicolor images.

6.2.12.3 Analysis of intersegmental vessels and the vascular network

6.2.12.3.1 Analysis of the diameter, number of nuclei and length of the intersegmental vessels

The diameter was measured at seven different locations along an ISV with Fiji. The average of these data points was statistically used as the diameter of the analyzed vessel.

The length of an ISV was determined with Fiji. The vessel was divided into segments according to the natural shape of the ISV. The length was determined from the DA roof to the ventral side of the DLAV, independent of arterial or venous identity. The sum of the segments was used as the length of the corresponding vessel in statistics.

The transgenic line $Tg(kdr:eGFP)^{S843}$ allows to manually count the number of nuclei in an ISV. The nuclei can be distinguished by strongly fluorescent ovaly shaped structures in the vessel.

6.2.12.3.2 Analysis of the vascular network

Figure 6-3 shows how the vascular network is defined, which area is object for quantification and how it is distinct in different genotypes. An area spanning four ISVs was defined at the level of the neural tube and the number of connecting vessels (segment) and sprouts (branching points) calculated.

The vascular network of both DLAV and ISV was assessed with a semi-automated analysis using Fiji. Stack projections of the acquired images were generated and a defined area of the dorsal part of the ISVs, at the position of the neural tube, was analyzed. In this defined area a skeleton of the vasculature was generated. Skeletonization was achieved using a Gaussian blur filter followed by a black/white threshold. The number of segments and branching points were calculated using the 'analyze skeleton' plugin.

6.2.12.4 Statistical analysis

The GraphPad Prism 6 software used for statistical analysis. If two groups were compared to each other, i.e. data of a morpholino or overexpression experiment, the data sets were first tested for normal distribution with the D'Agostino and Pearson test. Significance was calculated with either the unpaired parametric students t-test in case of normal distributed data sets or with the nonparametric Mann-Whitney U test if the data sets were non-normal distributed.

Data are represented as mean \pm standard error of the mean (s.e.m.). P-values of the

calculated significances are indicated as follows: ns (not significant), $p > 0.05$; *, $p \leq 0.05$; **, $p \leq 0.01$; ***, $p \leq 0.001$.

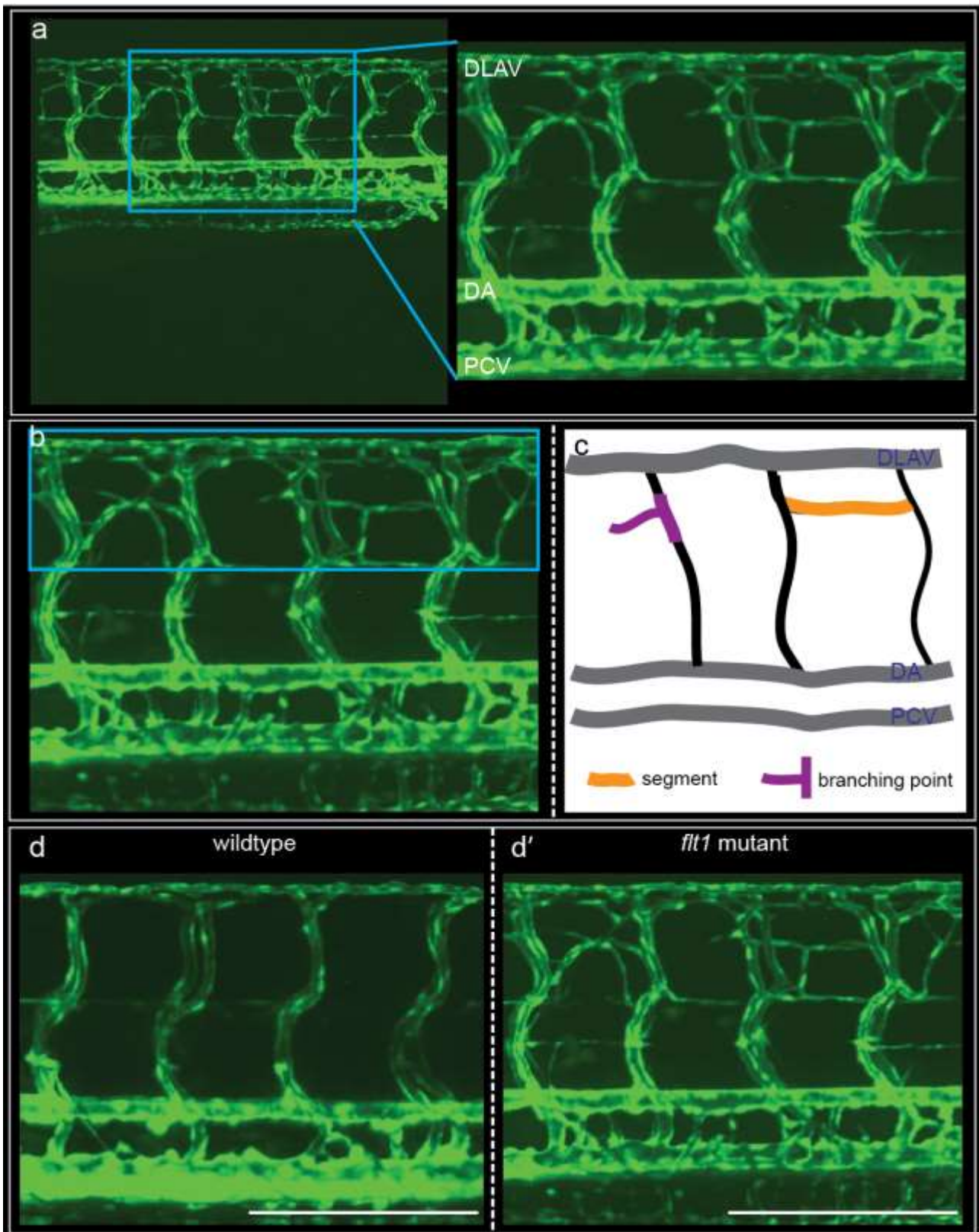


Figure 6-3. Quantification of the zebrafish vascular network at the neuro-vascular

interface. (a) z-stack of an original spinning disc microscope picture. The blue rectangle indicates the magnified area used for analysis of the blood vessel network. (b) Blue rectangle shows the defined area in which segments (a vessel is connected at each end to another one) and branching points (the sprout is joined to only one vascular structure) in the ISV and DLAV area will be calculated. (c) Graphical illustration how segments and branching points are defined. (d) Overview how the vascular system is arranged differently in the wildtype (d) and *flt1* mutant (d'). DA, dorsal aorta; DLAV, dorsal longitudinal anastomotic vessel; PCV, posterior cardinal vein. Scale bar 100 μm .

7 Bibliography

Abid, M. R. *et al.* (2006) 'Vascular endocan is preferentially expressed in tumor endothelium', *Microvascular Research*, 72(3), pp. 136–145. doi: 10.1016/j.mvr.2006.05.010.

Adams, R. H. and Alitalo, K. (2007) 'Molecular regulation of angiogenesis and lymphangiogenesis', *Nature Reviews Molecular Cell Biology*. Nature Publishing Group, 8, p. 464. Available at: <https://doi.org/10.1038/nrm2183>.

Adams, R. H. and Eichmann, A. (2010) 'Axon guidance molecules in vascular patterning.', *Cold Spring Harbor perspectives in biology*, 2(5), pp. 1–19. doi: 10.1101/cshperspect.a001875.

Annika, A., Alexandra, A. and Christer, B. (2005) 'Endothelial/Pericyte Interactions', *Circulation Research*. American Heart Association, 97(6), pp. 512–523. doi: 10.1161/01.RES.0000182903.16652.d7.

Arman, Y. *et al.* (2015) 'Effect of Glycemic Regulation on Endocan Levels in Patients With Diabetes: A Preliminary Study', *Angiology*. SAGE Publications Inc, 67(3), pp. 239–244. doi: 10.1177/0003319715585664.

Bai, L. and Morozov, A. V (2010) 'Gene regulation by nucleosome positioning', *Trends in Genetics*. Elsevier, 26(11), pp. 476–483. doi: 10.1016/j.tig.2010.08.003.

Balta, I. *et al.* (2013) 'Elevated serum levels of endocan in patients with psoriasis vulgaris: correlations with cardiovascular risk and activity of disease', *British Journal of Dermatology*. John Wiley & Sons, Ltd (10.1111), 169(5), pp. 1066–1070. doi: 10.1111/bjd.12525.

Balta, I. *et al.* (2014) 'Serum endocan levels as a marker of disease activity in patients with Behçet disease', *Journal of the American Academy of Dermatology*, 70(2), pp. 291–296. doi: <https://doi.org/10.1016/j.jaad.2013.09.013>.

Banfi, A. *et al.* (2018) 'Editorial: Vascularization for regenerative medicine', *Frontiers in Bioengineering and Biotechnology*, 6(NOV), pp. 4–6. doi: 10.3389/fbioe.2018.00175.

Bates, D. O. *et al.* (2002) 'VEGF165b, an inhibitory splice variant of vascular endothelial growth factor, is down-regulated in renal cell carcinoma', *Cancer Research*, 62(14), pp. 4123–4131.

Bechard, D. *et al.* (2000) 'Characterization of the secreted form of endothelial-cell-specific molecule 1 by specific monoclonal antibodies', *Journal of Vascular Research*, 37(5), pp. 417–425. doi: 10.1159/000025758.

Béchar, D. *et al.* (2001) 'Human Endothelial-Cell Specific Molecule-1 Binds Directly to the Integrin CD11a/CD18 (LFA-1) and Blocks Binding to Intercellular Adhesion Molecule-1', *The Journal of Immunology*, 167(6), pp. 3099 LP – 3106. doi: 10.4049/jimmunol.167.6.3099.

Becker, C. G. and Becker, T. (2008) 'Adult zebrafish as a model for successful central nervous system regeneration', *Restorative neurology and neuroscience*, 26(2–3), pp. 71–80.

Beil, J. *et al.* (2012) 'Is BAC transgenesis obsolete? State of the art in the era of designer nucleases', *Journal of biomedicine & biotechnology*. 2012/07/30. Hindawi Publishing Corporation, 2012, p. 308414. doi: 10.1155/2012/308414.

Bishop, J. R., Schuksz, M. and Esko, J. D. (2007) 'Heparan sulphate proteoglycans fine-tune mammalian physiology', *Nature*, 446(7139), pp. 1030–1037. doi: 10.1038/nature05817.

Blanco, R. and Gerhardt, H. (2013) 'VEGF and Notch in Tip and Stalk Cell Selection', *Cold Spring Harbor Perspectives in Medicine*, 3(1). doi: 10.1101/cshperspect.a006569.

Bluyssen, H. A. R. *et al.* (2004) 'Fibronectin is a hypoxia-independent target of the tumor suppressor VHL', *FEBS Letters*. John Wiley & Sons, Ltd, 556(1–3), pp. 137–142. doi: 10.1016/S0014-5793(03)01392-9.

Boilly, B. *et al.* (2000) 'FGF signals for cell proliferation and migration through different pathways', *Cytokine & Growth Factor Reviews*, 11(4), pp. 295–302. doi: [https://doi.org/10.1016/S1359-6101\(00\)00014-9](https://doi.org/10.1016/S1359-6101(00)00014-9).

Bota, M. and Swanson, L. W. (2007) 'The neuron classification problem', *Brain Research Reviews*, 56(1), pp. 79–88. doi: <https://doi.org/10.1016/j.brainresrev.2007.05.005>.

Bradford, Y. M. *et al.* (2017) 'Zebrafish Models of Human Disease: Gaining Insight into Human Disease at ZFIN', *ILAR Journal*, 58(1), pp. 4–16. doi: [10.1093/ilar/ilw040](https://doi.org/10.1093/ilar/ilw040).

Burri, P. H., Hlushchuk, R. and Djonov, V. (2004) 'Intussusceptive angiogenesis: Its emergence, its characteristics, and its significance', *Developmental Dynamics*, 231(3), pp. 474–488. doi: [10.1002/dvdy.20184](https://doi.org/10.1002/dvdy.20184).

Bussmann, J. *et al.* (2008) 'Zebrafish VEGF receptors: A guideline to nomenclature', *PLoS Genetics*, 4(5), pp. 4–5. doi: [10.1371/journal.pgen.1000064](https://doi.org/10.1371/journal.pgen.1000064).

Bussmann, J. *et al.* (2010) 'Arteries provide essential guidance cues for lymphatic endothelial cells in the zebrafish trunk', *Development*, 137(16), pp. 2653 LP – 2657. doi: [10.1242/dev.048207](https://doi.org/10.1242/dev.048207).

Bussmann, J. and Schulte-Merker, S. (2011) 'Rapid BAC selection for tol2-mediated transgenesis in zebrafish', *Development*, 138(19), pp. 4327–4332. doi: [10.1242/dev.068080](https://doi.org/10.1242/dev.068080).

Carmeliet, P. *et al.* (1996) 'Abnormal blood vessel development and lethality in embryos lacking a single VEGF allele', *Nature*, 380(6573), pp. 435–439. doi: [10.1038/380435a0](https://doi.org/10.1038/380435a0).

Carmeliet, P. *et al.* (2001) 'Synergism between vascular endothelial growth factor and placental growth factor contributes to angiogenesis and plasma extravasation in pathological conditions', *Nature Medicine*, 7(5), pp. 575–583. doi: [10.1038/87904](https://doi.org/10.1038/87904).

Carmeliet, P. (2003) 'Angiogenesis in health and disease', *Nature Medicine*, 9(6), pp. 653–660. doi: [10.1038/nm0603-653](https://doi.org/10.1038/nm0603-653).

Carmeliet, P., Wong, B. W. and De Bock, K. (2012) 'Treating diabetes by blocking a vascular growth factor', *Cell Metabolism*, 16(5), pp. 553–555. doi: [10.1016/j.cmet.2012.10.015](https://doi.org/10.1016/j.cmet.2012.10.015).

- Carninci, P. *et al.* (2006) 'Genome-wide analysis of mammalian promoter architecture and evolution', *Nature Genetics*, 38(6), pp. 626–635. doi: 10.1038/ng1789.
- Cébe-Suarez, S., Zehnder-Fjällman, A. and Ballmer-Hofer, K. (2006) 'The role of VEGF receptors in angiogenesis; complex partnerships', *Cellular and Molecular Life Sciences*, 63(5), p. 601. doi: 10.1007/s00018-005-5426-3.
- Celik, T. *et al.* (2015) 'Endocan, a novel marker of endothelial dysfunction in patients with essential hypertension: Comparative effects of amlodipine and valsartan', *Blood Pressure*. Taylor & Francis, 24(1), pp. 55–60. doi: 10.3109/08037051.2014.972816.
- Chappell, J. C. *et al.* (2009) 'Local Guidance of Emerging Vessel Sprouts Requires Soluble Flt-1', *Developmental Cell*. Elsevier Ltd, 17(3), pp. 377–386. doi: 10.1016/j.devcel.2009.07.011.
- Charkoudian, N. and Rabbitts, J. A. (2009) 'Sympathetic neural mechanisms in human cardiovascular health and disease', *Mayo Clinic proceedings*. Mayo Foundation for Medical Education and Research, 84(9), pp. 822–830. doi: 10.1016/S0025-6196(11)60492-8.
- Chávez, M. N. *et al.* (2016) 'Zebrafish as an Emerging Model Organism to Study Angiogenesis in Development and Regeneration', *Frontiers in Physiology*, 7, p. 56. doi: 10.3389/fphys.2016.00056.
- Childs, S. *et al.* (2002) 'Patterning of angiogenesis in the zebrafish embryo', *Development*, 129(4), pp. 973 LP – 982. Available at: <http://dev.biologists.org/content/129/4/973.abstract>.
- Conway, E. M., Collen, D. and Carmeliet, P. (2001) 'Molecular mechanisms of blood vessel growth', *Cardiovascular Research*, 49(3), pp. 507–521. doi: 10.1016/S0008-6363(00)00281-9.
- Cortés, F. *et al.* (1999) 'Differential expression of KDR/VEGFR-2 and CD34 during mesoderm development of the early human embryo', *Mechanisms of Development*, 83(1), pp. 161–164. doi: [https://doi.org/10.1016/S0925-4773\(99\)00030-1](https://doi.org/10.1016/S0925-4773(99)00030-1).

- Coultas, L., Chawengsaksophak, K. and Rossant, J. (2005) 'Endothelial cells and VEGF in vascular development', *Nature*, 438(7070), pp. 937–945. doi: 10.1038/nature04479.
- Cramer, L. P., Kay, R. R. and Zatulovskiy, E. (2018) 'Repellent and Attractant Guidance Cues Initiate Cell Migration by Distinct Rear-Driven and Front-Driven Cytoskeletal Mechanisms', *Current Biology*, 28(6), pp. 995-1004.e3. doi: <https://doi.org/10.1016/j.cub.2018.02.024>.
- Delehedde, M. *et al.* (2002) 'Proteoglycans in Inflammation', *Current Medicinal Chemistry - Anti-Inflammatory & Anti-Allergy Agents*, pp. 89–102. Available at: <https://www.ingentaconnect.com/content/ben/cmcaiaa/2002/00000001/00000002/art00001>.
- Delehedde, M. *et al.* (2013) 'Endocan in cancers: A lesson from a circulating dermatan sulfate proteoglycan', *International Journal of Cell Biology*, 2013. doi: 10.1155/2013/705027.
- Deryugina, E. I. and Quigley, J. P. (2008) 'Chapter 2 Chick Embryo Chorioallantoic Membrane Models to Quantify Angiogenesis Induced by Inflammatory and Tumor Cells or Purified Effector Molecules', in *Angiogenesis: In Vivo Systems, Part A*. Academic Press (Methods in Enzymology), pp. 21–41. doi: [https://doi.org/10.1016/S0076-6879\(08\)02802-4](https://doi.org/10.1016/S0076-6879(08)02802-4).
- Djonov, V. and Makanya, A. N. (2005) 'New insights into intussusceptive angiogenesis', in Clauss, M. and Breier, G. (eds) *Mechanisms of Angiogenesis*. Basel: Birkhäuser Basel, pp. 17–33. doi: 10.1007/3-7643-7311-3_2.
- Dumpich, M. and Theiss, C. (2015) 'VEGF in the nervous system: An important target for research in neurodevelopmental and regenerative medicine', *Neural Regeneration Research*. Editorial Board of Neural Regeneration Research, pp. 1725–1726. doi: 10.4103/1673-5374.170287.
- Dvorak, H. F. (2006) 'Discovery of vascular permeability factor (VPF)', *Experimental Cell Research*, 312(5), pp. 522–526. doi: <https://doi.org/10.1016/j.yexcr.2005.11.026>.

Eichmann, A. *et al.* (2005) 'Vascular development: From precursor cells to branched arterial and venous networks', *International Journal of Developmental Biology*, 49(2-3 SPEC. ISS.), pp. 259–267. doi: 10.1387/ijdb.041941ae.

Eichmann, A. and Thomas, J.-L. (2013) 'Molecular parallels between neural and vascular development', *Cold Spring Harbor perspectives in medicine*. Cold Spring Harbor Laboratory Press, 3(1), pp. a006551–a006551. doi: 10.1101/cshperspect.a006551.

Eilken, H. M. *et al.* (2017) 'Pericytes regulate VEGF-induced endothelial sprouting through VEGFR1', *Nature communications*. Nature Publishing Group UK, 8(1), p. 1574. doi: 10.1038/s41467-017-01738-3.

Eilken, H. M. and Adams, R. H. (2010) 'Dynamics of endothelial cell behavior in sprouting angiogenesis', *Current Opinion in Cell Biology*, 22(5), pp. 617–625. doi: <https://doi.org/10.1016/j.ceb.2010.08.010>.

Ellertsdóttir, E. *et al.* (2010) 'Vascular morphogenesis in the zebrafish embryo', *Developmental Biology*, 341(1), pp. 56–65. doi: <https://doi.org/10.1016/j.ydbio.2009.10.035>.

Etchin, J., Kanki, J. P. and Look, A. T. (2011) 'Chapter 13 - Zebrafish as a Model for the Study of Human Cancer', in Detrich, H. W., Westerfield, M., and Zon, L. I. (eds) *The Zebrafish: Disease Models and Chemical Screens*. Academic Press (Methods in Cell Biology), pp. 309–337. doi: <https://doi.org/10.1016/B978-0-12-381320-6.00013-8>.

Fearnley, G. W. *et al.* (2014) 'VEGF-A isoforms differentially regulate ATF-2–dependent VCAM-1 gene expression and endothelial–leukocyte interactions', *Molecular Biology of the Cell*. American Society for Cell Biology (mboc), 25(16), pp. 2509–2521. doi: 10.1091/mbc.e14-05-0962.

Fearnley, G. W. *et al.* (2015) 'VEGF-A isoform-specific regulation of calcium ion flux, transcriptional activation and endothelial cell migration', *Biology Open*, 4(6), pp. 731 LP – 742. doi: 10.1242/bio.201410884.

- Ferrara, N. (2004) 'Vascular Endothelial Growth Factor: Basic Science and Clinical Progress', *Endocrine Reviews*, 25(4), pp. 581–611. doi: 10.1210/er.2003-0027.
- Ferrara, N. (2005) 'VEGF as a Therapeutic Target in Cancer', *Oncology*, 69(suppl 3(Suppl. 3)), pp. 11–16. doi: 10.1159/000088479.
- Ferrara, N. (2009) 'Vascular Endothelial Growth Factor', *Arteriosclerosis, Thrombosis, and Vascular Biology*, 29(6), pp. 789–791. doi: 10.1161/ATVBAHA.108.179663.
- Ferrara, N. (2010) 'Binding to the extracellular matrix and proteolytic processing: two key mechanisms regulating vascular endothelial growth factor action', *Molecular biology of the cell*. The American Society for Cell Biology, 21(5), pp. 687–690. doi: 10.1091/mbc.E09-07-0590.
- Ferrara, N. and Davis-Smyth, T. (1997) 'The Biology of Vascular Endothelial Growth Factor', *Endocrine Reviews*, 18(1), pp. 4–25. doi: 10.1210/edrv.18.1.0287.
- Ferrara, N., Gerber, H. P. and LeCouter, J. (2003) 'The biology of VEGF and its receptors', *Nature Medicine*, 9(6), pp. 669–676. doi: 10.1038/nm0603-669.
- Ferrara, N. and Henzel, W. J. (1989) 'Pituitary follicular cells secrete a novel heparin-binding growth factor specific for vascular endothelial cells', *Biochemical and Biophysical Research Communications*, 161(2), pp. 851–858. doi: [https://doi.org/10.1016/0006-291X\(89\)92678-8](https://doi.org/10.1016/0006-291X(89)92678-8).
- Feucht, M., Christ, B. and Wilting, J. (1997) 'VEGF induces cardiovascular malformation and embryonic lethality', *American Journal of Pathology*, 151(5), pp. 1407–1416.
- Filep, J. G. (2006) 'Endocan or endothelial cell-specific molecule-1: A novel prognostic marker of sepsis?*', *Critical Care Medicine*, 34(2). Available at: https://journals.lww.com/ccmjournals/Fulltext/2006/02000/Endocan_or_endothelial_cell_specific_molecule_1__A.55.aspx.

- Filipowska, J. *et al.* (2017) 'The role of vasculature in bone development, regeneration and proper systemic functioning', *Angiogenesis*, 20(3), pp. 291–302. doi: 10.1007/s10456-017-9541-1.
- Fischer, C. *et al.* (2008) 'FLT1 and its ligands VEGFB and PlGF: Drug targets for anti-angiogenic therapy?', *Nature Reviews Cancer*, 8(12), pp. 942–956. doi: 10.1038/nrc2524.
- Flamme, I., Frölich, T. and Risau, W. (1997) 'Molecular mechanisms of vasculogenesis and embryonic angiogenesis', *Journal of Cellular Physiology*, 173(2), pp. 206–210. doi: 10.1002/(SICI)1097-4652(199711)173:2<206::AID-JCP22>3.0.CO;2-C.
- Flamme, I. and Risau, W. (1992) 'Induction of vasculogenesis and hematopoiesis in vitro', *Development*, 116(2), pp. 435–439.
- Folkman, J. (1995) 'Angiogenesis in cancer, vascular, rheumatoid and other disease', *Nature Medicine*, 1(1), pp. 27–30. doi: 10.1038/nm0195-27.
- Folkman, J. and D'Amore, P. A. (1996) 'Blood Vessel Formation: What Is Its Molecular Basis?', *Cell*, 87(7), pp. 1153–1155. doi: [https://doi.org/10.1016/S0092-8674\(00\)81810-3](https://doi.org/10.1016/S0092-8674(00)81810-3).
- Fong, G.-H. *et al.* (1995) 'Role of the Flt-1 receptor tyrosine kinase in regulating the assembly of vascular endothelium', *Nature*, 376(6535), pp. 66–70. doi: 10.1038/376066a0.
- Forster, J. *et al.* (2017) 'A review of the development of tumor vasculature and its effects on the tumor microenvironment', *Hypoxia*, Volume 5, pp. 21–32. doi: 10.2147/hp.s133231.
- Freeman, M. R. *et al.* (1995) 'Peripheral Blood T Lymphocytes and Lymphocytes Infiltrating Human Cancers Express Vascular Endothelial Growth Factor: A Potential Role for T Cells in Angiogenesis', *Cancer Research*, 55(18), pp. 4140 LP – 4145. Available at: <http://cancerres.aacrjournals.org/content/55/18/4140.abstract>.
- Gabhann, F. Mac and Popel, A. S. (2008) 'Systems biology of vascular endothelial growth factors', *Microcirculation*, 15(8), pp. 715–738. doi: 10.1080/10739680802095964.

Gallagher, John T. and Lyon, M. (2000) 'Molecular structure of heparan sulfate and interactions with growth factors and morphogens', in Iozzo, R. V. (ed.) *Proteoglycans: Structure, Biology and Molecular Interactions*. 1st edn. Boca Raton: CRC Press, pp. 27–59. doi: doi.org/10.1201/9780203909720.

Gamboa, N. T. *et al.* (2017) 'Neurovascular patterning cues and implications for central and peripheral neurological disease', *Surgical neurology international*. Medknow Publications & Media Pvt Ltd, 8, p. 208. doi: 10.4103/sni.sni_475_16.

Gerhardt, H. *et al.* (2003) 'VEGF guides angiogenic sprouting utilizing endothelial tip cell filopodia', *The Journal of Cell Biology*, 161(6), pp. 1163 LP – 1177. doi: 10.1083/jcb.200302047.

Geudens, I. and Gerhardt, H. (2011) 'Coordinating cell behaviour during blood vessel formation', *Development*, 138(21), pp. 4569 LP – 4583. doi: 10.1242/dev.062323.

Gimbrone, M. A. *et al.* (1972) 'Tumor dormancy in vivo by prevention of neovascularization', *Journal of Experimental Medicine*, 136(2), pp. 261–276. doi: 10.1084/jem.136.2.261.

Gore, A. V. *et al.* (2012) 'Vascular Development in the Zebrafish', *Cold Spring Harbor Perspectives in Medicine*, 2(5). doi: 10.1101/cshperspect.a006684.

Grigoriu, B. D. *et al.* (2006) 'Endocan Expression and Relationship with Survival in Human Non–Small Cell Lung Cancer', *Clinical Cancer Research*, 12(15), pp. 4575 LP – 4582. doi: 10.1158/1078-0432.CCR-06-0185.

Hagberg, C. E. *et al.* (2010) 'Vascular endothelial growth factor B controls endothelial fatty acid uptake', *Nature*, 464(7290), pp. 917–921. doi: 10.1038/nature08945.

Haigh, J. J. (2008) 'Role of VEGF in organogenesis', *Organogenesis*. Taylor & Francis, 4(4), pp. 247–256. doi: 10.4161/org.4.4.7415.

Harding, C. C. and S. P. (2011) 'Anti-VEGF Compounds in the Treatment of Neovascular Age Related Macular Degeneration', *Current Drug Targets*, pp. 173–181. doi: <http://dx.doi.org/10.2174/138945011794182674>.

Harper, S. J. and Bates, D. O. (2008) 'VEGF-A splicing: the key to anti-angiogenic therapeutics?', *Nature Reviews Cancer*. Nature Publishing Group, 8, p. 880. Available at: <https://doi.org/10.1038/nrc2505>.

Hatfield, K. J. *et al.* (2011) 'Serum levels of endothelium-derived endocan are increased in patients with untreated acute myeloid leukemia', *Hematology*. Taylor & Francis, 16(6), pp. 351–356. doi: 10.1179/102453311X13127324303434.

He, Y. *et al.* (1999) 'Alternative Splicing of Vascular Endothelial Growth Factor (VEGF)-R1 (FLT-1) pre-mRNA Is Important for the Regulation of VEGF Activity', *Molecular Endocrinology*, 13(4), pp. 537–545. doi: 10.1210/mend.13.4.0265.

Hellström, M. *et al.* (2007) 'Dll4 signalling through Notch1 regulates formation of tip cells during angiogenesis', *Nature*. Nature Publishing Group, 445, p. 776. Available at: <https://doi.org/10.1038/nature05571>.

Herbert, S. P., Cheung, J. Y. M. and Stainier, D. Y. R. (2012) 'Determination of Endothelial Stalk versus Tip Cell Potential during Angiogenesis by H2.0-like Homeobox-1', *Current Biology*. Elsevier, 22(19), pp. 1789–1794. doi: 10.1016/j.cub.2012.07.037.

Herbert, S. P. and Stainier, D. Y. R. (2011) 'Molecular control of endothelial cell behaviour during blood vessel morphogenesis', *Nature Reviews Molecular Cell Biology*, 12(9), pp. 551–564. doi: 10.1038/nrm3176.

Herzog, Y., Guttmann-Raviv, N. and Neufeld, G. (2005) 'Segregation of arterial and venous markers in subpopulations of blood islands before vessel formation', *Developmental Dynamics*, 232(4), pp. 1047–1055. doi: 10.1002/dvdy.20257.

Hiratsuka, S. *et al.* (1998) 'Flt-1 lacking the tyrosine kinase domain is sufficient for normal development and angiogenesis in mice', *Proceedings of the National Academy of Sciences of the United States of America*, 95(16), pp. 9349–9354. doi: 10.1073/pnas.95.16.9349.

Hiratsuka, S. *et al.* (2005) 'Membrane Fixation of Vascular Endothelial Growth Factor Receptor 1 Ligand-Binding Domain Is Important for Vasculogenesis and Angiogenesis in Mice', *Molecular and Cellular Biology*, 25(1), pp. 346 LP – 354. doi: 10.1128/MCB.25.1.346-354.2005.

Hogan, B. M. *et al.* (2009) 'Ccbe1 is required for embryonic lymphangiogenesis and venous sprouting', *Nature Genetics*, 41(4), pp. 396–398. doi: 10.1038/ng.321.

Hong, C. C., Kume, T. and Peterson, R. T. (2008) 'Role of Crosstalk Between Phosphatidylinositol 3-Kinase and Extracellular Signal-Regulated Kinase/Mitogen-Activated Protein Kinase Pathways in Artery–Vein Specification', *Circulation Research*, 103(6), pp. 573–579. doi: 10.1161/CIRCRESAHA.108.180745.

Hong, E. and Brewster, R. (2006) 'N-cadherin is required for the polarized cell behaviors that drive neurulation in the zebrafish', *Development*, 133(19), pp. 3895–3905. doi: 10.1242/dev.02560.

Houck, K. A. *et al.* (1991) 'The Vascular Endothelial Growth Factor Family: Identification of a Fourth Molecular Species and Characterization of Alternative Splicing of RNA', *Molecular Endocrinology*, 5(12), pp. 1806–1814. doi: 10.1210/mend-5-12-1806.

Houck, K. A. *et al.* (1992) 'Dual regulation of vascular endothelial growth factor bioavailability by genetic and proteolytic mechanisms.', *Journal of Biological Chemistry*, 267(36), pp. 26031–26037. Available at: <http://www.jbc.org/content/267/36/26031.abstract>.

Huang, G.-W., Tao, Y.-M. and Ding, X. (2009) 'Endocan Expression Correlated with Poor Survival in Human Hepatocellular Carcinoma', *Digestive Diseases and Sciences*, 54(2), pp. 389–394. doi: 10.1007/s10620-008-0346-3.

van Impel, A. *et al.* (2014) 'Divergence of zebrafish and mouse lymphatic cell fate

specification pathways', *Development (Cambridge)*, 141(6), pp. 1228–1238. doi: 10.1242/dev.105031.

Iozzo, R. V (1998) 'MATRIX PROTEOGLYCANS: From Molecular Design to Cellular Function', *Annual Review of Biochemistry*. Annual Reviews, 67(1), pp. 609–652. doi: 10.1146/annurev.biochem.67.1.609.

Isogai, S. *et al.* (2003) 'Angiogenic network formation in the developing vertebrate trunk', *Development*, 130(21), pp. 5281 LP – 5290. doi: 10.1242/dev.00733.

Isogai, S., Horiguchi, M. and Weinstein, B. M. (2001) 'The Vascular Anatomy of the Developing Zebrafish: An Atlas of Embryonic and Early Larval Development', *Developmental Biology*, 230(2), pp. 278–301. doi: <https://doi.org/10.1006/dbio.2000.9995>.

Iyer, S., Darley, P. I. and Acharya, K. R. (2010) 'Structural insights into the binding of vascular endothelial growth factor-B by VEGFR-1D2: Recognition and specificity', *Journal of Biological Chemistry*, 285(31), pp. 23779–23789. doi: 10.1074/jbc.M110.130658.

Jakobsson, L. *et al.* (2010) 'Endothelial cells dynamically compete for the tip cell position during angiogenic sprouting', *Nature Cell Biology*. Nature Publishing Group, a division of Macmillan Publishers Limited. All Rights Reserved., 12, p. 943. Available at: <https://doi.org/10.1038/ncb2103>.

Janke, J. *et al.* (2006) 'Adipose Tissue and Circulating Endothelial Cell Specific Molecule-1 in Human Obesity', *Horm Metab Res*, 38(01), pp. 28–33. doi: 10.1055/s-2006-924973.

Jin, S. W. *et al.* (2005) 'Cellular and molecular analyses of vascular tube and lumen formation in zebrafish', *Development*, 132(23), pp. 5199–5209. doi: 10.1242/dev.02087.

Jones, E. A. V (2011) 'The initiation of blood flow and flow induced events in early vascular development', *Seminars in Cell & Developmental Biology*, 22(9), pp. 1028–1035. doi: <https://doi.org/10.1016/j.semcdb.2011.09.020>.

Jones, E. A. V, le Noble, F. and Eichmann, A. (2006) 'What Determines Blood Vessel Structure? Genetic Prespecification vs. Hemodynamics', *Physiology*, 21(6), pp. 388–395. doi: 10.1152/physiol.00020.2006.

Joris, M. *et al.* (2017) 'Number of inadvertent RNA targets for morpholino knockdown in *Danio rerio* is largely underestimated: evidence from the study of Ser/Arg-rich splicing factors', *Nucleic acids research*. Oxford University Press, 45(16), pp. 9547–9557. doi: 10.1093/nar/gkx638.

Julius, A. *et al.* (2008) 'Brothers and Sisters', *Circulation Research*. American Heart Association, 103(9), pp. 929–939. doi: 10.1161/CIRCRESAHA.108.184937.

Juven-Gershon, T. *et al.* (2008) 'The RNA polymerase II core promoter — the gateway to transcription', *Current Opinion in Cell Biology*, 20(3), pp. 253–259. doi: <https://doi.org/10.1016/j.ceb.2008.03.003>.

Kali, A. and Rathan Shetty, K. S. (2014) 'Endocan: A novel circulating proteoglycan', *Indian Journal of Pharmacology*. Medknow Publications, pp. 579–583. doi: 10.4103/0253-7613.144891.

Kawamura, H. *et al.* (2008) 'Vascular Endothelial Growth Factor (VEGF)-A165b Is a Weak & In vitro Agonist for VEGF Receptor-2 Due to Lack of Coreceptor Binding and Deficient Regulation of Kinase Activity', *Cancer Research*, 68(12), pp. 4683 LP – 4692. doi: 10.1158/0008-5472.CAN-07-6577.

Keck, P. J. *et al.* (1989) 'Vascular permeability factor, an endothelial cell mitogen related to PDGF', *Science*, 246(4935), pp. 1309 LP – 1312. doi: 10.1126/science.2479987.

Kendall, R. L. and Thomas, K. A. (1993) 'Inhibition of vascular endothelial cell growth factor activity by an endogenously encoded soluble receptor', *Proceedings of the National Academy of Sciences*, 90(22), pp. 10705 LP – 10709. doi: 10.1073/pnas.90.22.10705.

Kim, S.-H., Turnbull, J. and Guimond, S. (2011) 'Extracellular matrix and cell signalling: the dynamic cooperation of integrin, proteoglycan and growth factor receptor', *Journal of Endocrinology*. Bristol, UK: BioScientifica, 209(2), pp. 139–151. doi: 10.1530/JOE-10-0377.

Kivelä, R. *et al.* (2014) 'VEGF-B-induced vascular growth leads to metabolic reprogramming and ischemia resistance in the heart', *EMBO Molecular Medicine*, 6(3), pp. 307–321. doi: 10.1002/emmm.201303147.

Klagsbrun, M. and Eichmann, A. (2005) 'A role for axon guidance receptors and ligands in blood vessel development and tumor angiogenesis', *Cytokine & Growth Factor Reviews*, 16(4), pp. 535–548. doi: <https://doi.org/10.1016/j.cytogfr.2005.05.002>.

Klems, A. (2017) *Flt1 determines the structural design of the arteriolar tree*, *Doctoral thesis*.

Koch, S. *et al.* (2011) 'Signal transduction by vascular endothelial growth factor receptors', *Biochemical Journal*, 437(2), pp. 169–183. doi: 10.1042/BJ20110301.

Koch, S. and Claesson-Welsh, L. (2012) 'Signal transduction by vascular endothelial growth factor receptors', *Cold Spring Harbor perspectives in medicine*. Cold Spring Harbor Laboratory Press, 2(7), pp. a006502–a006502. doi: 10.1101/cshperspect.a006502.

Kok, F. O. *et al.* (2015) 'Reverse genetic screening reveals poor correlation between morpholino-induced and mutant phenotypes in zebrafish', *Developmental cell*. 2014/12/18, 32(1), pp. 97–108. doi: 10.1016/j.devcel.2014.11.018.

Kolte, D., McClung, J. A. and Aronow, W. S. (2016) 'Chapter 6 - Vasculogenesis and Angiogenesis', in Aronow, W. S. and McClung, J. A. B. T.-T. R. in C. A. D. (eds). Boston: Academic Press, pp. 49–65. doi: <https://doi.org/10.1016/B978-0-12-802385-3.00006-1>.

Korn, C. and Augustin, H. G. (2015) 'Mechanisms of Vessel Pruning and Regression', *Developmental Cell*, 34(1), pp. 5–17. doi: <https://doi.org/10.1016/j.devcel.2015.06.004>.

Krebs, L. T. *et al.* (2004) 'Haploinsufficient lethality and formation of arteriovenous malformations in Notch pathway mutants', *Genes and Development*, 18(20), pp. 2469–2473. doi: 10.1101/gad.1239204.

Krueger, J. *et al.* (2011) 'Flt1 acts as a negative regulator of tip cell formation and branching morphogenesis in the zebrafish embryo', *Development*, 138(10), pp. 2111–2120. doi: 10.1242/dev.063933.

Krueger, J. (2012) *Novel insights into Flt1 mediated sprouting angiogenesis in zebrafish, Doctoral thesis.*

Kulik, M. *et al.* (2002) 'Disruption of acvr11 increases endothelial cell number in zebrafish cranial vessels.', *Development*, 129(12), pp. 3009–3019. Available at: <http://eutils.ncbi.nlm.nih.gov/entrez/eutils/elink.fcgi?dbfrom=pubmed&id=12050147&retmode=ref&cmd=prlinks%5Cnfile:///Files/96/965C18B8-F686-4E84-960E-87423C66636F.pdf>.

Kume, T. (2010) 'Specification of arterial, venous, and lymphatic endothelial cells during embryonic development', *Histology and histopathology*, 25(5), pp. 637–646. doi: 10.14670/HH-25.637.

Kwan, K. M. *et al.* (2007) 'The Tol2kit: A multisite gateway-based construction Kit for Tol2 transposon transgenesis constructs', *Developmental Dynamics*, 236(11), pp. 3088–3099. doi: 10.1002/dvdy.21343.

Kwon, H.-B. *et al.* (2012) 'AKAP12 regulates vascular integrity in zebrafish', *Experimental & Molecular Medicine*, 44(3), pp. 225–235. doi: 10.3858/emm.2012.44.3.017.

Kwon, H.-B. *et al.* (2013) 'The parallel growth of motoneuron axons with the dorsal aorta depends on Vegfc/Vegfr3 signaling in zebrafish', *Development*, 140(19), pp. 4081 LP – 4090. doi: 10.1242/dev.091702.

Lange, T. *et al.* (2003) 'VEGF162, A New Heparin-binding Vascular Endothelial Growth Factor Splice Form That Is Expressed in Transformed Human Cells ', *Journal of Biological Chemistry*, 278(19), pp. 17164–17169. doi: 10.1074/jbc.M212224200.

- Larrivé, B. *et al.* (2009) 'Guidance of Vascular Development', *Circulation Research*, 104(4), pp. 428–441. doi: 10.1161/CIRCRESAHA.108.188144.
- Lassalle, P. *et al.* (1996) 'ESM-1 Is a Novel Human Endothelial Cell-specific Molecule Expressed in Lung and Regulated by Cytokines', *Journal of Biological Chemistry*, 271(34), pp. 20458–20464. doi: 10.1074/jbc.271.34.20458.
- Law, S. H. W. and Sargent, T. D. (2014) 'The Serine-Threonine Protein Kinase PAK4 Is Dispensable in Zebrafish: Identification of a Morpholino-Generated Pseudophenotype', *PLOS ONE*. Public Library of Science, 9(6), p. e100268. Available at: <https://doi.org/10.1371/journal.pone.0100268>.
- Lawson, N. D. *et al.* (2001) 'Notch signaling is required for arterial-venous differentiation during embryonic vascular development', *Development*, 128(19), pp. 3675 LP – 3683. Available at: <http://dev.biologists.org/content/128/19/3675.abstract>.
- Lawson, N. D. *et al.* (2003) 'phospholipase C gamma-1 is required downstream of vascular endothelial growth factor during arterial development', *Genes & Development*, 17(11), pp. 1346–1351. doi: 10.1101/gad.1072203.
- Lawson, N. D., Vogel, A. M. and Weinstein, B. M. (2002) 'sonic hedgehog and vascular endothelial growth factor Act Upstream of the Notch Pathway during Arterial Endothelial Differentiation', *Developmental Cell*, 3(1), pp. 127–136. doi: [https://doi.org/10.1016/S1534-5807\(02\)00198-3](https://doi.org/10.1016/S1534-5807(02)00198-3).
- Lee, S. *et al.* (2005) 'Processing of VEGF-A by matrix metalloproteinases regulates bioavailability and vascular patterning in tumors', *The Journal of Cell Biology*, 169(4), pp. 681 LP – 691. doi: 10.1083/jcb.200409115.
- Lenhard, B., Sandelin, A. and Carninci, P. (2012) 'Metazoan promoters: emerging characteristics and insights into transcriptional regulation', *Nature Reviews Genetics*, 13(4), pp. 233–245. doi: 10.1038/nrg3163.

- Letrado, P. *et al.* (2018) 'Zebrafish: Speeding Up the Cancer Drug Discovery Process', *Cancer Research*, 78(21), pp. 6048 LP – 6058. doi: 10.1158/0008-5472.CAN-18-1029.
- Leung, D. W. *et al.* (1989) 'Vascular endothelial growth factor is a secreted angiogenic mitogen', *Science*. American Association for the Advancement of Science, 246(4935), pp. 1306–1309. doi: 10.1126/science.2479986.
- Liang, D. *et al.* (2001) 'The role of vascular endothelial growth factor (VEGF) in vasculogenesis, angiogenesis, and hematopoiesis in zebrafish development', *Mechanisms of Development*, 108(1), pp. 29–43. doi: [https://doi.org/10.1016/S0925-4773\(01\)00468-3](https://doi.org/10.1016/S0925-4773(01)00468-3).
- Liu, Y. *et al.* (2016) 'Targeting cellular mRNAs translation by CRISPR-Cas9', *Scientific Reports*. The Author(s), 6, p. 29652. Available at: <https://doi.org/10.1038/srep29652>.
- Lohela, M. *et al.* (2009) 'VEGFs and receptors involved in angiogenesis versus lymphangiogenesis', *Current Opinion in Cell Biology*, 21(2), pp. 154–165. doi: 10.1016/j.ceb.2008.12.012.
- Lortat-Jacob, H. (2009) 'The molecular basis and functional implications of chemokine interactions with heparan sulphate', *Current Opinion in Structural Biology*, 19(5), pp. 543–548. doi: <https://doi.org/10.1016/j.sbi.2009.09.003>.
- Lu, X. *et al.* (2004) 'The netrin receptor UNC5B mediates guidance events controlling morphogenesis of the vascular system', *Nature*, 432(7014), pp. 179–186. doi: 10.1038/nature03080.
- MacRae, C. A. and Peterson, R. T. (2015) 'Zebrafish as tools for drug discovery', *Nature Reviews Drug Discovery*. Nature Publishing Group, a division of Macmillan Publishers Limited. All Rights Reserved., 14, p. 721. Available at: <https://doi.org/10.1038/nrd4627>.
- Makita, T. *et al.* (2008) 'Endothelins are vascular-derived axonal guidance cues for developing sympathetic neurons', *Nature*, 452(7188), pp. 759–763. doi: 10.1038/nature06859.

Matsumoto, K. and Ema, M. (2014) 'Roles of VEGF-A signalling in development, regeneration, and tumours', *The Journal of Biochemistry*, 156(1), pp. 1–10. doi: 10.1093/jb/mvu031.

Matthews, W. *et al.* (1991) 'A receptor tyrosine kinase cDNA isolated from a population of enriched primitive hematopoietic cells and exhibiting close genetic linkage to c-kit', *Proceedings of the National Academy of Sciences of the United States of America*, 88(20), pp. 9026–9030. doi: 10.1073/pnas.88.20.9026.

Maurage, C. A. *et al.* (2009) 'Endocan expression and localization in human glioblastomas', *Journal of Neuropathology and Experimental Neurology*, 68(6), pp. 633–641. doi: 10.1097/NEN.0b013e3181a52a7f.

Meduri, G., Bausero, P. and Perrot-Applanat, M. (2000) 'Expression of Vascular Endothelial Growth Factor Receptors in the Human Endometrium: Modulation During the Menstrual Cycle¹', *Biology of Reproduction*, 62(2), pp. 439–447. doi: 10.1095/biolreprod62.2.439.

Mehta, D. and Malik, A. B. (2006) 'Signaling Mechanisms Regulating Endothelial Permeability', *Physiological Reviews*, 86(1), pp. 279–367. doi: 10.1152/physrev.00012.2005.

Melter, M. *et al.* (2000) 'Ligation of CD40 induces the expression of vascular endothelial growth factor by endothelial cells and monocytes and promotes angiogenesis in vivo', *Blood*, 96(12), pp. 3801 LP – 3808. Available at: <http://www.bloodjournal.org/content/96/12/3801.abstract>.

Menon, P., Kocher, O. N. and Aird, W. C. (2011) 'Endothelial Cell Specific Molecule-1 (ESM-1), a Novel Secreted Proteoglycan Stimulates Vascular Smooth Muscle Cell Proliferation and Migration', *Circulation*, 124(Suppl 21), p. A15455. Available at: http://circ.ahajournals.org/content/124/Suppl_21/A15455.abstract.

Mentzer, S. J. and Konerding, M. A. (2014) 'Intussusceptive angiogenesis: expansion and remodeling of microvascular networks', *Angiogenesis*, 17(3), pp. 499–509. doi: 10.1007/s10456-014-9428-3.

- Meyers, J. R. (2018) 'Zebrafish: Development of a Vertebrate Model Organism', *Current Protocols Essential Laboratory Techniques*. John Wiley & Sons, Ltd, 16(1), p. e19. doi: 10.1002/cpet.19.
- Miller, L. C. *et al.* (2010) 'Separating early sensory neuron and blood vessel patterning', *Developmental Dynamics*, 239(12), pp. 3297–3302. doi: 10.1002/dvdy.22464.
- Mione, M. C. and Trede, N. S. (2010) 'The zebrafish as a model for cancer', *Disease Models & Mechanisms*, 3(9–10), pp. 517 LP – 523. doi: 10.1242/dmm.004747.
- Moses, M. A. (1997) 'The Regulation of Neovascularization by Matrix Metalloproteinases and Their Inhibitors', *STEM CELLS*, 15(3), pp. 180–189. doi: 10.1002/stem.150180.
- Mukouyama, Y. *et al.* (2002) 'Sensory Nerves Determine the Pattern of Arterial Differentiation and Blood Vessel Branching in the Skin', *Cell*, 109(6), pp. 693–705. doi: [https://doi.org/10.1016/S0092-8674\(02\)00757-2](https://doi.org/10.1016/S0092-8674(02)00757-2).
- Mukouyama, Y. *et al.* (2005) 'Peripheral nerve-derived VEGF promotes arterial differentiation via neuropilin 1-mediated positive feedback', *Development*, 132(5), pp. 941 LP – 952. doi: 10.1242/dev.01675.
- Muller, Y. A. *et al.* (1997) 'Vascular endothelial growth factor: Crystal structure and functional mapping of the kinase domain receptor binding site', *Proceedings of the National Academy of Sciences*. National Academy of Sciences, 94(14), pp. 7192–7197. doi: 10.1073/pnas.94.14.7192.
- Mulligan, T. S. and Weinstein, B. M. (2014) 'Emerging from the PAC: Studying zebrafish lymphatic development', *Microvascular Research*, 96, pp. 23–30. doi: <https://doi.org/10.1016/j.mvr.2014.06.001>.
- Mythreya, K. and Blobel, G. C. (2009) 'Proteoglycan signaling co-receptors: Roles in cell adhesion, migration and invasion', *Cellular Signalling*, 21(11), pp. 1548–1558. doi: <https://doi.org/10.1016/j.cellsig.2009.05.001>.

Nakao, T., Ishizawa, A. and Ogawa, R. (1988) 'Observations of vascularization in the spinal cord of mouse embryos, With special reference to development of boundary membranes and perivascular spaces', *The Anatomical Record*, 221(2), pp. 663–677. doi: 10.1002/ar.1092210212.

Nasiadka, A. and Clark, M. D. (2012) 'Zebrafish breeding in the laboratory environment', *ILAR Journal*, 53(2), pp. 161–168. doi: 10.1093/ilar.53.2.161.

Niklason, L. and Dai, G. (2018) 'Arterial Venous Differentiation for Vascular Bioengineering', *Annual Review of Biomedical Engineering*, 20(1), pp. 431–447. doi: 10.1146/annurev-bioeng-062117-121231.

le Noble, F. *et al.* (2004) 'Flow regulates arterial-venous differentiation in the chick embryo yolk sac', *Development*, 131(2), pp. 361 LP – 375. doi: 10.1242/dev.00929.

le Noble, F. *et al.* (2005) 'Control of arterial branching morphogenesis in embryogenesis: go with the flow', *Cardiovascular Research*, 65(3), pp. 619–628. doi: 10.1016/j.cardiores.2004.09.018.

Novodvorsky, P. *et al.* (2015) 'klf2ash317 Mutant Zebrafish Do Not Recapitulate Morpholino-Induced Vascular and Haematopoietic Phenotypes', *PLOS ONE*. Public Library of Science, 10(10), p. e0141611. Available at: <https://doi.org/10.1371/journal.pone.0141611>.

Nyholm, M. K., Abdelilah-Seyfried, S. and Grinblat, Y. (2009) 'A novel genetic mechanism regulates dorsolateral hinge-point formation during zebrafish cranial neurulation', *Journal of Cell Science*. The Company of Biologists Ltd, 122(12), pp. 2137–2148. doi: 10.1242/jcs.043471.

Olofsson, B. *et al.* (1996) 'Vascular endothelial growth factor B, a novel growth factor for endothelial cells', *Proceedings of the National Academy of Sciences of the United States of America*, 93(6), pp. 2576–2581. doi: 10.1073/pnas.93.6.2576.

Olsson, A.-K. *et al.* (2006) 'VEGF receptor signalling ? in control of vascular function', *Nature Reviews Molecular Cell Biology*, 7(5), pp. 359–371. doi: 10.1038/nrm1911.

Pajusola, K. *et al.* (1992) 'FLT4 Receptor Tyrosine Kinase Contains Seven Immunoglobulin-like Loops and Is Expressed in Multiple Human Tissues and Cell Lines', *Cancer Research*, 52(20), pp. 5738 LP – 5743. Available at: <http://cancerres.aacrjournals.org/content/52/20/5738.abstract>.

Pan, Q. *et al.* (2007) 'Blocking Neuropilin-1 Function Has an Additive Effect with Anti-VEGF to Inhibit Tumor Growth', *Cancer Cell*, 11(1), pp. 53–67. doi: 10.1016/j.ccr.2006.10.018.

Park, J. E. *et al.* (1994) 'Placenta growth factor. Potentiation of vascular endothelial growth factor bioactivity, in vitro and in vivo, and high affinity binding to Flt-1 but not to Flk-1/KDR.', *Journal of Biological Chemistry*, 269(41), pp. 25646–25654. Available at: <http://www.jbc.org/content/269/41/25646.abstract>.

Park, J. E., Keller, G. A. and Ferrara, N. (1993) 'The vascular endothelial growth factor (VEGF) isoforms: differential deposition into the subepithelial extracellular matrix and bioactivity of extracellular matrix-bound VEGF.', *Molecular Biology of the Cell*. American Society for Cell Biology (mboc), 4(12), pp. 1317–1326. doi: 10.1091/mbc.4.12.1317.

Parng, C. (2005) 'In vivo zebrafish assays for toxicity testing', *Current opinion in drug discovery & development*, 8(1), p. 100–106.

Patan, S. *et al.* (2001) 'Vascular Morphogenesis and Remodeling in a Model of Tissue Repair', *Circulation Research*, 89(8), pp. 723–731. doi: 10.1161/hh2001.097870.

Peretz, D. *et al.* (1992) 'Glycosylation of vascular endothelial growth factor is not required for its mitogenic activity', *Biochemical and Biophysical Research Communications*, 182(3), pp. 1340–1347. doi: [https://doi.org/10.1016/0006-291X\(92\)91880-Y](https://doi.org/10.1016/0006-291X(92)91880-Y).

Peri, F. and Nüsslein-Volhard, C. (2008) 'Live Imaging of Neuronal Degradation by Microglia Reveals a Role for v0-ATPase a1 in Phagosomal Fusion In Vivo', *Cell*, 133(5), pp. 916–927. doi: 10.1016/j.cell.2008.04.037.

Perrimon, N. and Bernfield, M. (2000) 'Specificities of heparan sulphate proteoglycans in developmental processes', *Nature*, 404(6779), pp. 725–728. doi: 10.1038/35008000.

Phng, L.-K. and Gerhardt, H. (2009) 'Angiogenesis: A Team Effort Coordinated by Notch', *Developmental Cell*, 16(2), pp. 196–208. doi: <https://doi.org/10.1016/j.devcel.2009.01.015>.

Phng, L.-K., Stanchi, F. and Gerhardt, H. (2013) 'Filopodia are dispensable for endothelial tip cell guidance', *Development*. The Company of Biologists Ltd, 140(19), pp. 4031–4040. doi: 10.1242/dev.097352.

Plouët, J. *et al.* (1997) 'Extracellular Cleavage of the Vascular Endothelial Growth Factor 189-Amino Acid Form by Urokinase Is Required for Its Mitogenic Effect', *Journal of Biological Chemistry*, 272(20), pp. 13390–13396. doi: 10.1074/jbc.272.20.13390.

Pociute, K., Schumacher, J. A. and Sumanas, S. (2019) 'Clec14a genetically interacts with Etv2 and Vegf signaling during vasculogenesis and angiogenesis in zebrafish', *BMC Developmental Biology*, 19(1), p. 6. doi: 10.1186/s12861-019-0188-6.

Pollman, M. J. *et al.* (1996) 'Vasoactive substances regulate vascular smooth muscle cell apoptosis: Countervailing influences of nitric oxide and angiotensin II', *Circulation Research*. Lippincott Williams and Wilkins, 79(4), pp. 748–756. doi: 10.1161/01.RES.79.4.748.

Pötgens, A. J. *et al.* (1994) 'Covalent dimerization of vascular permeability factor/vascular endothelial growth factor is essential for its biological activity. Evidence from Cys to Ser mutations.', *Journal of Biological Chemistry*, 269(52), pp. 32879–32885. Available at: <http://www.jbc.org/content/269/52/32879.abstract>.

Pudliszewski, M. and Pardanaud, L. (2005) 'Vasculogenesis and angiogenesis in the mouse embryo studied using quail/mouse chimeras', *International Journal of Developmental Biology*, 49(2-3 SPEC. ISS.), pp. 355–361. doi: 10.1387/ijdb.041956mp.

Rafii, S. and Carmeliet, P. (2016) 'VEGF-B Improves Metabolic Health through Vascular Pruning of Fat', *Cell Metabolism*, 23(4), pp. 571–573. doi: 10.1016/j.cmet.2016.03.012.

Risau, W. (1995) 'Differentiation of Endothelium', *Faseb*, 9(10), pp. 926–933.

- Risau, W. (1997) 'Mechanisms of angiogenesis', *Nature*, 386(6626), pp. 671–674. doi: 10.1038/386671a0.
- Risau, W. (2008) 'Mechanisms of angiogenesis', *Biochemistry (Moscow)*, 73(7), pp. 751–762. doi: 10.1134/S0006297908070031.
- Risau, W. and Flamme, I. (1995) 'Vasculogenesis', *Annual Review of Cell and Developmental Biology*, 11(1), pp. 73–91. doi: 10.1146/annurev.cb.11.110195.000445.
- Robinson, C. J. and Stringer, S. E. (2001) 'The splice variants of vascular endothelial growth factor (VEGF) and their receptors', *Journal of Cell Science*. The Company of Biologists Ltd, 114(5), pp. 853–865. Available at: <https://jcs.biologists.org/content/114/5/853>.
- Roca, C. and Adams, R. H. (2007) 'Regulation of vascular morphogenesis by Notch signaling', *Genes and Development*, 21(20), pp. 2511–2524. doi: 10.1101/gad.1589207.
- Rocha, S. F. *et al.* (2014) 'Esm1 modulates endothelial tip cell behavior and vascular permeability by enhancing VEGF bioavailability', *Circulation Research*, 115(6), pp. 581–590. doi: 10.1161/CIRCRESAHA.115.304718.
- Roodhart, J. *et al.* (2008) 'The Molecular Basis of Class Side Effects Due to Treatment with Inhibitors of the VEGF/VEGFR Pathway', *Current Clinical Pharmacology*. Bentham Science Publishers Ltd., 3(2), pp. 132–143. doi: 10.2174/157488408784293705.
- van Rooijen, E. *et al.* (2011) 'A Zebrafish Model for VHL and Hypoxia Signaling', *Methods in Cell Biology*, 105(December), pp. 163–190. doi: 10.1016/B978-0-12-381320-6.00007-2.
- Rossi, A. *et al.* (2015) 'Genetic compensation induced by deleterious mutations but not gene knockdowns', *Nature*. Nature Publishing Group, a division of Macmillan Publishers Limited. All Rights Reserved., 524, p. 230. Available at: <https://doi.org/10.1038/nature14580>.
- Rossi, A. *et al.* (2016) 'Regulation of Vegf signaling by natural and synthetic ligands', *Blood*, 128(19), pp. 2359–2366. doi: 10.1182/blood-2016-04-711192.

Rostand, K. S. and Esko, J. D. (1997) 'Microbial adherence to and invasion through proteoglycans', *Infection and immunity*, 65(1), pp. 1–8. Available at: <https://www.ncbi.nlm.nih.gov/pubmed/8975885>.

Roudnicky, F. *et al.* (2013) 'Endocan is upregulated on tumor vessels in invasive bladder cancer where it mediates VEGF-A-induced angiogenesis', *Cancer Research*, 73(3), pp. 1097–1106. doi: 10.1158/0008-5472.CAN-12-1855.

Roy, H., Bhardwaj, S. and Ylä-Herttuala, S. (2006) 'Biology of vascular endothelial growth factors', *FEBS Letters*, 580(12), pp. 2879–2887. doi: <https://doi.org/10.1016/j.febslet.2006.03.087>.

Rubinstein, A. L. (2003) 'Zebrafish: From disease modeling to drug discovery', *Current Opinion in Drug Discovery and Development*, 6(2), pp. 218–223.

Ruhrberg, C. *et al.* (2002) 'Spatially restricted patterning cues provided by heparin-binding VEGF-A control blood vessel branching morphogenesis', *Genes & Development*, 16(20), pp. 2684–2698. doi: 10.1101/gad.242002.

Ruhrberg, C. (2003) 'Growing and shaping the vascular tree: multiple roles for VEGF', *BioEssays*, 25(11), pp. 1052–1060. doi: 10.1002/bies.10351.

Ruhrberg, C. and Bautch, V. L. (2013) 'Neurovascular development and links to disease', *Cellular and Molecular Life Sciences*, 70(10), pp. 1675–1684. doi: 10.1007/s00018-013-1277-5.

Sandelin, A. *et al.* (2007) 'Mammalian RNA polymerase II core promoters: insights from genome-wide studies', *Nature Reviews Genetics*, 8(6), pp. 424–436. doi: 10.1038/nrg2026.

Santoriello, C. and Zon, L. I. (2012) 'Hooked! Modeling human disease in zebrafish', *The Journal of Clinical Investigation*. The American Society for Clinical Investigation, 122(7), pp. 2337–2343. doi: 10.1172/JCI60434.

Sarrazin, S. *et al.* (2006) 'Endocan or endothelial cell specific molecule-1 (ESM-1): A potential novel endothelial cell marker and a new target for cancer therapy', *Biochimica et Biophysica Acta - Reviews on Cancer*, 1765(1), pp. 25–37. doi: 10.1016/j.bbcan.2005.08.004.

Sarrazin, S. *et al.* (2010) 'Characterization and binding activity of the chondroitin/dermatan sulfate chain from Endocan, a soluble endothelial proteoglycan', *Glycobiology*, 20(11), pp. 1380–1388. doi: 10.1093/glycob/cwq100.

Sarrazin, S., Lamanna, W. C. and Esko, J. D. (2011) 'Heparan Sulfate Proteoglycans', *Cold Spring Harbor Perspectives in Biology*, 3(7). doi: 10.1101/cshperspect.a004952.

Sasisekharan, R. *et al.* (2002) 'Roles of heparan-sulphate glycosaminoglycans in cancer', *Nature Reviews Cancer*, 2(7), pp. 521–528. doi: 10.1038/nrc842.

Scherpereel, A. *et al.* (2003) 'Overexpression of Endocan Induces Tumor Formation', *Cancer Research*, 63(18), pp. 6084 LP – 6089. Available at: <http://cancerres.aacrjournals.org/content/63/18/6084.abstract>.

Scherpereel, A. *et al.* (2006) 'Endocan, a new endothelial marker in human sepsis*', *Critical Care Medicine*, 34(2). Available at: https://journals.lww.com/ccmjournals/Fulltext/2006/02000/Endocan,_a_new_endothelial_marker_in_human_sepsis_.35.aspx.

Schmidtchen, A., Frick, I.-M. and Björck, L. (2001) 'Dermatan sulphate is released by proteinases of common pathogenic bacteria and inactivates antibacterial α -defensin', *Molecular Microbiology*. John Wiley & Sons, Ltd (10.1111), 39(3), pp. 708–713. doi: 10.1046/j.1365-2958.2001.02251.x.

Senger, D. R. *et al.* (1983) 'Tumor cells secrete a vascular permeability factor that promotes accumulation of ascites fluid', *Science*. American Association for the Advancement of Science, 219(4587), pp. 983–985. doi: 10.1126/science.6823562.

Shalaby, F. *et al.* (1995) 'Failure of blood-island formation and vasculogenesis in Flk-1-deficient mice', *Nature*, 376(6535), pp. 62–66. doi: 10.1038/376062a0.

Shalaby, F. *et al.* (1997) 'A Requirement for Flk1 in Primitive and Definitive Hematopoiesis and Vasculogenesis', *Cell*. Elsevier, 89(6), pp. 981–990. doi: 10.1016/S0092-8674(00)80283-4.

Shibuya, M. *et al.* (1990) 'Nucleotide sequence and expression of a novel human receptor-type tyrosine kinase gene (flt) closely related to the fms family.', *Oncogene*, 5(4), pp. 519–524. Available at: <https://app.dimensions.ai/details/publication/pub.1078397375>.

Shibuya, M. (2014) 'VEGF-VEGFR Signals in Health and Disease', *Biomolecules & therapeutics*. The Korean Society of Applied Pharmacology, 22(1), pp. 1–9. doi: 10.4062/biomolther.2013.113.

Shimojo, H., Ohtsuka, T. and Kageyama, R. (2011) 'Dynamic expression of notch signaling genes in neural stem/progenitor cells', *Frontiers in neuroscience*. Frontiers Research Foundation, 5, p. 78. doi: 10.3389/fnins.2011.00078.

Shin, D. *et al.* (2001) 'Expression of EphrinB2 Identifies a Stable Genetic Difference Between Arterial and Venous Vascular Smooth Muscle as Well as Endothelial Cells, and Marks Subsets of Microvessels at Sites of Adult Neovascularization', *Developmental Biology*, 230(2), pp. 139–150. doi: <https://doi.org/10.1006/dbio.2000.9957>.

Shin, J. W., Huggenberger, R. and Detmar, M. (2008) 'Transcriptional profiling of VEGF-A and VEGF-C target genes in lymphatic endothelium reveals endothelial-specific molecule-1 as a novel mediator of lymphangiogenesis', *Blood*, 112(6), pp. 2318 LP – 2326. doi: 10.1182/blood-2008-05-156331.

Siekman, A. F. and Lawson, N. D. (2007) 'Notch signalling limits angiogenic cell behaviour in developing zebrafish arteries', *Nature*. Nature Publishing Group, 445, p. 781. Available at: <https://doi.org/10.1038/nature05577>.

- Smet, F. De *et al.* (2009) 'Mechanisms of Vessel Branching', *Arteriosclerosis, Thrombosis, and Vascular Biology*, 29(5), pp. 639–649. doi: 10.1161/ATVBAHA.109.185165.
- Smith, G. A. *et al.* (2016) 'VEGFR2 Trafficking, Signaling and Proteolysis is Regulated by the Ubiquitin Isopeptidase USP8', *Traffic*. John Wiley & Sons, Ltd (10.1111), 17(1), pp. 53–65. doi: 10.1111/tra.12341.
- Spillmann, D. (2001) 'Heparan sulfate: Anchor for viral intruders?', *Biochimie*, 83(8), pp. 811–817. doi: [https://doi.org/10.1016/S0300-9084\(01\)01290-1](https://doi.org/10.1016/S0300-9084(01)01290-1).
- Stéphane, S. *et al.* (2010) 'Endocan as a biomarker of endothelial dysfunction in cancer', *Journal of Cancer Science and Therapy*, pp. 47–52. doi: 10.4172/1948-5956.1000022.
- Strasser, G. A., Kaminker, J. S. and Tessier-Lavigne, M. (2010) 'Microarray analysis of retinal endothelial tip cells identifies CXCR4 as a mediator of tip cell morphology and branching', *Blood*, 115(24), pp. 5102 LP – 5110. doi: 10.1182/blood-2009-07-230284.
- Stuttfield, E. and Ballmer-Hofer, K. (2009) 'Structure and function of VEGF receptors', *IUBMB Life*, 61(9), pp. 915–922. doi: 10.1002/iub.234.
- Suchting, S. *et al.* (2007) 'The Notch ligand Delta-like 4 negatively regulates endothelial tip cell formation and vessel branching', *Proceedings of the National Academy of Sciences*. National Academy of Sciences, 104(9), pp. 3225–3230. doi: 10.1073/pnas.0611177104.
- Sun, H. *et al.* (2019) 'Circulating ESM-1 levels are correlated with the presence of coronary artery disease in patients with obstructive sleep apnea', *Respiratory Research*, 20(1), p. 188. doi: 10.1186/s12931-019-1143-6.
- Swift, M. R. and Weinstein, B. M. (2009) 'Arterial–Venous Specification During Development', *Circulation Research*, 104(5), pp. 576–588. doi: 10.1161/CIRCRESAHA.108.188805.
- Takahashi, H. and Shibuya, M. (2005) 'The vascular endothelial growth factor (VEGF)/VEGF receptor system and its role under physiological and pathological conditions', *Clinical Science*, 109(3), pp. 227–241. doi: 10.1042/CS20040370.

Tam, S. J. and Watts, R. J. (2010) 'Connecting Vascular and Nervous System Development: Angiogenesis and the Blood-Brain Barrier', *Annual Review of Neuroscience*. Annual Reviews, 33(1), pp. 379–408. doi: 10.1146/annurev-neuro-060909-152829.

Tammela, T. *et al.* (2008) 'Blocking VEGFR-3 suppresses angiogenic sprouting and vascular network formation', *Nature*. Macmillan Publishers Limited. All rights reserved, 454, p. 656. Available at: <https://doi.org/10.1038/nature07083>.

Tata, M., Ruhrberg, C. and Fantin, A. (2015) 'Vascularisation of the central nervous system', *Mechanisms of Development*, 138, pp. 26–36. doi: <https://doi.org/10.1016/j.mod.2015.07.001>.

Taylor, K. R. and Gallo, R. L. (2006) 'Glycosaminoglycans and their proteoglycans: host-associated molecular patterns for initiation and modulation of inflammation', *The FASEB Journal*. Federation of American Societies for Experimental Biology, 20(1), pp. 9–22. doi: 10.1096/fj.05-4682rev.

Terman, B. I. *et al.* (1992) 'Identification of the KDR tyrosine kinase as a receptor for vascular endothelial cell growth factor', *Biochemical and Biophysical Research Communications*, 187(3), pp. 1579–1586. doi: [https://doi.org/10.1016/0006-291X\(92\)90483-2](https://doi.org/10.1016/0006-291X(92)90483-2).

Tischer, E. *et al.* (1991) 'The human gene for vascular endothelial growth factor. Multiple protein forms are encoded through alternative exon splicing.', *Journal of Biological Chemistry*, 266(18), pp. 11947–11954. Available at: <http://www.jbc.org/content/266/18/11947.abstract>.

del Toro, R. *et al.* (2010) 'Identification and functional analysis of endothelial tip cell-enriched genes', *Blood*. 2010/08/12. American Society of Hematology, 116(19), pp. 4025–4033. doi: 10.1182/blood-2010-02-270819.

Trowbridge, J. M. and Gallo, R. L. (2002) 'Dermatan sulfate: new functions from an old glycosaminoglycan', *Glycobiology*, 12(9), pp. 117R-125R. doi: 10.1093/glycob/cwf066.

Ulrich, F. *et al.* (2011) 'Neurovascular development in the embryonic zebrafish hindbrain', *Developmental Biology*, 357(1), pp. 134–151. doi: <https://doi.org/10.1016/j.ydbio.2011.06.037>.

Vincenti, V. *et al.* (1996) 'Assignment of the Vascular Endothelial Growth Factor Gene to Human Chromosome 6p21.3', *Circulation*, 93(8), pp. 1493–1495. doi: [10.1161/01.CIR.93.8.1493](https://doi.org/10.1161/01.CIR.93.8.1493).

Visconti, R. P., Richardson, C. D. and Sato, T. N. (2002) 'Orchestration of angiogenesis and arteriovenous contribution by angiopoietins and vascular endothelial growth factor (VEGF)', *Proceedings of the National Academy of Sciences*, 99(12), pp. 8219 LP – 8224. doi: [10.1073/pnas.122109599](https://doi.org/10.1073/pnas.122109599).

Waltenberger, J. *et al.* (1994) 'Different signal transduction properties of KDR and Flt1, two receptors for vascular endothelial growth factor.', *Journal of Biological Chemistry*, 269(43), pp. 26988–26995. Available at: <http://www.jbc.org/content/269/43/26988.abstract>.

Wang, H. U., Chen, Z.-F. and Anderson, D. J. (1998) 'Molecular Distinction and Angiogenic Interaction between Embryonic Arteries and Veins Revealed by ephrin-B2 and Its Receptor Eph-B4', *Cell*, 93(5), pp. 741–753. doi: [https://doi.org/10.1016/S0092-8674\(00\)81436-1](https://doi.org/10.1016/S0092-8674(00)81436-1).

Wang, S. and Olson, E. N. (2009) 'AngiomiRs—Key regulators of angiogenesis', *Current Opinion in Genetics & Development*, 19(3), pp. 205–211. doi: <https://doi.org/10.1016/j.gde.2009.04.002>.

Watson, O. *et al.* (2013) 'Blood flow suppresses vascular Notch signalling via dll4 and is required for angiogenesis in response to hypoxic signalling', *Cardiovascular Research*, 100(2), pp. 252–261. doi: [10.1093/cvr/cvt170](https://doi.org/10.1093/cvr/cvt170).

Whitelock, J. M., Melrose, J. and Iozzo, R. V (2008) 'Diverse Cell Signaling Events Modulated by Perlecan', *Biochemistry*. American Chemical Society, 47(43), pp. 11174–11183. doi: [10.1021/bi8013938](https://doi.org/10.1021/bi8013938).

Whittaker, J. R. (1966) 'An analysis of melanogenesis in differentiating pigment cells of ascidian embryos', *Developmental Biology*, 14(1), pp. 1–39. doi: [https://doi.org/10.1016/0012-1606\(66\)90003-0](https://doi.org/10.1016/0012-1606(66)90003-0).

Wild, R. (2016) *Neuronal Flt1 controls spinal cord vascularization involving venous endothelium with high angiogenic potential*.

Wild, R. *et al.* (2017) 'Neuronal sFlt1 and Vegfaa determine venous sprouting and spinal cord vascularization', *Nature Communications*, 8(May 2016). doi: 10.1038/ncomms13991.

Yang, J. *et al.* (2015) 'Endocan: A new marker for cancer and a target for cancer therapy', *Biomedical reports*. 2015/02/26. D.A. Spandidos, 3(3), pp. 279–283. doi: 10.3892/br.2015.438.

Yaniv, K. *et al.* (2006) 'Live imaging of lymphatic development in the zebrafish', *Nature Medicine*, 12(6), pp. 711–716. doi: 10.1038/nm1427.

Yella, V. R., Kumar, A. and Bansal, M. (2018) 'Identification of putative promoters in 48 eukaryotic genomes on the basis of DNA free energy', *Scientific Reports*, 8(1), p. 4520. doi: 10.1038/s41598-018-22129-8.

Yilmaz, M. I. *et al.* (2014) 'Plasma endocan levels associate with inflammation, vascular abnormalities, cardiovascular events, and survival in chronic kidney disease', *Kidney International*, 86(6), pp. 1213–1220. doi: <https://doi.org/10.1038/ki.2014.227>.

Young, P. P. and Schäfer, R. (2015) 'Cell-based therapies for cardiac disease: A cellular therapist's perspective', *Transfusion*, 55(2), pp. 441–451. doi: 10.1111/trf.12826.

Zhang, F. *et al.* (2009) 'VEGF-B is dispensable for blood vessel growth but critical for their survival, and VEGF-B targeting inhibits pathological angiogenesis', *Proceedings of the National Academy of Sciences*, 106(15), pp. 6152 LP – 6157. doi: 10.1073/pnas.0813061106.

Zhang, L. (2010) 'Glycosaminoglycan (GAG) biosynthesis and GAG-binding proteins', in *Progress in Molecular Biology and Translational Science*. doi: 10.1016/S1877-1173(10)93001-9.

Zhao, Y., Vanhoutte, P. M. and Leung, S. W. S. (2015) 'Vascular nitric oxide: Beyond eNOS', *Journal of Pharmacological Sciences*, 129(2), pp. 83–94. doi: <https://doi.org/10.1016/j.jphs.2015.09.002>.

Zhong, T. P. *et al.* (2001) 'Gridlock signalling pathway fashions the first embryonic artery', *Nature*, 414(6860), pp. 216–220. doi: 10.1038/35102599.

Zhu, D. *et al.* (2017) 'Vegfa Impacts Early Myocardium Development in Zebrafish', *International journal of molecular sciences*. MDPI, 18(2), p. 444. doi: 10.3390/ijms18020444.

8 List of figures

Figure 3-1	The architecture of blood vessels
Figure 3-2	Vasculogenesis and angiogenesis
Figure 3-3	Development of the zebrafish trunk vasculature
Figure 3-4	The distinct physiological sprouting types establish the vascular network of the zebrafish trunk
Figure 3-5	The tip-stalk cell model
Figure 3-6	VEGFs and their receptors
Figure 4-1	<i>Esm1</i> expression is enhanced in <i>Vegfaa</i> GOF models
Figure 4-2	Target site of the <i>esm1</i> whole mount <i>in situ</i> probe
Figure 4-3	Spatial location of <i>esm1</i> mRNA in the wildtype
Figure 4-4	Spatial expression of <i>esm1</i> mRNA in <i>flt1</i> mutants
Figure 4-5	<i>Esm1</i> promoter activity in the heart and blood vessels
Figure 4-6	<i>Esm1</i> promoter activity during development of the trunk vasculature
Figure 4-7	The <i>esm1</i> promoter is active in <i>flt1</i> mutants
Figure 4-8	The <i>esm1</i> promoter is preferentially active in endothelial cells of arterial identity
Figure 4-9	Activation of the <i>esm1</i> promoter in neurons of the spinal cord
Figure 4-10	<i>Esm1</i> in the <i>flt1</i> LOF model attenuates tertiary sprouting
Figure 4-11	Verification of the <i>esm1</i> morpholino dosage in <i>esm1</i> mutants
Figure 4-12	Generation and verification of <i>esm1</i> mutants
Figure 4-13	Establishing <i>esm1;flt1</i> double mutants
Figure 4-14	Vascular patterning in <i>esm1</i> and <i>flt1</i> LOF models at the level of the spinal cord
Figure 4-15	Graphical illustration of the mutation in the <i>esm1</i> ^{sa11057} line
Figure 4-16	Hypersprouting upon <i>flt1</i> knock down is less severe in <i>esm1</i> ^{sa11057} mutants
Figure 4-17	Global increase of <i>esm1</i> results in augmented tertiary sprouting
Figure 4-18	<i>Esm1</i> overexpressed in blood vessels results in elevated ectopic sprouting
Figure 4-19	<i>Esm1</i> levels affect spinal cord vascularization in the <i>vh1</i> mutant
Figure 4-20	The trunk vascular pattern in <i>esm1</i> zebrafish mutants was not altered during early development
Figure 4-21	Trunk vessels show a mild phenotype in <i>esm1</i> knock out fish
Figure 5-1	Hypothesis how <i>Esm1</i> modulates bioavailability of <i>Vegfaa</i> for <i>Kdr1</i>
Figure 6-1	Illustration of the BAC recombineering process and establishing transgenesis for studying promoter activity
Figure 6-2	The eGFP-p2a system
Figure 6-3	Quantification of the zebrafish vascular network at the neuro-vascular interface

9 List of tables

Table 6-1	Zebrafish reporter lines
Table 6-2	Zebrafish mutant lines
Table 6-3	Composition of solutions and buffer
Table 6-4	Enzymes
Table 6-5	Commercial kits
Table 6-6	Primer sequences for real-time qPCR or genotyping
Table 6-7	Primer sequences for construct cloning
Table 6-8	Morpholino
Table 6-9	crRNA target sequences used for CRISPR/Cas9 mutagenesis
Table 6-10	Plasmids generated elsewhere
Table 6-11	Plasmids generated in this work
Table 6-12	Online tools and softwares used
Table 6-13	mRNA generation from different plasmids

10 Abbreviations

aISV	arterial intersegmental vessel
BAC	bacterial artificial chromosome
bp	base pairs
BV	blood vessel
Cas9	CRISPR associated protein 9
cDNA	complementary DNA
CMV	cytomegalovirus
CNS	central nervous system
CRISPR	Clustered Regularly Interspaced Short Palindromic Repeats
crRNA	CRISPR RNA
DA	dorsal aorta
DIG	digoxigenin
DLAV	dorsal longitudinal anastomotic vessel
DII4	delta-like 4
DNA	deoxyribonucleic acid
DNase	deoxyribonuclease
dNTP	deoxynucleotide triphosphate
dpf	days post fertilization
EC	endothelial cell
ECM	extracellular matrix
EDTA	ethylene diamine tetraacetic acid
eGFP	enhanced green fluorescent protein
ESM1	Endothelial cell-specific molecule 1
fli1a	Fli1a proto-oncogene
Flk1	Fetal liver kinase-1
Flt1	Fms-like tyrosine kinase 1/VEGFR-1
Flt4	Fms-like tyrosine kinase 4/VEGFR-4
GAG	glycosaminoglycan
GFP	green fluorescent protein
GOF	gain-of-function
hpf	hours post fertilization
Ig	immunoglobulin
ISH	<i>in situ</i> hybridization
ISV	intersegmental vessel
Kb	kilo base pairs
kDa	kilo Dalton
Kdrl	kinase insert domain receptor-like
LOF	loss-of-function
MAPK	mitogen-activated protein kinases
mRNA	messenger RNA
NRP	Neuropilin
NT	neural tube
NTP	nucleotide triphosphate
PBS	phosphate buffered saline
PBS-T	phosphate buffered saline with Tween 20
PCR	polymerase chain reaction
PCV	posterior cardinal vein

PFA	paraformaldehyde
PG	proteoglycan
PI3Ks	phosphoinositide 3 –kinases
PlGF	placental growth factor
RNA	ribonucleic acid
RNase	ribonuclease
rpm	revolutions per minute
RTK	receptor tyrosine kinase
s.e.m	standard error of the mean
sFlt1	soluble Flt1
sgRNA	single guide RNA
Tg	transgenic
tracrRNA	trans-activating crRNA
Tris	tris(hydroxymethyl)-aminomethane
VEGF	vascular endothelial growth factor
VEGFR	vascular endothelial growth factor receptor
vhl	von Hippel-Lindau
vISV	venous intersegmental vessel
WISH	whole mount <i>in situ</i> hybridization
wt	wildtype
YFP	yellow fluorescent protein

11 Publications

Seifert, Anne, David F Werheid, Silvana M Knapp and Edda Tobiasch. 2015. "Role of Hox genes in stem cell differentiation." *World J Stem Cell* 7(3):583-95. doi:10.4252/wjsc.v7.i3.583.